



HAL
open science

Remotely sensed rivers in the Anthropocene: state of the art and prospects

Hervé Piégay, Fanny Arnaud, Barbara Belletti, Mélanie Bertrand, Simone Bizzi, Patrice Carbonneau, Simon Dufour, Frédéric Liébault, Virginia Ruiz-villanueva, Louise Slater

► To cite this version:

Hervé Piégay, Fanny Arnaud, Barbara Belletti, Mélanie Bertrand, Simone Bizzi, et al.. Remotely sensed rivers in the Anthropocene: state of the art and prospects. *Earth Surface Processes and Landforms*, 2019, 45 (1), pp.157-188. 10.1002/esp.4787. hal-02485109

HAL Id: hal-02485109

<https://hal.science/hal-02485109v1>

Submitted on 6 Jan 2025

HAL is a multi-disciplinary open access archive for the deposit and dissemination of scientific research documents, whether they are published or not. The documents may come from teaching and research institutions in France or abroad, or from public or private research centers.

L'archive ouverte pluridisciplinaire **HAL**, est destinée au dépôt et à la diffusion de documents scientifiques de niveau recherche, publiés ou non, émanant des établissements d'enseignement et de recherche français ou étrangers, des laboratoires publics ou privés.

1 Remotely Sensed Rivers in the Anthropocene: 2 State of the Art and Prospects

3
4 H. Piégay¹, F. Arnaud¹, B. Belletti², M. Bertrand³, S. Bizzi⁴, P. Carbonneau⁵, S. Dufour⁶, F.
5 Liebault³, V. Ruiz-Villanueva^{1,7}, L. Slater⁸

6
7 ¹ University of Lyon, UMR 5600 CNRS EVS, École Normale Supérieure de Lyon, 15 Parvis René Descartes, F-69342
8 Lyon, France

9
10 ² Politecnico di Milano, Department of Electronics, Information and Bioengineering, Piazza Leonardo da Vinci 32, 20133
11 Milano, Italy

12
13 ³ University of Grenoble Alpes, Irstea, ETNA, F-38 000 Grenoble, France.

14
15 ⁴ Department of Geosciences, University of Padova, Padua, Italy.

16
17 ⁵ Durham University, Department of Geography, Durham, United Kingdom, DH1 3LE

18
19 ⁶ University of Rennes 2, CNRS UMR LETG, Place Le Moal, F-35000, Rennes, France

20
21 ⁷ University of Geneva, Institute for Environmental Sciences (ISE), 66 Boulevard Carl-Vogt, 1205 Geneva, Switzerland

22
23 ⁸ University of Oxford, School of Geography and the Environment, South Parks Road, Oxford OX1 3QY, UK

24
25
26 **ABSTRACT:** The rivers of the world are undergoing accelerated change in the Anthropocene, and
27 need to be managed at much broader spatial and temporal scales than before. Fluvial remote sensing
28 now offers a technical and methodological framework that can be deployed to monitor the processes
29 at work and to assess the trajectories of rivers in the Anthropocene. In this paper, we review research
30 investigating past, present and future fluvial corridor conditions and processes using remote sensing
31 and we consider emerging challenges facing fluvial and riparian research. We introduce a suite of
32 remote sensing methods designed to diagnose river changes at reach to regional scales. We then focus
33 on identification of channel patterns and acting processes from satellite, airborne or ground
34 acquisitions. These techniques range from grain scales to landform scales, and from real time scales
35 to inter-annual scales. We discuss how remote sensing data can now be coupled to catchment scale
36 models that simulate sediment transfer within connected river networks. We also consider future
37 opportunities in terms of datasets and other resources which are likely to impact river management
38 and monitoring at the global scale. We conclude with a summary of challenges and prospects for
39 remotely sensed rivers in the Anthropocene.

40
41 **Key Words:** remote sensing, GIS, drone, fluvial geomorphology, biogeomorphology, channel
42 changes, riparian vegetation, sediment transport modelling, grain size, fluvial corridor

43 44 45 1. **Introduction**

46
47 The concept of the Anthropocene proposed by Crutzen (2002) suggests that the geophysical
48 influence of humans on Earth is such that we have fundamentally modified global landscape
49 characteristics and entered a new era. Humans are changing the world's ecosystem processes and

50 functioning, and need to adapt to the consequences of these changing conditions. With the “Great
51 Acceleration” of landscape changes since the 20th century (Steffen et al. 2007), it has become crucial
52 to characterize evolutionary trajectories of Earth’s environments in order to infer future conditions.
53 Even though the concept of the Anthropocene is still debated, there is a pressing need to quantify the
54 human impacts on physical systems in recent decades. Moreover, the concept of the Anthropocene
55 also helps identify the driving processes of landscape change (Moore, 2015). Thus, although the
56 concept focuses predominantly on large spatio-temporal scales, human societies produce different
57 types of change, and not all regions of the world follow the same trajectories. In other words, multi-
58 scale approaches are needed to explore the characteristics of the Anthropocene from local to global
59 scales. Lastly, the concept of the Anthropocene also highlights the key principles of rehabilitation
60 and restoration as tools to preserve our landscapes and their ecological integrity.

61 The Anthropocene is notably of interest for river scientists and fluvial geomorphologists who
62 explore future changes and are engaged in management applications and decision-making support.
63 Comprehensive reviews of research on river morphology and riverine environments in the
64 Anthropocene have been recently proposed by Downs and Piégay (2019) and Wohl (2019). The
65 Anthropocene reshapes river management perspectives by encouraging conservation and restoration
66 processes and introduces humans as a boundary condition to be taken into account in the definition
67 of management options (Mould & Fryirs, 2018). The concept also suggests that fluvial systems are
68 now socio-ecological hybrids and that human constructions can be perceived as potentially valuable,
69 as is discussed with the novel ecosystem concept (Hobbs et al. 2006). There is an urgent need to work
70 on highly modified river systems and not only the most natural systems, in order to understand the
71 physical processes and improve their functioning (Thorel et al. 2018). Fluvial geomorphologists have
72 made considerable progress in reading the landscape (Fryirs & Brierley, 2012), interpreting the range
73 of past channel processes, understanding the biophysical and anthropogenic drivers of channel
74 trajectories, and predicting future changes (Brierley et al., 2013; Wohl, 2014; Brown et al., 2018).
75 However, our ability to quantify interactions between local hydromorphological processes and fluvial
76 system functioning at the basin scale is still largely conceptual (Fryirs, 2013; Bracken et al., 2015),
77 as is our ability to predict likely future channel trajectories (Surian & Rinaldi, 2003; Brierley & Fryirs,
78 2008; Dufour & Piégay, 2009). Recent scientific contributions are emerging in this domain based on
79 geospatial resources (Schmitt et al. 2018b; Grill et al. 2019). Factors that influence evolutionary
80 trajectories can be natural or anthropogenic and may act at both reach and catchment scales; they can
81 be progressive (e.g. climate or land use change), impulsive (e.g. floods, earthquakes) or
82 discontinuous, e.g. either a transient (e.g. sediment mining) or a permanent disturbance (e.g. dam,
83 bank protection), forming a complex set of drivers (Dufour & Piégay, 2009). A temporal analysis of
84 past river processes and natural inheritance is necessary to understand present river conditions,
85 sensitivity and resilience (Brierley & Fryirs, 2005; Gurnell et al., 2016; Brown et al., 2018) and to
86 support river restoration and management (Grabowski et al., 2014). In the context of the
87 Anthropocene, one of the major challenges is to isolate the role of natural and anthropogenic driving
88 forces on past and present river trajectories to anticipate future change. Local changes (flooding,
89 erosion, ecological alteration, water resource availability) must always be considered with an
90 integrated catchment perspective (Figure 1). Fluvial changes are not only driven by water and
91 sediment but also by changing vegetation and human interactions in a fairly complex system of
92 drivers, pressures, and impacts. The assessment of river status, trajectory and functioning requires a
93 space-time framework much broader than the one employed traditionally by river engineers and
94 managers. A complete understanding of fluvial trajectories cannot only come from the field, even if

95 geomorphology has a long tradition of field-based investigation, because of the temporal and spatial
96 limitations of field data. Understanding the Anthropocene is therefore intimately linked with remote
97 sensing (RS). Recent advances in remote sensing have produced a step-change in the spatial and
98 temporal scales of data that can be used to characterise the impacts of humans on river systems.

99 The science of remote sensing includes a range of techniques and methods to acquire
100 information about spatial objects (e.g. a river corridor and its associated features and characteristics)
101 and phenomena (river processes and changes) without any physical contact. It includes sensors
102 (digital cameras, video-cameras, thermal-, infra-red-, hyper-, multi-spectral sensors, Light Detection
103 and Ranging (LiDAR), Ground-Penetrating Radar (GPR), or geophones) mounted on platforms
104 (satellite, airborne, or even ground) (see details on Fluvial Remote Sensing in Carbonneau & Piégay
105 (2012) or more recent publications (Gilvear et al., 2016; Entwistle et al., 2018; Tomsett & Leyland,
106 2019). RS can help understand morphological trajectories because of new spatial and temporal
107 resolution and detection capabilities (e.g. applications of hyperspectral imagery or green-LiDAR).
108 The capabilities and spatial extent of these techniques have grown considerably since the early 2000s.
109 Piégay et al. (2015) highlighted a shift in the kind of tools used by geomorphologists to understand
110 river systems. Remote sensing acquisition has partly informed the “Great Acceleration” with data
111 archives, so we can increasingly work within a BACI (Before-After-Control-Impact) design (Green,
112 1979) based on robust hypothesis-driven protocols to assess changes and their drivers in comparative
113 settings. When used alone, most field techniques only allow a short temporal perspective and access
114 to a limited spatial context with no clear appraisal of processes occurring upstream or even laterally
115 (notably in forested or large river systems). Integrative approaches, where field data, archived
116 documentation (i.e. aerial photos, maps, topographic surveys) and remotely sensed information
117 (which can be programmed, planned, repeated, and archived) are combined allow fluvial
118 geomorphologists to widen their spatial and temporal perspectives. RS sensors are now largely
119 employed by river scientists in the field (e.g. Terrestrial Laser Scan; aerial photos from drones; ground
120 cameras, etc.) and RS data validation is usually based on intensive field surveys (See Carbonneau &
121 Piégay, 2012; Bizzi et al., 2016). In summary, remote sensing offers new opportunities based on: (i)
122 greater temporal resolution (i.e. repeated snapshots of the targeted landscape); (ii) larger spatial
123 extents; (iii) higher spatial resolution; and (iv) use of contactless or non-invasive techniques (i.e. not
124 disturbing the landscape).

125 Gilvear and Bryant (2016) in their early review on the application of remote sensing in fluvial
126 geomorphology highlighted that remote sensing is often the only way to obtain an “overall picture”
127 of river functioning at large scales. This overall picture is fundamental to understand channel
128 behaviour and changes, especially for the purposes of river planning and management frameworks,
129 as highlighted for instance in Europe by the Water Framework Directive. Even if existing
130 management-oriented frameworks are still mainly based on the acquisition of a large amount of local
131 in situ data and require specific expertise of the river catchments to derive large-scale interpretations,
132 they recognize the value and encourage the use of data and methods from remote sensing.

133
134 Societies are shaping and modifying the landscape to a degree that has never occurred in the
135 past. One of the key challenges for understanding remotely sensed rivers in the Anthropocene is to
136 use the new, rapidly evolving technologies which provide an unprecedented ability to observe and
137 understand the landscape. With this perspective in mind, we review research that investigates past,
138 present and future fluvial conditions and processes, and summarise insights and challenges for new
139 research.

140
141
142
143
144
145
146
147
148
149
150
151
152
153
154
155
156
157
158
159
160
161
162
163
164
165
166
167
168
169
170
171
172
173
174
175
176
177
178
179
180
181
182
183
184

Figure 1. General framework of geomorphic studies: diagnosis and project appraisal, top-down and bottom-up strategies (source: Piégay et al. 2016, chapter 22)

2. Remote sensing to explore past conditions within the Anthropocene

2.1. Data and methodological framework to diagnose river changes

Aerial photography

Reconstructing river trajectories requires the use of historical data, and especially remote sensing information (Grabowski & Gurnell, 2016). Early studies mostly relied on the use of oblique and vertical aerial photography in the visible domain. The use of remote sensing to explore past conditions starts with the advent of aerial photography around the 1930s, with mainly black and white images before the 1970s (Gilvear & Bryant, 2016). In many European countries, national aerial surveys were conducted with decadal frequency or even less from the 1950s (e.g. the historical archives of the French Geographical Institute: <https://remonterletemps.ign.fr/>).

Given the relatively coarse spatial resolution of early civilian airborne remote sensing data (typically from 5 to 0.5 m), the smallest spatial scale that can be characterized over time corresponds to river features (e.g. changes in flow channel areas, emerged bare ground units, islands or riparian vegetation; Toone et al., 2014; Lallias-Tacon et al., 2017). The 2D reconstruction of channel planform dynamics from historical aerial photographs, sometimes combined with historical maps, has largely improved our understanding of channel metamorphosis (*sensu* Schumm, 1969), meander migration and channel shifting (Hookes, 2003; Alber & Piégay, 2017). Early studies (e.g. Petts et al., 1989; Gurnell et al., 1994; Hooke, 2003) focused on 2D interpretation but did not quantify geomorphic work or sediment volumes, which limited the understanding of channel response. Historical aerial photographs have been used to detect channel changes in recent decades (e.g. Liébault and Piégay, 2002; Kondolf et al., 2007; Surian et al., 2009; Comiti et al., 2011; Arnaud et al., 2015; Marchese et al., 2017) to corroborate conclusions derived from traditional field-survey methods; to understand the causes of channel changes (Rollet et al., 2013; Grabowski & Gurnell, 2016; Bizzi et al., 2019); and to isolate human impacts on rivers since the 1950s, especially since the “Great Acceleration” of impacts in the Anthropocene era (Brown et al., 2017).

Satellites

Historical analyses of changing river systems now also use satellite products. Landsat TM multi-spectral data at 30 m resolution covers a temporal extent of 30 years (<http://landsat.usgs.gov>) but this is still limited to main river branches (Donchyts et al., 2016). Dewan et al. (2017) assessed channel changes of the Ganges-Padma River over 200 km and 38 years, and found significant channel shifting over the 1973-2011 period related to changes in the hydrological regime but no real geomorphic changes which may be attributed to upstream dams. Pekel et al. (2016) quantified

185 changes in surface freshwater globally using the entire Landsat 5, 7 and 8 archives over the past 32
186 years (1984-2015; ca 3 millions images). An increasing number of papers have recently been
187 published on channel changes based on such Landsat archives because the images are free of charge
188 and the temporal range is now sufficient to detect channel response to specific drivers (mainly
189 damming), in the case of responsive rivers.

190 Satellite images are becoming increasingly available with a resolution allowing users to
191 explore smaller riverine systems globally. However, with the exception of Landsat, the temporal
192 window covered by satellite data is still too short for historical analysis. Satellite imagery is therefore
193 accurate to characterize processes at an inter- and intra-annual scale, but not yet for detecting channel
194 changes over decades beyond last 30-40 years. [For longer channel temporal trajectories, or smaller
195 rivers, satellite records are insufficient.](#) Data can be supplemented by historical map data to extend
196 data records, as used by Ricaurte et al. (2012) to compare the contemporary and historical distribution
197 of vegetated islands in sections of the Danube, Rhine and Olt rivers.

198

199 *Complementary field data*

200

201 Remote sensing data can be complemented with more traditional field approaches to increase
202 the set of convergent evidence confirming changes in channel morphology and their drivers.
203 Historical hydrometric archives of stream gauging stations are commonly used to quantify long-term
204 changes in channel width, depth, and riverbed elevation, and to understand the driving processes
205 (James 1999, Stover & Montgomery 2001, Slater & Singer 2013, Phillips & Jerolmack 2016; Pfeiffer
206 et al., 2018). Long profiles are also available at regional or national scales, sometimes with historical
207 resources (Liébault et al., 2013). Additionally, time series of discharge and stage can be used
208 conjointly to estimate changes in channel depth and conveyance (e.g. Biedenharn & Watson, 1997;
209 Pinter & Heine, 2005). Finally, hydrometric data are increasingly being used to quantify the influence
210 of changes in channel conveyance on flood frequency (Slater et al., 2015).

211

212

213 2.2. Reach-scale changes

214

215

216 *Classical approach from airborne images*

217

218 A classic approach to analyze reach-scale channel adjustments over multiple kilometres is to
219 compile historical aerial photographs. Series of photographs are selected at least every ten years,
220 depending on the availability of archived photos and flood dates, and integrated in a GIS environment
221 to extract geomorphic variables, e.g. active channel width or sinuosity, gravel bar area (Gilvear et al.,
222 2000; Ollero, 2010; Michalkova et al., 2011; Rollet et al., 2013; Toone et al., 2014; Arnaud et al.,
223 2015; Lallias-Tacon et al., 2017; Scorpio et al., 2018) and landscape unit characteristics (e.g. Dufour
224 et al., 2015; Solins et al., 2018). Image georeferencing and vectorization of river features from
225 historical datasets are still mostly manual and time-consuming tasks which require real expertise. By
226 analyzing the temporal series of historical remote sensing data, we can detect discontinuities in the
227 spatio-temporal trajectories of rivers. Homogeneous sub-reaches in terms of magnitude of change can
228 be statistically delineated using tests for stationarity (Alber & Piégay, 2011; Roux et al., 2015). Aerial
229 photographs are also broadly used to study patterns of pioneer and woody riparian vegetation related

230 to regional/climatic factors and human disturbance, and link these changes with river pattern changes
231 to assess vegetation controls (Aguiar & Ferreira, 2005; Dufour et al., 2007; Kondolf et al., 2007;
232 Cadol et al., 2010; Dufour et al., 2012; Belletti et al., 2015; Surian et al., 2015; Kui et al., 2017; Safran
233 et al., 2017). Dépret et al. (2017) and Tena et al. (*in review*) analysed a set of aerial photographs from
234 different sites of the Rhône river and underlined effects of channel regulation on cutoff channel life
235 span and groyne field terrestrialization (Figure 2A). Decadal changes in species composition and
236 landscape configuration can also be surveyed with satellite images (Rodríguez-González et al., 2017).

237

238 *Added value of combining field and airborne data*

239

240 Archived aerial photos and field surveys can be used jointly to assess both planform and vertical
241 channel changes or vegetation properties. For example, Arnaud et al. (2015) exploited seven sets of
242 aerial photos and three cross sections series from the 1950s to the 2010s to quantify channel
243 narrowing/widening and bed degradation/flood terrace aggradation rates on the dammed Rhine River.
244 Belletti et al. (2014) assessed the influence of floods on riverscape organization of twelve braided
245 reaches (French Rhône basin) by using five archived aerial photos series and sediment regime
246 information from archived longitudinal profiles (Liébault et al., 2013). Sequences of archive images
247 and field measures of standing tree volumes have been also used to determine wood recruitment
248 through time and contribute to wood budgeting (Lassetre et al. 2008; Boivin et al. 2017). With the
249 emergence of new remote sensing technologies, it is now much easier to combine sequences of
250 archive imagery with topographic information, and to move a step forward towards the reconstruction
251 of 3D multi-decadal channel responses. For instance, sequential aerial photos since the 1940s-1950s
252 and present-day LiDAR data were combined to reconstruct floodplain formation and relate this with
253 vegetation properties along three alpine braided rivers in France (Figure 2B, Lallias-Tacon et al.,
254 2017). RS has also been used to estimate riverbank erosion volumes for different river reaches in
255 New Zealand (Spiekermann et al., 2017).

256 The time periods covered by national aerial photograph series are typically too short to explore
257 lowland rivers that are less responsive to change. In these larger river systems, RS data must be
258 combined with other data such as sedimentological information from coring or geophysics to access
259 information ranging from the medieval period to the 20th century (Vauclin et al., 2019).

260

261 *Figure 2. Temporal evolution of surface areas through time based on a series of aerial photographs:*
262 *(A) example of the terrestrialisation of the natural (dashed line) and artificial (thick line) abandoned*
263 *channels of the Rhône River – Grange Ecrasée is the only one case of expansion right after cut-off*
264 *and then shrinking (Source: Figure 1, Dépret et al. 2017, Geomorphology) (B) reconstruction of bed-*
265 *level evolution of a small alpine gravel-bed stream from the combination of historical aerial*
266 *photographs (from 1948 to 2010) and a recent airborne LiDAR survey (2010) (modified after Lallias-*
267 *Tacon et al., 2017); historical aerial photographs have been used to date recent terraces, and*
268 *airborne LiDAR data to extract elevation differences between dated terraces to reconstruct the*
269 *floodplain formation history*

270

271 Vertical information can also be derived directly from archived aerial photographs using digital
272 photogrammetry (Lane, 2000; Gilvear & Bryant, 2016; Bakker & Lane, 2017). For example, Carley
273 et al. (2012) assess post-dam channel changes by combining elevation contour maps acquired from
274 aerial photogrammetry, *in situ* bathymetric surveys, and point cloud models acquired from a total
275 station (TS). On the other hand, geomorphic metrics extracted from archived aerial photographs or

276 3D bed topography offer input/validation data for linking hydraulic modelling with channel change
277 (Santos et al., 2011; Gilvear & Bryant, 2016; Serlet et al., 2018). However, extracting channel change
278 information from archived data (e.g. old aerial photographs) is not straightforward and requires an
279 assessment of error production and propagation to allow its application for quantitative geomorphic
280 analysis (James et al., 2012; Bakker & Lane, 2017). For example, it has been demonstrated that SfM
281 data processing of historical air photos of braided channels can produce a quality of information
282 equivalent to classical photogrammetric approaches, provided that image texture and overlap are
283 sufficiently high for tie-point detection and matching (Bakker and Lane, 2017). However, the
284 persistence of systematic centimetre- to decimetre-scale elevation errors after coregistration of point
285 clouds indicates that topographic differencing using SfM processing of archival imagery is still
286 limited for the quantitative analysis of sediment budgets.

287 The integration of large-scale historical data (beyond remote sensing) is often used to better
288 contextualise reach-scale changes within a catchment and landscape context. For example, Ziliani
289 and Surian (2012) combine catchment-scale datasets on river pressures (e.g. bank protection,
290 sediment mining, chronology and location of torrential control works), RS-derived information (land
291 use changes), historical maps, and aerial photos to disentangle the contribution of local vs. large-scale
292 drivers in the evolutionary trajectory of channel morphology along the nearly-natural Tagliamento
293 river (north-western Italy).

294

295

296 2.3. Regional network changes

297

298 Reach-scale river trajectory assessment, combining field data, manual editing of historical
299 remotely sensed information and qualitative expert-based interpretation of process evidence, is a
300 research challenge that requires careful harmonization and consistency when implemented at regional
301 or network scales (several thousands of km of river length). Two strategies are usually implemented:
302 i) assessing inter-reach differences at the network scale to infer controlling factors, ii) observing
303 continuous network changes.

304

305 *Assessing inter-reach differences at the network scale to identify controlling factors*

306

307 Past evolutionary trajectories can be explained, and future trajectories can sometimes be
308 predicted, through *location-for-time* substitution which infers a temporal trend from a study of
309 different aged sites, permitting regional assessment of channel changes (Pickett, 1989; Fryirs et al.,
310 2012) or *location-for-condition* evaluation allowing to identify factors explaining observed changes.
311 This *location-for-time* approach builds on the well-known channel-evolution model of Schumm et al.
312 (1984) and Simon and Hupp (1986). Such historical large-scale studies are usually based on relatively
313 few observations (at best decadal), mainly aerial photos (e.g. Belletti et al., 2014), manually digitized
314 historical maps (Scorpio et al., 2016; Meybeck & Lestel, 2017) or a combination of aerial photos and
315 maps (e.g. Surian et al., 2009). Regional active corridor changes are estimated through *location-for-*
316 *condition* evaluation by sampling a set of river reaches or river features within a hydrographic
317 network which can be compared in space and time (Belletti et al., 2015). The approach mainly
318 consists in combining present remote sensing data and spatially distributed historical information
319 within a catchment to interpret controls of present channel conditions. Belletti et al. (2015) explored
320 active channel width evolution between the 1950s-2000s in French braided rivers that showed general

321 narrowing in the northern reaches versus more complex patterns in the southern reaches. Applying
322 the *location-for-condition* evaluation, Bertrand and Liébault (2019) studied the impact of nickel
323 mining activities on the river beds in New Caledonia by comparing the spatial patterns of present
324 active channel width normalized by the catchment area in a set of undisturbed versus impacted
325 reaches, identified on recent orthophotos. They demonstrated that the increase in coarse sediment
326 supply induced sediment waves which propagated from the major mining sources, widening and
327 aggrading active channels along the stream network. An advanced approach in this domain by
328 Liébault et al. (2002) showed from Co-inertia Analysis that differences in channel changes in twenty
329 mountain streams (channel narrowing, bed degradation and armouring) were largely controlled by
330 watershed morphometry and land use, permitting to better understand sub-catchment sensitivity to
331 change. Recently, Alber and Piégay (2017) predicted potential bank retreat at an entire network scale
332 from stream power and active channel width based on a set of sites/observations where bank retreat
333 was assessed over a 50-year period from two series of aerial photos.

334

335 *Observing continuous network changes*

336

337 This second approach has become possible in the last ten years thanks to a better temporal and
338 spatial resolution in remote sensing data. It relies on the integration of optical, multi-spectral
339 (orthophotos or satellite images) and topographic (LiDAR) data. Macfarlane et al. (2017) combined
340 Landsat imagery and a modelled estimate of pre-European settlement land cover, and showed, over
341 50,000 km of rivers, that 62% of Utah rivers and 48% of the Columbia River Basin network exhibited
342 significant differences in riparian vegetation compared to historic conditions due to land-use impacts
343 and flow and disturbance regime changes. Bizzi et al. (2019) derived in the Piedmont river network
344 (Italy) historical and current hydraulic scaling laws by integrating a recent regional geomorphic
345 database based on remotely sensed datasets (Demarchi et al., 2017), sparse historical field
346 measurements of channel cross sections, and evidence from unaltered river systems in similar Alpine
347 regions in France (Figure 3) (Piégay et al., 2006; Gob et al., 2014). It has long been recognized that
348 past changes in channel characteristics can be used to predict long-term trajectories of channel
349 morphology. Comparing these relationships with present channel measurements provides an
350 indication of the level of channel modification at the regional scale due to human pressures over the
351 last century. Such approaches are promising for understanding river evolution over much larger scales
352 in the future.

353 Historical maps are rare and not so widely used as additional layers to quantify temporal
354 changes at a regional level because of limitations (geometric distortion, simplified representation of
355 features, notably the hydrography) (Dunesme et al., 2018). But there are some opportunities in
356 countries such as Switzerland or Belgium that have very good historical map resources covering the
357 19th century and for which automatic vectorization is possible (Horacio et al., on line).

358

359 *Figure 3. Classes of channel changes combining incision and narrowing based on regional LiDAR,*
360 *aerial photos and field/archived data to established reference: severe changes indicate significant*
361 *narrowing (>50-100% of their current width) and riverbed incision (2-5 m) over the last century,*
362 *moderate changes indicate mostly river reaches that show substantial narrowing and moderate*
363 *channel incision (source: Figure 12, Bizzi et al., 2018 in ESPL)*

364

365

366 **3. Remote sensing to identify patterns and acting processes**

367 368 3.1 Characterizing rivers from ground, sky, and space

369

370 Remotely sensed approaches of river systems can be classified according to the scale of
371 observation, ranging from ground-based and close-range surveying techniques to airborne and
372 spaceborne platforms (Table 1).

373

374

375 *Ground-based and close-range surveying techniques*

376

377 Field-based approaches in fluvial geomorphology increasingly use terrestrial remote sensing
378 to survey the topography and to measure the fluxes of water, sediment or wood passing through a
379 river section. For example, Terrestrial Laser Scanning (TLS) is now commonly employed to produce
380 dense 3D point clouds of river channels (e.g. Milan et al., 2007; Heritage & Milan, 2009; Hodge et
381 al., 2009). Although this technique is mostly used at scales ranging from small gravel patches to short
382 channel reaches of several hundreds of metres, combining TLS with mobile platforms allows for
383 coverage of several kilometres of non-wetted area in complex river channels (Williams et al., 2014).
384 Time-lapse cameras (Džubáková et al., 2015), video recordings (Le Coz et al., 2010; MacVicar &
385 Piégay, 2012), seismic sensors (Burtin et al., 2016) or active RFID tracers (Cassel et al., 2017) are
386 now in the modern toolkit for the ground-based observation of fluvial forms and processes. The main
387 limitation of ground-based observations remains the small spatial coverage of investigation.

388

389 *Airborne techniques*

390

391 Airborne surveys can be made using a range of platforms, from the most affordable and flexible ones
392 (poles, lighter-than-air balloons or blimps, small Unmanned Aerial Vehicle (UAV) also called
393 Unmanned Aerial Systems (UAS)) to manned aircraft (ultralight trikes, helicopters, planes) (Figure
394 4). Blimps (Vericat et al., 2009; Fonstad et al., 2013) and poles (Bird et al., 2010) used to get high
395 resolution images in short river reaches, typically less than 1 km in length, are particularly appropriate
396 in narrow river channels partially or totally masked by forest canopy. UAVs can more easily cover
397 several km of wide river reaches (e.g. Woodget et al., 2015; Vázquez-Tarrío et al., 2017). Airborne
398 observations allow for the investigation of larger spatial scales with constraints of flight duration,
399 optical properties of the sensor and flying height of the platform. In co-evolution with UAV and
400 ultralight trikes, Structure from Motion (SfM) photogrammetry has largely resolved the issue of
401 image orthorectification and Digital Elevation Model (DEM) production (James & Robson, 2012;
402 Westoby et al., 2012; Fonstad et al., 2013). Such low-cost platforms are usually equipped with
403 commercial digital cameras, with varied configurations and technical options as technology is rapidly
404 evolving (Marcus & Fonstad, 2010; Bertoldi et al., 2012; MacVicar et al., 2012; Entwistle et al.,
405 2018). More recently, there is a growing availability of drones equipped with real-time kinematic
406 (RTK) GPS allowing for cm accuracy positioning of the imagery. The popular Phantom series of
407 drones produced by DJI inc. now has a model equipped with such RTK-GPS technology and the cost
408 is of approximately 7000 € (in early 2019). This technical development should further enhance the
409 ease of use of UAVs for geomorphological investigations. As a consequence of these key
410 technological advances, published papers on the use of UAVs in river settings have appeared at an

411 accelerated pace with a Google Scholar search for keywords ‘UAV River’ returning over 9000 items
412 published since 2015. Drones are now equipped with LiDAR sensors, multi- and hyper-spectral
413 sensors, even RFID tracking technology (Cassel et al., *in review*).

414 However, we note that this rapid growth of technologies with increasing levels of automation
415 has not been without negative effects. In the case of SfM-photogrammetry, the major drawback of
416 the high levels of automation has in fact been a net loss, or at the very least a stagnation in growth, of
417 photogrammetric expertise in the geomorphology community. Modern softcopy SfM-
418 photogrammetry packages will often deliver visually stunning results and extremely high data
419 volumes irrespective of the quality of the input data. Since it is increasingly difficult to validate a
420 significant percentage of these outputs with field data, they are too often accepted as good without
421 detailed examination. After the appearance of the first papers on the topic of SfM in 2012/2013, it
422 has taken several years and multiple contributions to recognise that SfM-photogrammetry, whilst still
423 strongly rooted in photogrammetry, requires its own expertise. The best example is the debate around
424 optimal flight patterns and camera calibrations. Given that nadir image acquisition had been the norm
425 in the first 50 years of photogrammetry, SfM-photogrammetry acquisitions initially employed this
426 approach. But some early papers (Wrackow and Chandler 2008, 2011; James and Robson 2014;
427 Woodget et al., 2015) started to document a doming deformation whereby the centre of a digital
428 elevation model produced with SfM-photogrammetry was either depressed or elevated along a
429 parabolic shape. The simulation work of James and Robson (2014) and laboratory experiments of
430 Wrachow and Chandler (2011) further demonstrated that this doming deformation was due to poor
431 camera calibration due to the exclusive use of nadir imagery. It is now well recognised that for SfM-
432 photogrammetry with low-cost cameras, the acquisition of off-nadir imagery with convergent views
433 is critical. Significant photogrammetric expertise is required to correctly adapt SfM technology to a
434 geomorphic context. This is also true for hardware. UAV-based LiDAR systems are now increasingly
435 common; however, anecdotal evidence (Lejot, *pers. comm.*) suggests that getting these systems to an
436 operational state is not straightforward. Once again, very significant technical expertise is required.
437 Overall, airborne acquisition technology has advanced considerably, but potential users must be
438 aware that significant expertise and time is still a critical requirement for successful deployment of
439 these technologies.

440

441

442 *Spaceborne techniques*

443

444 For working at larger spatial scales, satellite images are also becoming an important source of
445 data. Since the advent of multi-spectral satellite images (around the late 1970s for the Landsat TM),
446 satellites provide access to further information derived from electromagnetic radiation that is
447 complementary to field-based data or aerial photographs, mainly for large rivers (e.g. Salo et al.,
448 1986; Henshaw et al., 2013). Landsat 7 and 8 with images at 15 and 30 m resolution and a revisit
449 capacity of 16 days are often used at large scales, e.g. for characterizing thermal patterns
450 (Wawrzyniak et al., 2016) or channel morphology (Xie et al., 2018). Early work using Landsat-5
451 images focused on channel migration in the Peruvian Amazon (Salo et al., 1986). The main advantage
452 is that these images are globally available and free of charge to users. If metric-scale resolutions are
453 required, commercial satellite products become the only option. SPOT 5 imagery has been used
454 associated with LiDAR and Very High Resolution (VHR) QuickBird images to map riparian zone
455 features (Johansen et al., 2010). Since 2015, SPOT 6 and 7 programs now offer daily images at 1.5

456 m in panchromatic mode. The Pleiades program (launched in 2011-2012) produces daily images at
457 70 cm resampled at 50 cm which have been used to map aquatic areas in river corridors and assess
458 their spatial extent according to discharge (Wawrzyniak et al., 2014). These data sources provide
459 VHR images but the acquisition costs can be particularly high for large scale or multitemporal studies.
460 In recent years, there has been an increase in the number of studies using Sentinel images both in
461 visible, infrared and radar domains (e.g. Spada et al., 2018 who combine data from the CORONA,
462 Landsat and Sentinel-2 missions) that are publicly-accessible and provide high spatial resolution (10
463 to 60 m) images in Europe every 5 days (if no cloud), or weekly or sub-monthly, at the global scale.
464

465 Over the past few decades, geomorphologists have advocated for an increase in spatial
466 resolution whereas now, some of the geomorphic questions are solved when resolution is reduced
467 (e.g. channel bathymetry from radiometric information). An issue is then to determine the optimal
468 resolution and level of change detection for solving geomorphic questions.
469

470 In recent years, satellites have increased in spatial resolution (reaching sub-meter scales) and
471 frequency of acquisition (sub-weekly acquisition), collecting multispectral and radar information and
472 in some cases (such as Pleiades) stereoscopic datasets for topographic/DEM reconstruction. We are
473 entering an era where river channel planforms and processes can be observed and classified from
474 satellites almost weekly for large rivers worldwide. This opportunity requires specific and
475 interdisciplinary expertise as well as access to funding/resources to be properly realized. For this
476 reason, this new satellite information has not yet produced a concrete advance in river process
477 understanding. Remote sensing derived information has so far mostly been used to test existing
478 concepts and their range of applications, rather than for generating new concepts or theory. The time
479 has come to translate our request for data (now partially satisfied) into efforts to use this data to pose
480 specific research questions to advance fluvial geomorphology scientific understanding.
481

482 *Figure 4. Example of platforms used by scientific teams to acquire hyperspatial imagery: A)*
483 *Octocopter ; B) Hexacopter equipped with an active RFID antenna; C) Ultralight trike equipped with*
484 *RGB and thermal cameras; D) Unmanned Control Helicopter (Sources : A) Kristell Michel; B)*
485 *Mathieu Cassel; C) Baptiste Marteau and D) Philippe Grandjean)*
486

488 3.2. Detection and characterization of fluvial forms and their attributes

489 *Grain size and shape measurement*

491
492 The grain-size distribution (GSD) of river channels is critical for understanding the interactions
493 between hydraulics, sediment transport, and channel form, and for the characterization of physical
494 habitats. Investigations of the spatial variability of river sedimentology is at the core of many works
495 dedicated to sediment sorting patterns and processes of fluvial environments (e.g. Dietrich et al.,
496 1989; Rice & Church, 1998; Guerit et al., 2014). Collecting data about surficial GSD has been for a
497 long time only possible through laborious and time-consuming field samplings, such as the well-
498 known pebble count protocol (Wolman, 1954). Remotely-sensed solutions started to emerge in the
499 late 1970s, with the development of “photo-sieving” image analysis tools. Initially, photosieving
500 methods relied on manual measurement of clasts visible on images taken from the ground (e.g.
501 Adams, 1979; Ibbeken & Schleyer, 1986). Later solutions became based on the automatic

502 segmentation and size extraction of single particles on close-range images of gravel patches (Butler
503 et al., 2002; Graham et al., 2005 a and b; Detert & Weitbrecht, 2012). At similar scales, other methods
504 started to emerge which relied on statistical properties of images. Image-based sedimentological
505 extraction initially used a grain-size calibration with image texture, semivariance or entropy (e.g.
506 Carbonneau et al., 2004; Tamminga et al., 2015; Woodget et al., 2018). Wavelet analysis and
507 autocorrelation have also been demonstrated as being capable of extracting grain-size information
508 from imagery (Rubin, 2004; Buscombe, 2008; Buscombe & Masselink, 2009; Buscombe et al., 2010).
509 Chardon et al. (*in review*) tested the automatic Buscombe procedure on underwater images and
510 showed solar lighting conditions and particles petrography influence significantly the GSD. They
511 proposed procedures to correct these effects and determine the optimal sampling area to accurately
512 estimate the different grain size percentiles when using such a technique, which is still the only
513 accurate approach to characterize grain size underwater. Similar approaches would later be applied
514 to airborne data in order to extend the spatial coverage of remotely sensed grain size mapping
515 approaches (Figure 5).

516 As an alternative, the 3D point cloud-based technique uses roughness metrics to approximate
517 grain-size (e.g. Heritage & Milan, 2009; Brasington et al., 2012; Vázquez-Tarrío et al., 2017). Only
518 few recent works proposed a comparison between these techniques. Woodget et al. (2018) tested a
519 2D image texture approach and a 3D topographic roughness approach in a small gravel-bed river in
520 UK and obtained a better grain-size prediction with the 3D approach. However, another field
521 experiment showed that the texture of single UAV images is more efficient than 3D roughness metrics
522 for grain-size prediction, provided that UAV images are acquired with a mechanical stabilization
523 system (gimbal) to avoid blurring effect (Woodget et al., 2018). First attempts to predict grain-size
524 with 3D point clouds were based on local standard deviation of elevations which were determined by
525 scale-dependent submeter kernels (Entwistle & Fuller, 2009; Heritage & Milan, 2009). More recent
526 works demonstrated that detrending the local micro-topography (e.g. bank slope, edges of gravel bars)
527 before computing the roughness metrics is crucial for grain-size prediction (Brasington et al., 2012;
528 Rychov et al., 2012; Vázquez-Tarrío et al., 2017).

529 Recently, Carbonneau et al. (2018) demonstrated a method that leverages Direct
530 Georeferencing (DG) in order to roboticize the grain-size mapping process. By using the on-board
531 GPS of a drone, and by flying at very low altitudes (below 10 m), the authors demonstrated that drone
532 images could be combined in a DG workflow which uses particle recognition software. As a result,
533 the method of Carbonneau et al. (2018) allows a drone to act as a fully autonomous robotic field
534 worker that measures grain-size data over local areas. With the advent of hyperspatial remote sensing
535 solutions at larger scales, grain-scale information can now cover entire river reaches of several
536 kilometres in length. The airborne LiDAR topographic survey can also accurately generate grain-size
537 maps when the point density is high (38 to 49 points/m², mean distance between points of 0.08 m to
538 0.09 m) and the laser spot size fairly low (0.12 m at NADIR; see Chardon et al., *in review*),
539 comparatively to observed grain sizes, allowing to cover areas much larger than with drones.

540

541

542 *Figure 5. Long profile of median grain size over 80 km of the Sainte Marguerite River, Québec from*
543 *image processing and showing link cutoff points (vertical lines), numbered 1–8 as determined by*
544 *Davey and Lapointe (unpublished report, 2004) and an example of an “error column” structure*
545 *caused by glare at the water surface (Source: Carbonneau et al., 2005, Figure 5.).*

546

547 The study of longitudinal grain shape evolution helps understand the downstream fining and
548 rounding processes and enhances our ability to decipher the transport history of river sediment
549 (Domokos et al., 2014; Litty and Schlunegger, 2016) and interpret gravel provenance (Lindsey et al.,
550 2007) (Figure 6). From traditional field measures which emerged in the 1930s (Wadell, 1932), image
551 processing and Fourier grain shape analysis were used in the 1990s in the first attempts to
552 automatically measure particle shape and roundness (Diepenbroek et al., 1992). This approach was
553 further developed in the late 2000s using automatic ground imagery procedures to get a set of
554 roundness and shape indexes and explore spatial patterns at reach to network scales (Roussillon et
555 al., 2009; Cassel et al., 2018). A digital approach has been also proposed to estimate roundness of
556 individual particles using 3D laser scanner, but it is still at an experimental level without in situ results
557 (Hayakawa and Oguchi, 2005). Using a large set of SfM field data, Pearson et al. (2017) highlighted
558 effects of particle shape or grain packing structure on roughness/grain-size relationships, opening
559 new issues to potentially characterize particle shape from imagery without sampling particles and
560 disrupting the bed surface. However, particle roundness characterization needs an accurate detection
561 of particle boundaries, therefore such measurement is still difficult to imagine without field sampling.

562
563 *Figure 6. (A) Evolutions of the ratios of perimeters rP according to the distance travelled through 36*
564 *km from the headwater of Progo river (Indonesia) (dark grey) or in an annular flume (red). $rP =$*
565 *P_g/P_e with P_g the pebble perimeter and P_e the ellipse perimeter, both having the same surface area.*
566 *The single clear grey boxplot with red borders represents values distributions of rounded pebbles*
567 *which were collected 30 km downstream the Progo spring Boxplots represent distributions of shape*
568 *parameter values at a given distance and provide 10th, 25th, 50th, 75th and 90th percentiles values.*
569 *White circles represent median values. (B) Example of picture of angular pebbles taken for roundness*
570 *analysis. (Source: Cassel et al., 2018, Figure 11 and Figure 3).*

571

572

573 *Bathymetry and water depth*

574

575 Water depth is arguably the most fundamental parameter in fluvial morphology and has been
576 the topic of considerable work in fluvial remote sensing. We can distinguish three main approaches
577 to water depth mapping: radiometric depth retrieval, direct measurement with photogrammetry and
578 active measurements with bathymetric LiDAR. Radiometric depth retrieval uses the Beer-Lambert
579 law of absorption and correlates the brightness levels in an image with the depth of water. Crucially,
580 the bottom of the river must be clearly visible. This empirical approach has been frequently used and
581 reported (Winterbottom and Gilvear, 1997; Marcus, 2002; Fonstad and Marcus, 2005, Carbonneau et
582 al., 2006). In these cases where the stream is clear, the full bathymetry of the channel can be retrieved
583 with photogrammetry either using a classic approach (Westaway et al., 2003; Fuerer et al., 2008;
584 Lane et al. 2010), or a SfM approach (Woodget et al., 2015, Dietrich 2016). Finally, bathymetric
585 LiDAR using a green laser has been in use for several years and is now available for deployment in
586 rivers using manned airborne platforms (e.g. Kinzel et al., 2007; Bailly et al., 2010; Legleiter et al.,
587 2015). However, readers should note that all these methods suffer from the same limitation: water
588 clarity. Radiometry and photogrammetry methods must have a clear view of the riverbed and are
589 therefore limited to very low-levels of turbidity and suspended sediment. Active methods based on
590 LiDAR are somewhat more robust since a laser pulse is capable of penetrating turbid water, but in
591 practice, the increased signal noise caused by suspended particles means that the improvement is

592 marginal. Ultimately, ground remote sensing with intensive measurements from boat are the only
593 way to obtain accurate depth predictions for heavily turbid flows.

594
595 *Characterization of fluvial corridor features: from reach to network and global scales*

596
597 At the reach scale, river corridors can be seen as complex mosaics of distinct spatial units
598 resulting from interactions between sediment, water, and vegetation. Fryirs & Brierley (2012) define
599 these landforms as the “building blocks” of the fluvial mosaic, but other terms have been proposed,
600 like geomorphic units, hydraulic units, physical habitats, meso-habitats or biotopes (Milan et al.,
601 2010; Wyrick et al., 2014; Wheaton et al., 2015; Belletti et al., 2017). Some recent works combine
602 multisource remote sensing data from different sensors to better classify, characterize, and model
603 these building blocks (Bertoldi et al., 2011; Legleiter, 2012; Williams et al., 2014; Wyrick et al.,
604 2014; Demarchi et al., 2016), as well as their physical properties, such as temperature (Wawrzyniack
605 et al., 2016).

606 Reach-scale features are traditionally mapped by means of expert-based approaches based on
607 interpretation of available imagery, which may be used in complement with high resolution
608 topography (e.g. Dietrich 2016). Topographic and morphometric signatures can be systematically
609 extracted from high resolution DEMs, allowing the prediction of fluvial landscape features such as
610 channel heads (Clubb et al., 2014), floodplains and terraces (e.g. Clubb et al., 2017), morphological
611 units (Cavalli et al. 2008) or river reach features (Schmitt et al., 2014). Automatic or semi-automatic
612 algorithms to map river features started to emerge recently to improve the reproducibility of mapping
613 products, and to reduce the time for mapping. Image classification is often a first step required to
614 focus the application of algorithms to specific features in the image. To this day, a cost-effective
615 method for classifying river features is still lacking and the first step of data processing is often one
616 of the most laborious. Over the last decade, Object Based Image Analysis (OBIA) has slowly
617 developed as a step change allowing for enhanced image classification (Blaschke, 2010; Blaschke et
618 al., 2014). In contrast, the rapid developments in machine learning, deep learning and artificial
619 intelligence are now beginning to cross-over in the environmental sciences. Casado et al. (2015)
620 demonstrated that a low-complexity, shallow, artificial neural network (i.e. a multilayer perceptron)
621 was capable of identifying geomorphic features in a short river reach with an accuracy of 81%.
622 Recently, Buscombe and Ritchie (2018) use a large dataset to demonstrate that a convolutional neural
623 network (CNN) could be adapted to fluvial imagery in order to classify images and report mean F1
624 scores ranging from 88% to 98%. Carbonneau et al. (*in revision*) developed a novel approach dubbed
625 ‘CNN-Supervised Classification’ which uses a pre-trained convolutional neural network to replace
626 the user input in traditional supervised classification. They report mean F1 scores ranging from 90%
627 to 98%. The result of 90% reported in Carbonneau et al. (*in revision*) is for rivers that were never
628 seen by the classifier during the training phase. This suggests that deep learning could deliver a quasi-
629 universal classifier capable of matching human performance when visually establishing the semantic
630 classes of a river image.

631 In the case of vegetation and the riparian zone, the last years have seen significant gains in
632 terms of resolution and detail (Bertoldi et al., 2011; Dufour et al., 2012, Kasprak et al., 2012;
633 Abalharth et al., 2015; Atha & Dietrich, 2016). The ability to identify vegetation composition,
634 including at species scale, and to describe vegetation structure has greatly increased (Kaneko &
635 Nohara, 2014; Riedler et al., 2015; Husson et al., 2016; Michez et al., 2016; Bywater-Reyes et al.,
636 2017; Hortobágyi et al., 2017; Loicq et al., 2018). This is due to the integration of structural

637 information provided notably by LiDAR data (Charlton et al., 2003; Farid et al., 2006; Antonarakis
638 et al., 2008; Geerling et al., 2009; Johansen et al., 2010; Michez et al., 2017; Laslier et al., 2019a).
639 Indeed, LiDAR data can be used at the reach scale to assess vegetation roughness (Straatsma &
640 Baptist, 2008), to monitor vegetation volume changes following a flood event at a very fine scale
641 (Milan et al., 2018), to identify tree genera at individual scale (Ba et al., 2019), and many other
642 attributes such as vegetation height, crown diameter canopy closure, vegetation density, age class or
643 stream shading (Michez et al., 2017; Laslier et al., 2019a). The ability to identify vegetation
644 composition, including at species scale, has been also greatly increased with the development of
645 hyperspatial (Kaneko & Nohara, 2014; Husson et al., 2016; Michez et al., 2016; Bedell et al., 2017,
646 Laslier et al., 2019b) and hyperspectral data (e.g. Peerbhay et al., 2016; Rodríguez-González et al.,
647 2017). Mapping efforts from remote sensing data also detect specific features such as instream wood
648 distribution (Atha, 2014; Ulloa et al., 2015), wood deposits (Marcus et al. 2002, 2003) or instream
649 wood characteristics and volumes in riverine environments (Boivin & Buffin-Bélanger, 2010; Tonon
650 et al., 2014).

651

652

653 *Figure 7. Riparian genres map obtained from LiDAR data and tree morphological patterns (Sélune*
654 *River, western France). Tree crown morphology and internal structure indicators were computed*
655 *from the 3D points clouds of two surveys (summer and winter; n = 144 indicators) and the most*
656 *discriminant indicators were selected using a stepwise Quadratic Discriminant Analysis allowing the*
657 *number of indicators to be reduced to less than 10 relevant indicators. The selected indicators were*
658 *used as variables for classification using Support Vector Machine. Overall accuracy ranges from*
659 *80% for 3 genres to 50% for 8 genres. With 8 genres, the identification remains a challenge as*
660 *for one tree crown predicted pixels can be mixed (Source: Ba et al., 2019)*

661

662 In recent decades, important efforts have been made for network-scale mapping of fluvial
663 environments (Alber & Piégay, 2011; Demarchi et al., 2016) and riparian zones (Goetz, 2006;
664 Johansen et al., 2007; Clerici et al., 2014; Michez et al., 2017). Notebaert and Piégay (2013) studied
665 the present variability of floodplain width in the entire Rhône basin by combining digital terrain
666 models, historical maps and other GIS layers (hydro-ecoregions, geological maps). They highlighted
667 the contribution of inherited landscapes from tectonic processes and glaciations. Such approaches
668 have also been used to map geomorphic units using aerial infrared orthophotos only (Bertrand et al.,
669 2013a) or combined with LiDAR DEM (Demarchi et al., 2017). Another example is the method for
670 regional scale automatic mapping of unvegetated patches in headwater catchments based on an
671 object-based image analysis of infrared orthophotos and Landsat 7 ETM+ images developed by
672 Bertrand et al. (2017). This has been successfully applied in the Southern French Alps to assess
673 regional-scale sediment supply conditions in relation to debris-flow triggering, and more recently to
674 link suspended load hysteresis patterns and sediment sources configuration in alpine catchments
675 (Misset et al., 2019). Concerning the riparian zone, the method can be used from large scale
676 delineation of buffers to the description of the zone characteristics at watershed to continental scales
677 (Johansen et al., 2010; Clerici et al., 2014; Cunningham et al., 2018). Fine scale approaches now
678 extend to the network scale. Michez et al. (2017) compared rivers of different regions in Belgium
679 based on the ratios of channel width and depth to the basin area.

680

681 *Figure 8. Workflow of the multilevel, object-based methodology developed for the classification of*
682 *riverbank units and in-stream mesohabitats. Top row shows data type used (multispectral and Lidar*
683 *derived DTM); central row describes the OBIA steps to derive topographically and spectrally*

684 *homogenous units; the bottom row displays classification results for riverscape units (on the left) and*
685 *mesohabitats (on the right). (Source: Demarchi et al. 2016 Figure 5)*

686

687 Comprehensive, systematic analyses of the different predictors of fluvial patterns, as well as
688 predictions of future channel evolution (if any of these predictors are altered), may now be achieved
689 at a global level, at least for medium-size rivers, using existing pre-processed, remotely-sensed
690 archives and platforms. For instance, the Global Width Database for Large Rivers (GWD-LR)
691 contains channel widths between 60S and 60N extracted using the SRTM Water Body Database
692 (Yamazaki et al., 2014). Considerable advances may be achieved by using global archives to
693 interrogate or predict channel form, e.g. using remotely-sensed measurements of global surface water
694 (Pekel et al., 2016), global river widths extracted from gauging stations worldwide (Allen & Pavelsky,
695 2018), or a global geospatial river reach hydrographic information database (including river networks,
696 watershed boundaries, drainage directions, and flow accumulations) derived from SRTM high-
697 resolution elevation data (HydroSHEDS; Lehner et al., 2008). Recently, a Global River Classification
698 (GloRiC) database has been built on such global archives (Ouellet Dallaire et al., 2019). Global River
699 Classification (GloRiC) database provides 127 river reach types for all rivers globally, based on
700 variables such as hydrology, physiography and climate, fluvial geomorphology, water chemistry and
701 aquatic biology (Ouellet-Dallaire et al., 2019). Pan-European riparian corridors have been generated
702 also (Weissteiner et al., 2016).

703

704

705 3.3. Fluvial processes: from decadal landform changes to real time observations

706

707 The notable advances in fluvial remote sensing during the last two decades have been
708 particularly helpful for the investigation of channel responses to environmental driving forces in a
709 very large variety of physical settings, and for the assessment of fluvial processes.

710

711

712 *Riverscape changes*

713

714 Landform changes (sediment erosion, deposition, channel shifting) investigated at decadal scales are
715 now approached at inter-annual or even event-based scales. Until the mid 1990s, when the first high-
716 resolution DEMs of river channels have been reported (Lane et al., 1994; Lane et al., 1995), it was
717 only possible to constrain erosion and deposition processes acting in river channels by using time-
718 consuming repeated terrestrial topographic surveys, generally along predefined monumented cross-
719 sections positioned at regularly-spaced intervals along river reaches. With the advent of modern
720 topographic surveying solutions, it is possible to rapidly cover several km of river reaches with dense
721 3D point clouds of high accuracy and precision. LiDAR surveys (ground-based or airborne) and SfM
722 photogrammetry are the two technological solutions available for a rapid and continuous topographic
723 survey of river channels. Both solutions offer comparable precision, accuracy, and density of
724 information for unvegetated and exposed terrains (a compilation of precision and accuracy values for
725 airborne LiDAR datasets in gravel-bed rivers is available in Lallias-Tacon et al., 2014), but with
726 LiDAR, it is possible to capture the topography of vegetated surfaces, provided that the density of the
727 vegetation cover is not too high (e.g. Charlton et al., 2003). The most recent advances in LiDAR
728 technology also offer the possibility to combine different LiDAR wavelengths to capture during the

729 same flight the topography of exposed and submerged surfaces of river channels (Mandlbürger et al.,
730 2015), which can be a decisive advantage for large river channels. Case studies making use of
731 sequential and distributed high-resolution remote sensing data to reconstruct short-term channel
732 changes are now common in the literature (see recent review from Vericat et al., 2017). Differential
733 topography based on sequential LiDAR or SfM datasets is used to produce distributed maps of erosion
734 and deposition of channel reaches, to use this information to reconstruct sediment budgets, and also
735 to back-calculate bedload transport using the morphological approach (Passalacqua et al., 2015;
736 Vericat et al., 2017; Antoniazza et al., 2019). The order of magnitude of detectable elevation changes
737 with those data is generally around 10–20 cm, but this depends on the sensor accuracy or flight height
738 as well as the properties of the investigated surfaces. Several studies document the negative effect of
739 vegetation, local slope, and surface roughness on the level of detection of topographic change in river
740 channels (e.g. Wheaton et al., 2010; Milan et al., 2011; Lallias-Tacon et al., 2014). It is also
741 recognized that these data need a careful inspection and correction of systematic errors in spatial
742 positioning or elevation before computing a sediment budget, as this error may have a strong impact
743 on the integrated volumes of sediment erosion and deposition (Anderson, 2019). Stable areas may be
744 used to evaluate the systematic error, and to coregister the sequential datasets before computing the
745 sediment budget (e.g. Lallias-Tacon et al., 2014; Passalacqua et al., 2015; Anderson, 2019).
746 Topographic differencing using high resolution datasets have been successfully used to investigate a
747 large range of fluvial processes, such as bank erosion (Thoma et al., 2005; Jugie et al., 2018), braided
748 channel responses to flow events (Lane et al., 2003; Milan et al., 2007; Hicks et al., 2009; Lallias-
749 Tacon et al., 2014), channel response to restoration projects (Campana et al., 2014; Heckmann et al.,
750 2017) (Figure 9).

751

752

753 *Figure 9. Monitoring of sediment wave propagation following a gravel replenishment operation*
754 *downstream of a dam in the Buëch River (Southern French Prealps), using repetitive airborne LiDAR*
755 *surveys and UHF active RFID tags (source: Brousse et al, online); the combination of HR*
756 *topographic differencing before and after a 5-yr flood and bedload tracing successfully allow to*
757 *detect the propagation of the artificially-induced sediment wave, with a front located at 2.5 km from*
758 *the dam*

759

760 Classically, vegetation dynamics have been analysed using temporal series of remotely-sensed
761 images (satellites, aerial, UAV, terrestrial, etc.) to monitor management actions such as ecological
762 restoration (Norman et al., 2014; Nunes et al., 2015; Martínez-Fernández et al., 2017; Bauer et al.,
763 2018; Martinez et al., 2018). In many cases, the monitored processes impose a given temporal
764 resolution and thus a given sensor/vector couple. For example, single events and intra-annual
765 processes can be monitored using close range terrestrial photography (Bonin et al., 2014; Džubáková
766 et al., 2015) or UAV (Laslier et al., 2019b), and inter-annual succession processes using UAV
767 (Hervouet et al., 2011; Räßle et al., 2017) or airborne orthophotos (e.g. Michez et al., 2017).

768

769

770 *Real time monitoring of fluvial processes*

771

772 Fluvial processes can now be monitored in real time using ground-based imagery with high
773 temporal or spatial resolution. Tauro et al. (2018) review the most commonly used and new

774 techniques to measure and observe different hydrological variables, and notably the latest optical flow
775 tracking techniques to estimate flow velocity and discharge, including large-scale particle image
776 velocimetry (LSPIV; Le Coz et al., 2010), particle tracking velocimetry (PTV; Tauro et al., 2019),
777 and Kanade-Lucas-Tomasi (KLT) flow tracking (Perks et al., 2016). These techniques allow the
778 computation of flow surface velocities using images of the river surface sampled with UAV (Perks
779 et al., 2016), ground-based cameras, or screenshots extracted from film (Le Boursicaud et al., 2016).
780 Natural tracers present at the flow surface are tracked, such as boils, surface ripples, driftwood, or
781 artificial tracers, such as cornstarch chips (Le Coz et al., 2010). They have been increasingly used to
782 measure and estimate surface flow velocity and discharge during floods (Muste et al., 2011; Tauro et
783 al., 2016) in both gauged and ungauged basins, and proved to be a powerful approach when standard
784 techniques fail or are difficult to deploy (Le Coz et al., 2010).

785
786 Manual and automatic procedures have been also developed to monitor instream wood fluxes
787 using ground cameras (MacVicar et al., 2009). Kramer and Wohl (2014) used a time-lapse camera to
788 observe and quantify wood fluxes in the subarctic Slave River and stressed that an appropriate and
789 site-specific sampling interval is key to achieve unbiased estimates. MacVicar and Piégay (2012)
790 pioneered installing a video camera on the Ain River in France to describe the relation between wood
791 transport and water discharge, and to construct and validate a wood budget for the reach upstream of
792 the camera (Figure 10A&B). Boivin et al. (2017) used two video cameras to monitor the passage of
793 wood during floods and ice-breakup events in the Saint-Jean River in Canada. As for flood discharge
794 data (Le Coz et al., 2016), web crowdsourced home movies have been recently used to define and
795 characterize wood-laden flows (Ravazzolo et al., 2017; Ruiz-Villanueva et al., 2019) (Figure 10C).
796 Automatic and semi-automatic wood detection procedures have been developed to track and quantify
797 the wood discharge in the images (Benacchio et al., 2017), but the systematic application still requires
798 further research (Piégay et al., 2019). Despite the limitations, monitored sites with cameras have
799 significantly increased in the last years and will continue in the future.

800
801 *Figure 10: (A) Wood detection procedure using a video camera in the Ain River, France. Images*
802 *show the region of interest (ROI) based on a visual detection of wood including measurement of date*
803 *and time from time stamp, the precise location of end and side points to define the piece length,*
804 *diameter, and first position, and the definition of second position after advancing a user-determined*
805 *number of frames to allow calculation of velocity and angular velocity; (B) Flood hydrograph and*
806 *wood flux estimated based on video records during the event on April 10–13, 2008 (Modified from*
807 *MacVicar and Piégay, 2012); (C) Wood transport regimes characterized using home movies; the*
808 *small images show the same river section (North Creek, US) at different times (t), h : water depth*
809 *and z : wood flow depth; d_w : wood piece diameter; k : coefficient >1 (Modified from Ruiz-Villanueva*
810 *et al., 2019).*

811
812 Ground-based remote sensing techniques for the indirect monitoring of bedload transport are also in
813 an active phase of development. Seismic sensors like impact sensors, geophones or seismometers are
814 increasingly used as non-intrusive devices to detect and characterize bedload transport from ground
815 vibrations generated by grain impacts (Burtin et al., 2011; Downs et al., 2016; Burtin et al., 2016;
816 Roth et al., 2016). Their deployment in the near proximity to river channels, in relatively safe
817 positions, is a great advantage compared to traditional seismic methods based on the deployment of
818 plates or pipes in the active zone of bedload transport (e.g. Mizuyama et al., 2010; Rickenmann et al.,

819 2012). The monitoring of bedload in large rivers with high water depths is also now possible with the
 820 use of acoustic sensors, like hydrophones (Belleudy et al., 2010; Geay et al., 2017). Although reliable
 821 estimates of bedload flux with seismic and acoustic sensors still implies time-consuming field efforts
 822 for calibration with physical bedload samples, these RS solutions offer valuable continuous proxy
 823 records of sediment transport. These records have been successfully used to inform incipient motion,
 824 hysteresis in bedload rating curves, or to detect the passage of sediment pulses at river cross-sections
 825 (Belleudy et al., 2010; Geay et al., 2017; Burtin et al., 2016).

826
 827 Table 1 – A few examples of corridor features and attributes remotely sensed from a set of
 828 platforms/sensors within specific space-time frameworks
 829

Riverscape features and attributes	Ground	UAV/UAS/Ultralight	Plane/helicopter	Satellite	Spatial coverage	Multitemporal survey	Type of Data sensed	References
Grain characters								
Grain size	X				1 m ²	no	TLS	Hodge et al., 2009
	X				180 m ²	no	TLS	Heritage and Milan 2009
	X				Flume and field sampling (~1 m ²)	no	Ground photos	Stähly et al., 2017
	X				0.5 m ²	no	Ground photos	Purinton & Bookhagen, 2019
		X			2.5 km	yes	Aerial photos (RGB)	Vázquez-Tarrió et al., 2017
		X			Reach Scale	no	UAV/SfM	Carbonneau et al. 2018
	X		X			no	Ground photos, airborne LiDAR	Chardon et al., <i>in review</i>
Grain shape	X				Reach and catchment scale	no	Ground photos	Litty and Schlunegger, 2016
Grain roundness	X				Catchment scale	no	Ground photos	Roussillon et al., 2009
	X				Gravel bar	no	TLS	Hayakawa & Oguchi, 2005
	X				Catchment scale	no	Ground photos	Cassel et al., 2018
Channel characters								
Geomorphic features		X			Javoří brook (1-km-long stretch, catchment : 11 km ²)	no	Aerial photos (RGB)	Langhammer, J. & Vacková, 2018
			X			no	Airborne LiDAR	Wheaton et al., 2015
			X		Drôme network (1640 km ²)	no	Orthophotos (RGB and NIR)	Bertrand et al. 2013 a
			X		Piemont region (1200 km of rivers).	no	Aerial photos (with multispectral information, RGB and NIR), low resolution airborne LiDAR	Demarchi et al. 2017

			X		Set of reaches (n=53) – regional network	yes	Aerial orthophotos and historic aerial photos, high-resolution (< 1 m)	Belletti et al., 2015
				X	All Red River Basin (21000 km of rivers), Vietnam	no	Google EARTH (based on Digital Globe Quikbird and CNES Spot Image), topographic data (ASTER V2 GDEM), discharge data, and sediment rating curve	Schmitt et al, 2014
Instream wood size and distribution		X			Several river reaches along the Blanco River	no	UAV/SfM with a RGB camera	Sanhueza et al., 2018
		X						
			X		River reach	no	Airborne LiDAR	Atha and Dietrich, 2016
			X		Lamar River and the Cooke City Reach of Soda Butte Creek	no	Airborne hyperspectral imagery	Marcus et al. 2002, 2003
				X	146 river reaches along the Queets River	no	Google Earth imagery	Atha 2014
Instream wood volume		X			6 river reaches along the Clear Creek	no	UAV-SfM with a RGB camera	Truksa, 2017
			X		River reach	no	Airborne LiDAR	Atha and Dietrich 2016
				X	10 km along the Blanco River	yes	Digital Globe satellite imagery and three-band imagery derived from an airborne LiDAR survey	Ulloa et al. 2015
		X			Several reaches along the Blanco River	no	UAV/SfM with a RGB camera	Sanhueza et al., 2018
	X				14 ha of the Piave River	no	TLS	Tonon et al., 2014
		X			River reach Kuzlovec Torrent	no	TLS	Grigillo et al., 2015
Topography (excluding bathymetry)	X				Proglacial fan of Glacier du Mont Miné and Ferpècle, Swiss alps (5800 m ²)	yes	TLS	Milan et al., 2007
			X		Bès River, 7 km	yes	Airborne LiDAR	Lallias-Tacon et al., 2014
Topography (including bathymetry)	X		X		Rees River, 2.5 km	no	TLS, and aerial photos (RGB)	Williams et al., 2014
		X			Elbow River, 1 km	no	Aerial photos (RGB)	Tamminga et al., 2015
		X			White River, 0.25 km	no	Aerial photos (RGB)	Dietrich 2017
			X		Waimakariri River, 3.3 km	yes	Airborne LiDAR, and aerial photos (RGB)	Lane et al., 2003
			X		2 reaches on Soda Butte Creek, 0.385 km and 0.440 km	yes	Airborne LiDAR, and aerial photos (RGB)	Legleiter 2012

			X		Pielach River, 1-2 km	yes	Green airborne LiDAR	Mandlbürger et al., 2015
			X		Ste-Marguerite River, 80km	no	RGB camera	Carbonneau et al., 2006
Water, sediment and wood fluxes								
Water level		X			Ridracoli reservoir	yes	UAV with a RGB camera	Ridolfi and Manciola, 2018
				X	Ganges and Brahmaputra Rivers	yes	AMSR-E and TRMM sensor	Hirpa et al., 2013
Flow velocity	X				River reach	no	Home movies from YouTube and LSPIV	Le Boursicaud et al., 2016
	X				Laboratory small scale experiments and field sites on La Morge River at Voiron (<1km ²)	yes	Ground camera images (B&W)	Jodeau et al., 2017
	X				Yufeng Creek (cross section width of 15~30 m)	yes	Ground camera images (RGB)	Huang et al., 2018
		X			River reach	no	UAV and the Kande–Lucas–Tomasi (KLT) algorithm	Perks et al., 2016
Pebble mobility	X				2.3 km	yes	Passive RFID tags	Liébault et al., 2012
		X			22 ha, Büech River	no	Active RFID antenna mounted on a drone	Cassel et al., <i>in review</i>
Instream wood flux	X				River reach along the Ain River	yes	Video camera	MacVicar and Piégay, 2012
	X				River reach	yes	Time-lapse photography	Kramer and Wohl, 2014;
	X				Génissiat reservoir on the Rhône River (section about 0.35km ²)	yes	Ground images (RGB)	Benacchio et al., 2017
	X		X	X	River reach along the Saint-Jean River	yes	Aerial and satellite imagery	Boivin et al., 2017
	X				27 rivers reaches	yes	Home movies from YouTube	Ruiz-Villanueva et al., 2019

830
831
832
833
834
835
836
837
838
839
840
841

4. Developing predictive models using RS information

RS technologies open new opportunities to assess future changes and potential physical or ecological responses. The technologies can be used to develop scenarios of change (Baker et al., 2004), pressure-impact models (Tormos et al., 2012), risk assessment (Bertrand et al., 2013 a and 2013 b), and increasingly process-based models. Remote sensing technology is moving toward the possibility to map entire river networks consistently, extensively (from geomorphic features and processes to acting pressures), and over time (Carbonneau et al., 2012).

842

843 *Biogeomorphic models*

844

845 Abiotic and biotic interactions have long been an important part of fluvial geomorphology,
846 given the role of riparian vegetation (Corenblit et al., 2007, 2009; Gurnell et al., 2012) and large wood
847 (Ruiz-Villanueva et al., 2016), but also aquatic macrophytes/biofilm (which can be a constraint to
848 extract water depth or grain size from remote sensing data) and the other biotic components.

849 There is scope to increase the linkage between disciplines by incorporating remotely-sensed
850 information (such as land cover change or NDVI) within future predictive models of river changes.
851 Models are able to simulate complex fluvial processes including water–sediment–vegetation–wood
852 feedbacks. First attempts have been made to model the effect of flow and climate change on
853 vegetation dynamics (Hammersmark et al., 2010), the succession of riparian vegetation as a function
854 of scour disturbance, shear stress, and flood duration using the CASiMiR-vegetation model
855 (Benjankar et al., 2014) or the effects of vegetation growth on meander bank stability (Perucca et al.,
856 2007). Recent developments have enhanced computational fluid dynamic models by including
857 vegetation and wood dynamics (Bertoldi et al., 2014; Ruiz-Villanueva et al., 2014b) (Figure 11).
858 These advanced models open the door for investigations of how changes in the water, sediment or
859 wood regime may affect the fluvial response, which is fundamental for river management. Still the
860 full coupling of hydro-, morpho- and vegetation dynamics remains challenging. One key constraint
861 is to gather the required high-resolution input and validation data.

862

863 *Figure 11: (A) Aerial images of the Magra River near Aulla (Italy) in 2007 (up) and in 2011 (down)*
864 *and bed topography before a simulated flood sequence, after four floods and simulated biomass*
865 *distribution (From Bertoldi et al., 2014).(B) Simulated water depth and logs deposited along the*
866 *Czarny Dunajec River reach at a discharge of 28m³/s. From Ruiz-Villanueva et al., 2017.*

867

868 *Catchment-scale models*

869

870 Until a few years ago, catchment scale models were limited by the lack of suitable datasets, but
871 are now flourishing research area which is providing valuable evidence to support the management
872 and planning of river systems. Catchment-scale models have become feasible due to the availability
873 of DEMs with a high enough resolution to represent river features (e.g. Passalacqua et al., 2015). The
874 coupling of DEMs with large scale distributed hydrological models (Van Der Knijff et al., 2010) can
875 now be used to characterize sediment and nutrient transport across entire networks (Jain et al., 2006;
876 Barker et al., 2009; Bizzi & Lerner, 2015). This context has fostered the development of sediment
877 models to assess how sediment is routed through a network and how the various sediment sources
878 within the basin generate different sediment connectivity patterns (Cavalli et al., 2013; Heckmann &
879 Schwanghart, 2013; Czuba and Foufoula-Georgiou, 2014; Heckmann et al., 2015 Parker et al., 2015;
880 Czuba, 2018; Heckmann et al. 2018). For instance, the CATCHment Sediment Connectivity And
881 DELivery (CASCADE) modelling framework enables a quantitative, spatially explicit analysis of
882 network sediment connectivity with potential applications in both river science and management
883 (Schmitt et al., 2016) (Figure 12). In the Mekong delta, understanding the cumulative effects of
884 constructed and planned dams helps identify new solutions addressing both economic and
885 environmental objectives (Schmitt et al., 2018a, 2018b, 2019).

886

887 *Figure 12. Examples of plots obtained from CASCADE toolbox (source: Tangi et al, 2019). The tool*
888 *allows analysing various properties of sediment connectivity in an interactive manner. Panel a shows*
889 *the total sediment transported in Kg/s in the network. b visualizes patterns of deposition for a single*
890 *sediment class out of the 18 considered in the model (in this case boulders/cobbles). c shows the*
891 *changes in total sediment transport caused by the removal of one dam and two external sediment*
892 *flows. d shows an analysis of grain size distribution, sediment sources and deposition and*
893 *entrainment in a specific reach. Each step can be interactively controlled by the user using a*
894 *graphical interface.*

895

896 Similarly, in the case of instream large wood (i.e. fallen trees, trunks, rootwads and branches),
897 models have been developed to assess wood supply and transfer through catchments using novel
898 datasets (Ruiz-Villanueva et al., 2016). Wood is supplied to rivers by complex recruitment processes
899 (e.g. landslides, bank erosion) with large spatial and temporal variability, which makes predictions
900 challenging. Models fed with remotely sensed data, such as aerial imagery and forest cover
901 information, enable the simulation and identification of recruitment processes and sources and the
902 estimation of wood supplied volumes (Gregory & Meleason, 2003; Mazzorana et al., 2009; Ruiz-
903 Villanueva et al., 2014 a; Cislighi et al., 2018). High-resolution canopy models obtained from LiDAR
904 or photogrammetry may provide more accurate estimation of wood volumes (Steeb et al., 2017;
905 Gasser et al., 2019). Scenarios based on forecasted climate change alterations of vegetation cover,
906 flow regimes, and human activities can be also designed to explore and quantify the range of
907 variability of instream wood supply, and to make predictions about how differences in river and forest
908 management may alter instream wood supply (e.g. Cislighi et al., 2018).

909 Understanding future changes consistently at the network scale to inform river management
910 requires an integrated approach, combining local field data with current large data archives and
911 computational tools and drawing upon a range of disciplines such as hydrology, climatology, or
912 ecology. Hydrology can help us understand patterns in remotely sensed rivers by better incorporating
913 information on flow non-stationarity, catchment characteristics, large-scale river flow archives, and
914 hydrologic modelling. Integrating geomorphological analyses with climatology is increasingly
915 important for understanding how climate change and large-scale climate variability may alter
916 sediment dynamics, vegetation patterns, streamflow, and ultimately channel adjustment (Darby et al.,
917 2013; Slater et al., 2019a).

918

919

920

921 **5. Forthcoming resources**

922

923 Emerging data, tools and geospatial analyses are generating cost-effective and promising
924 opportunities to inform river management worldwide. This section provides an overview of datasets,
925 tools and web resources available to assess river status and changes.

926

927 *New acquisition opportunities*

928

929 One of the principal technological challenges in remote sensing is to increase the scale and
930 spatial coverage at which it is possible to obtain a continuous and high-resolution reconstruction of

931 the Earth's surface. This in turn allows an increase in the number of forms and processes that can be
932 identified using a variety of spatial and spectral information. However, the cost of remote sensing
933 technology generally increases rapidly with increasing resolution, along with associated costs in terms
934 of data handling and processing and the technical skills required to analyze the products of new
935 aforementioned sensors. Despite the growing availability of low-cost airborne solutions such as UAV,
936 the challenge of surveying entire rivers at sub-decimeteric resolutions remains considerable.

937 In recent years, the growing popularity of the consumer drone market has meant that models
938 equipped with moderate quality imaging sensors are now available at less than 2500 € (in 2019). The
939 drive to produce imagery and video footage for mass consumption has benefited scientists who
940 require images with relatively low distortion and a good dynamic range. Furthermore, ease of
941 operations for the mass consumer market means that these low-cost airborne platforms are capable
942 of automated flight, have single-phase, non-corrected, GPS systems and, increasingly, active collision
943 avoidance systems. Expanding the area of operations for drone surveys remains at the research
944 frontier. There are two important issues to confront. First, the current regulatory trend in most nations
945 is to limit drone operations to the line of sight of the pilot. This obviously constrains the range of
946 operations to a radius of a few hundred meters per flight. In practice, this means that a well-trained
947 team of operators can currently survey 3-5 km of river corridor per day depending on the relocation
948 conditions and the amount of ancillary data required, such as surveyed ground control. Second, this
949 use of ground control, long held as an absolute requirement, is currently being challenged (e.g.
950 Carbonneau and Dietrich, 2017; James et al., 2017).

951 If we look towards the near future, the resolution of Earth Observation data from satellites is
952 such that soon it should provide more information to characterize large to mid-sized river features
953 and changes almost continuously in space and time. Mini-satellites provide almost daily images
954 globally at 3-5 m resolution in the RGB and near-infrared bands (see <https://www.planet.com/>), and
955 the SWOT satellite will soon observe major lakes, rivers and wetlands with unprecedented resolution.
956 In the next few years, two major programs will supply more frequent images with better quality:
957 Landsat 9 which will be launched in 2020, and Pleiades Neo will be composed of 4 satellites that will
958 revisit the same scene twice daily, producing panchromatic images at 30 cm resolution, a higher
959 spatial resolution than for airborne campaigns done by many national institutions since 1940s.

960

961 *The increasing global data availability*

962 High resolution topographic and observed hydrological data have only been available for a few
963 years at the global scale and are providing new ways to characterize river characteristics and
964 trajectories. Better understanding of how fluvial systems vary globally will require close integration
965 of geomorphic datasets with a range of hydrologic, climatic, topographic, and biological data
966 archives. Hydrologic data have become available for many countries via the GRDB and the World
967 Meteorological Organisation's Hydrological Observing System (WHOS). Crochemore et al. (2019)
968 provide an analysis of the quality of 21,586 river flow time series from 13 openly-accessible
969 hydrological archives. Recent global datasets such as the Global Streamflow Indices and Metadata
970 Archive (Do et al., 2018) have used these archives to compute global river catchment attributes.
971 Global discharge reanalysis data from 1979 to near real time has also recently become available
972 through the Copernicus Climate Data Store (CEMS GloFAS 2019). DEM-derived topographic
973 signatures (e.g. Amatulli et al., 2018) may also be used to provide a more systematic assessment of
974 the spatial distribution of different river types, with the advent of high resolution DEMs such as
975 MERIT (Yamazaki et al., 2017) or the 90-m resolution TanDEM-X (Archer et al., 2018). A

976 systematic understanding of channel signatures will also require the integration of these topographic
977 signatures with large-scale climatic and anthropogenic data, e.g. by using global high-resolution
978 reanalysis products such as ERA5 from Copernicus ECMWF (Hersbach et al., 2018), information on
979 global reservoirs and dams (Lehner et al., 2011; Grill et al., 2019)(Figure 13), or suspended sediment
980 data (e.g. the Land2Sea database; Peucker-Ehrenbrink, 2009).

981

982

983 *Figure 13. Dominant pressure indicator for global river reaches below a given Connectivity Status*
984 *Index (CSI) threshold (95%). Pressure indicators include the DOF (degree of fragmentation), DOR*
985 *(degree of regulation), SED (sediment trapping), USE (consumptive water use) and URB (urban*
986 *areas). The inset shows the number and proportion of river reaches per dominant pressure indicator*
987 *at the global scale. (Source: Grill et al., 2019; Figure 2)*

988

989 *Emerging geoprocessing tools*

990

991 Data are increasingly available from a number of freely and openly accessible repositories.
992 However, to realize the full potential of big data, rapid access and efficient processing capabilities
993 are required (Giuliani et al., 2017). With the development of new data and sensors we must also
994 develop our collective ability to manage and analyze these data. The increasing development of 3D
995 information provided by photogrammetry and LiDAR or infra-annual time-series of VHR images,
996 for instance, potentially opens many scientific and applied issues related to the interpretation and
997 understanding of riverscape functioning, but also raises the question of the chain of actors involved
998 in data acquisition, processing and utilization.

999 Deriving insights on fluvial characteristics from very large datasets requires computational
1000 tools and automation. There has been a rise in computational hydrology, ecology, and geomorphology
1001 over the last decade thanks to the uptake of open-source programming languages like R and Python.
1002 For example, hydrologists have developed many packages supporting the entire hydrological
1003 ‘workflow’, including meteorological and hydrological data retrieval via application programming
1004 interfaces; data extraction at catchment scales from global gridded data; many different catchment
1005 hydrological models; and packages specifically designed for statistical analyses, and data
1006 visualization (Slater et al., 2019b). Many hydrological and ecological packages already exist for
1007 automated satellite image processing, handling and manipulating remote sensing data, correcting and
1008 rescaling satellite imagery, or for analyzing remotely sensed vegetation data. For R users, the CRAN
1009 Task Views provide lists of packages for different areas of research, many of which are relevant for
1010 fluvial geomorphology, including areas such as time series analysis, reproducible research, machine
1011 learning, or spatial data analysis (<https://cran.r-project.org/web/views/>). Supervised classification is
1012 on the verge of undergoing a fundamental change whereby general pre-trained deep learning models
1013 are used to obviate the labour-intensive phase of manual image labelling for land-cover classification.
1014 Most notably, the machine learning algorithms used by Carbonneau et al. (*in revision*) are fully in the
1015 open-source realm. It would therefore seem likely that artificial intelligence approaches are set to
1016 overtake, or perhaps absorb, existing approaches of ‘object-based image analysis’.

1017 Computational fluvial geomorphologists are also increasingly using and developing toolboxes
1018 to understand and quantify river landscape change (for a recent review see Fryirs et al. 2019). For
1019 instance, the open-source LSDTopoTools software is used for topographic analysis, channel network
1020 extraction, chi analysis, calculation of erosion rates, hilltop flow routing and relief metrics, and/or

1021 topographic extraction of floodplains and terraces (Mudd et al., 2018). The RiVMAP MATLAB
1022 toolbox or the cmgo R package can be used to measure channel widths, the locations and rates of
1023 migration, accretion and erosion, and the space-time characteristics of cutoff dynamics (Golly &
1024 Turowski, 2017; Schwenk et al., 2017). The CASCADE toolbox (Tangi et al., 2019) provides
1025 assessment of sediment connectivity at the network scale and enables screening impacts of many
1026 infrastructure portfolios. Other toolboxes include the Fluvial Corridor Toolbox
1027 (<https://github.com/EVS-GIS/Fluvial-Corridor-Toolbox-ArcGIS>; Roux et al., 2015), the NCED
1028 Stream Restoration Toolbox (Lauer, 2006), the River Bathymetry Toolkit (McKean et al., 2009) or
1029 the RVR Meander toolbox (Abad & García, 2006) to measure channel features and processes (e.g.
1030 migration rates). The River Analysis and Mapping engine (RivaMap) has been developed to facilitate
1031 the computation of large-scale hydrography datasets (i.e. extracting the river centerline and width)
1032 from Landsat data in a short time period (Isikdogan et al., 2017). The Valley Bottom Extraction Tool
1033 (V-BET) (Gilbert et al., 2016) and the Valley Bottom Confinement Tool (VBCT) (O'Brien et al.,
1034 subm.) used across networks, allow to categorize channel confinement categories and degrees. The
1035 shape/morphology of different channel units (i.e. concave, convex and planar surfaces) can be
1036 mapped along reaches using the Geomorphic Unit Tool (GUT) (Wheaton et al., 2015; Kramer et al.,
1037 2017) as well as the Geomorphic change detection (GCD) software for sediment budgeting (Wheaton
1038 et al., 2010) (see www.riverscapes.xyz). Digital grain sizing algorithms developed by Buscombe
1039 (2013) (pyDGS - <http://digitalgrainsize.org/>) and Detert and Weitbrecht (2012) (Basegrain -
1040 <https://basement.ethz.ch/download/tools/basegrain.html>) are also available online as well as an
1041 algorithm for calculating roundness index (Cassel et al., 2018) ([https://github.com/EVS-GIS/2D-
1042 Roundness-Toolbox](https://github.com/EVS-GIS/2D-Roundness-Toolbox)). Most of these datasets and toolboxes are free to use, globally applicable and
1043 represent a valuable resource for researchers and managers worldwide.

1044
1045
1046 *Figure 14. Example of tools/interfaces available online to measure characters of fluvial corridors :*
1047 *A) The Fluvial Corridor Toolbox – FCT - within the ArcGIS Arc Toolbox (Roux et al. 2015) and view*
1048 *of generic spatial units for characterizing aggregated geographical objects at the network scale*
1049 *(<https://github.com/EVS-GIS/Fluvial-Corridor-Toolbox-ArcGIS>); B) website views (tutorial and*
1050 *dataset example) of the Geomorphic Change Detection software (<http://gcd.riverscapes.xyz/>)*
1051 *(Wheaton et al., 2010a); and C) Example of image output showing grain detection using BaseGrain*
1052 *software ([https://www.ethz.ch/content/specialinterest/baug/laboratory-
1053 vaw/basement/en/download/tools/basegrain.html](https://www.ethz.ch/content/specialinterest/baug/laboratory-vaw/basement/en/download/tools/basegrain.html)) (Detert et Weitbrecht, 2012)*

1054 1055 *Online platforms and repositories*

1056
1057 Sharing data and knowledge is an indispensable component of stakeholder-integrated problem-
1058 solving (Lehmann et al., 2017; Dick et al., 2018). The wide range of automatic feature extraction
1059 toolboxes listed above indicates that mapping/detecting geomorphic features is possible. However,
1060 collective organization and repository tools are needed. One example is the international long-term
1061 ecological research (ILTER) network which gathers more than 600 sites worldwide in a broad variety
1062 of terrestrial, freshwater, and marine environments (Haase et al., 2016; Dick et al., 2018). Networking
1063 is based on the DEIMS-SDR data system (Dynamic Ecological Information Management System –
1064 Site and Dataset Registry: <https://data.lter-europe.net/deims/>), which includes repository of remotely-
1065 sensed data. Similarly, a spatial data infrastructure (SDI) has been developed within the Human-
1066 Environment Observatories network which brings together 13 French and international observatories,

1067 including river observatories (Chenorkian, 2012). Web GIS, metadata and other visualization tools
1068 developed in this SDI are available for scientists and stakeholders. Additionally, the Data Center of
1069 the San Francisco Estuary Institute provides a broad range of tools and web services to upload, access,
1070 and visualize remotely-sensed datasets and other GIS layers to support and inform natural resource
1071 management in the area (Grosso & Azimi-Gaylon, 2018; <https://www.sfei.org/sfeidata.htm>). In the
1072 Earth surface sciences, the Community Surface Dynamics Modeling System (CSDMS) maintains a
1073 code and metadata repository for numerical models and scientific software tools
1074 (<https://csdms.colorado.edu>). In hydrology, Lehman et al. (2014) reviewed innovative global
1075 observation solutions which provide a suite of hydrological standard specifications to BRIdging
1076 Services Information and Data for Europe (BRISEIDE) project to visualize, manage and process
1077 geospatial resources useful for hydrological model development. Google Earth or NASA WorldWind
1078 also offer capabilities to visualize spatio-temporal data. An example is the Global Dam Watch
1079 initiative (<http://globaldamwatch.org/>), which aims to maintain the world's most comprehensive and
1080 freely available global dam data, including repository for the GLObal georeferenced Database of
1081 Dams (GOOD²) obtained from Google Earth satellite imagery, and an open list of existing dam data
1082 available at regional and global scales.

1083 1084 1085 **6. Prospects for the remote sensing of Anthropocene rivers**

1086
1087 Remote sensing has become a key tool to characterize past, current and future fluvial corridor
1088 conditions, and provides information almost as important as field information. In recent decades,
1089 fluvial RS has mainly been used in the sciences, but now these techniques are increasingly used by
1090 consultants too. Many river management consultancies utilise drones, equipped with different
1091 sensors, as well as SfM techniques or classical images in monitoring studies. Ground cameras are
1092 also widely employed to study processes in action. RS has become one of the most common tools in
1093 the geomorphologist's toolkit and one might almost say the "field tradition" is in the past! What are
1094 thus the future research prospects for RS? Some research objectives are likely to be rapidly attained
1095 whereas others are still inaccessible. Ten future avenues for RS of Anthropocene rivers include:

1096
1097 1) Exploring existing data more deeply such as national (maps and aerial photos) or satellite (Landsat
1098 archives) resources to assess channel behaviour and trajectories. This gap is particularly important in
1099 regions of the world where river corridor studies are rare, or where human activities such as damming
1100 are an issue (e.g. where channel sensitivity or bedload transport are not monitored). Additionally,
1101 recent advances in the digitisation of old archives and maps, alongside increasing computational
1102 power and the availability of novel geomatic toolboxes, are opening new opportunities to generate
1103 vast databases of digital historical information, ready for big-data analysis. More work may be done
1104 on derivation of DEMs from stereo-photo pairs. Recent (10-20 years) dynamics could be detected by
1105 stereoscopic acquisitions from airplane or satellite high resolution images. Some satellites acquire
1106 now at sub-meter resolution in stereoscopic mode (e.g., Pleiades and WorldView) and it would be
1107 worth testing their accuracy to explore what kind of earth surface process monitoring they can be
1108 exploited for. Finally, we might also question if after almost a decade of methodological development,
1109 more efforts could be made to use the existing new data and place more collective effort on
1110 geomorphic understanding, theory and practice, rather than always seeking technological
1111 development.

1112
1113 2) Merging data sources and scales of analysis to obtain new information, with careful data quality
1114 control and validation. Drone data can for instance be used to validate information from satellites.
1115 Assessing vegetation growth patterns and health is now possible by combining hyperspectral LiDAR
1116 information and age unit layers from aerial photo series. A major challenge in the future is to build a
1117 modifiable, methodological framework integrating different sensors (optical, hyperspectral, LiDAR,
1118 SAR, etc.), as well as different spatial (from local to regional) and temporal (daily to annual or greater)
1119 approaches. We will need to combine the strengths of each sensor and approach to improve
1120 understanding of channel trajectories and behaviour. Traditional measurements (such as stream
1121 gauging measurements, width/depth ratios, hydraulic scaling laws) are not obsolete but – quite the
1122 contrary – are increasingly indispensable to validate, integrate and generalize RS-based
1123 characterization and assessments. More data with higher resolution does not mean necessarily more
1124 knowledge. A key challenge and a goal for future river science will be to translate information into
1125 knowledge and to critically consider the data quality, metadata and resolution accuracy.
1126

1127 3) Accessing high temporal resolution RS information to provide input for water policy. Considerable
1128 efforts have been made to characterize the status of rivers but only a few studies have focused on the
1129 changes of river status through time. Monitoring these changes is crucial to understand channel
1130 responses to management actions. Obtaining bottom-up feedback on the potential success of
1131 implemented measures from RS is a real issue in river restoration. Similarly, top-down strategies can
1132 be also based on high temporal resolution RS. Combining LiDAR data at regional scales should soon
1133 provide inter-annual information (e.g., in Belgium, Switzerland or Denmark) to detect major changes
1134 in channel geometry as well as riparian vegetation and identify the most critical reaches, and to design
1135 planning strategy to target actions.
1136

1137 4) Implementing large scale models and upscaling catchment characterisation to continental or global
1138 scales. We are at the beginning of large/network scale modelling. In the future, river scientists should
1139 invest efforts to generate consistent hydrological, morphological and biotic datasets at global scales,
1140 working with local, national and international environmental agencies/institutions to characterize
1141 river status and develop model frameworks capable of tackling the network scale at which most
1142 fluvial processes operate. Some of the key challenges are: to integrate the sediment cascade, supply,
1143 transfer and functional connectivity; to combine riparian vegetation recruitment, growth and even
1144 diversity; and to quantify channel evolution, including shifting, incision, and aggradation. Bio-
1145 geomorphic diagnostics that use RS to detect differences in health conditions (and explore potential
1146 links with stationary conditions, such as water resource availability) should soon be possible.
1147 Sediment or wood budgeting is expected to relate with human pressures and land use changes at these
1148 large scales. With new resources available, RS is becoming a key technology for monitoring river
1149 trajectories and scenarios of change alongside process-based models.
1150

1151 5) Developing real time monitoring from ground sensors. Real time tools and early-warning systems
1152 are increasingly available for monitoring wood flux, bank retreat, sediment transport or hydro-
1153 meteorological extreme events. Discharge is already available online in real time. In the future, it is
1154 conceivable that websites will provide real-time monitoring of in-channel wood flux, potentially with
1155 alerts based on threshold values, as is already the case with water discharge gauging stations or debris-

1156 flow hazards in steep slope torrents. Similar systems might be developed for bedload transport with
1157 geophones, hydrophones or seismographs.

1158

1159 6) Exploring new knowledge frontiers that are still a challenge for RS. Accessing underwater
1160 environments remains a key challenge, notably when monitoring channel responses to restoration and
1161 aquatic habitat improvement. The main challenge for surficial grain size mapping in rivers remains
1162 the characterization of submerged areas, for which we still lack efficient remote sensing solutions.
1163 Bathymetry is still challenging for many rivers and it is not clear when it is appropriate to collect RS
1164 bathymetric data. Another critical challenge is the investigation of the subsurface sedimentology of
1165 river channels, notably the subsurface grain size for which geophysical solutions are still lacking to
1166 obtain reliable grain size distribution. Bank material characterization, floodplain geomorphic units,
1167 and sediment supply are all examples of relevant river components which cannot be easily assessed
1168 by RS, even with semi-automated procedures.

1169 RS also still fails to capture key information on rapid phenomena such as the changes and bedload
1170 transport that occur in river channels during floods (high-frequency monitoring). Much of the RS
1171 techniques allow extracting ‘snapshots’ of riverine landscapes These can be compared to analyse net
1172 changes (i.e. integrate changes during the period between snapshots). Two snapshots of a given
1173 landscape might look the same even though the channel has experience considerable change during
1174 the period between snapshots (e.g. compensation). For example, how does a channel or the bed
1175 material adjust during a competent flood event? Field work will remain the only feasible method to
1176 generate this type of information in the near future. However, this issue might be solved with new
1177 emerging ground sensors (which are also RS) rather than classic airborne imagery. We expect a new
1178 step of knowledge production to emerge from this ground sensor technology - notably in terms of
1179 process understanding at high temporal resolution – relying on the creativity of researchers to adapt
1180 these technologies to solve geomorphic questions.

1181 A new era is also emerging in this domain with Big Earth Data. It seems we are just at the beginning
1182 of this new period. Fluvial geomorphologists do not really use Big Data yet. There are almost no
1183 deep learning papers in the river literature because the data is not available. This is especially true
1184 with VHR airborne data where there are no papers on multiple catchments. River scientists still lack
1185 a shared global infrastructure to compile and organise data collectively. This is a new avenue for
1186 fluvial geomorphologists and satellite archives are one of the key resources suitable for a Big Data
1187 approach.

1188

1189 7) Developing long term integrative science observatories within which RS data are shared, managed
1190 and archived. Compiling data on river basins is critical to validate modelling studies and to develop
1191 simulations and scenarios. Field campaigns (such as grain size characterization, sediment sources
1192 identification, sediment transport monitoring) and river diagnosis (such as multi-temporal aerial
1193 photo series) take time, and the processed data are often lost even though subsequent projects could
1194 build on these efforts. Archiving long-term data is also critical for practitioners who may access
1195 scenarios of change and incorporate them into policy strategies. Here is also a clear need to share
1196 efforts in knowledge production. Some river scientists must specialise in data acquisition (i.e. data
1197 collectors). It is a research task in itself. There are new opportunities to acquire original data at
1198 unprecedented scales (i.e. produce repeated near real-time facsimiles of the landscape features) and
1199 this implies learning new techniques, designing new sampling and post-processing strategies taking
1200 into account data precision, accuracy and different sources of errors. These tasks are time-consuming

1201 and sometimes require a never-ending learning process due to the continuous advances in terms of
1202 sensors, platforms and software. Peer-reviewed journals must provide space for such methodological
1203 research, even if they do not always reach geomorphic answers because practical tests, experiments,
1204 descriptions of new techniques are needed to inject new tools and data in the research domain. The
1205 geomorphology community must organise itself to support complementary research and engineering,
1206 sharing the geomorphic data and tools, and not only methodological developments. Research teams
1207 must thus join methodologists and thematologists. A network strategy can also be necessary when
1208 experts cannot be present on a local academic site.

1209
1210 8) Sharing data and processing tools online. River science requires collective efforts to improve
1211 access to data, geoprocessing tools, and algorithms. Building a geomorphological repository of tools
1212 and data for monitoring/benchmarking fluvial change, as well as associated literature and tutorials is
1213 urgent to accelerate research and uptake of these tools within the community. Data and tools can be
1214 shared among scientists and practitioners, as both would benefit. Data sharing can induce both
1215 bottom-up and top-down strategies: practitioners can provide local data (bottom-up) to implement
1216 basin-scale or national-scale tools and use these tools to better contextualise their own catchments
1217 within the large-scale framework in terms of river status, functionality, or responsiveness (top-down).
1218 Collecting and managing these data is a long-term investment, which can be enhanced by
1219 collaborating with local institutions in charge of data management. Existing archives can be used to
1220 characterize large-scale historical trajectories and then advance our capacity to predict future change.
1221 Participatory approaches and citizen science are also a key future avenue to obtain information on
1222 channel geometry, status, and attributes (e.g. grain size), for quality control or validation and for
1223 knowledge transfer.

1224
1225 9) Using RS to reexplore theories. Many concepts that were developed in the 20th century using small
1226 datasets can now be quantified and tested systematically using RS over much larger scales and at
1227 greater temporal resolutions than ever before. RS generates new opportunities to disentangle and
1228 quantify the role of natural and anthropogenic drivers in shaping river systems, rank them in terms of
1229 impact, identify the mosaics of riverscape conditions, better understand the time scales of adjustment
1230 and lag times, generate conclusions and assess their range of applicability. Increasingly, it is
1231 becoming possible to monitor short-term river trajectories consistently at local, basin, regional or
1232 even national scales and to predict future trajectories of change. These advances allow us to test
1233 concepts such as river sensitivity (which has been so far introduced mostly theoretically in science
1234 and management; Fryirs, 2017), or resilience of river channels to human disturbances, and assess
1235 their contextual applications. Large scale data can also be used in retrospective hydraulic modelling
1236 to assess past changes in channel geometry, morphodynamics, sensitivity to changes and bedload
1237 transport. Real time ground monitoring also allows us to better understand the processes at work and
1238 reconsider physical drivers to improve modelling approaches. The time has come to translate our
1239 requests for more data (which are now partially satisfied) into efforts to use this data to review and
1240 advance the basic concepts and theories at the core of fluvial geomorphology.

1241
1242 10) Promoting a critical approach to RS practices. It is clear that some of the “emergent” remote-
1243 sensing techniques are no longer new. These techniques are already available for the community,
1244 with clear workflows and freely-available tools, and, consequently, we need to use them for specific
1245 objectives, avoiding further methodological developments and improving the knowledge we have in

1246 terms of understanding how rivers work (both natural and disturbed systems) and their future
1247 trajectories. Furthermore, the intensive use of RS tools to characterize environmental processes is not
1248 neutral: depending on the context and the issue, these methods may exclude certain stakeholders,
1249 limit the understanding of phenomena, and/or generate controversial data. Thus, the use of RS tools
1250 needs to be combined with a critical understanding of their sociological and cultural effects, and
1251 complementary approaches to counterbalance any potential negative effects. Thus, interdisciplinary
1252 scientific teams are required to generate integrative river science. Collaborative engagement and co-
1253 development of decision-support tools are required to identify solutions to problems faced by specific
1254 stakeholders.

1255

1256

1257

1258 **6. Conclusions**

1259

1260 Research in remote sensing is essential to address one of the major challenges of the
1261 Anthropocene: understanding and managing the relationship between society and the environment.
1262 Field data alone is insufficient to tackle complex geomorphic questions, and the reverse (remote
1263 sensing without field data for validation and field observation) is also true. While geomorphologists
1264 still need to spend time in the field observing the complexity of processes and landforms, geomorphic
1265 understanding can also emerge from image observations. Remote sensing resources provide much
1266 greater insight into the spatial variability of channel forms and processes than ever before – from the
1267 scale of the cross section to that of entire river networks. However, even with the enhanced
1268 availability of data, river scientists still need to develop appropriate scientific questions, ground-truth
1269 measurements at relevant space and time scales, and interpret the data.

1270 Remote sensing is no longer only a scientific tool; it is a set of data and techniques for informing
1271 river managers at local to basin scales. River scientists need to move beyond simple methodological
1272 development (eureka it works!) by sharing tools, transferring knowledge, and developing critical
1273 understanding of where, how and when methods can be accurately incorporated in applied
1274 geomorphology. Remote sensing can be used to help implement and monitor management measures,
1275 identify criticalities, tipping points, future trajectories, pressures and their effects, better than in the
1276 past. Merging field observations with RS information will allow us to understand rivers in the
1277 Anthropocene and identify the best management scenarios for their (and our) future.

1278

1279

1280 **7. Acknowledgments**

1281

1282 We thank colleagues and students, including 40 PhD students who have worked with us during these
1283 25 years of exciting research on emerging RS techniques applied to riverine sciences. This work was
1284 performed within the framework of the ZABR, the EUR H₂O'Lyon (ANR-17-EURE-0018) of
1285 Université de Lyon (UdL) and the Observatoire Hommes-Milieus Vallée du Rhône (OHM VR) of
1286 the Labex DRIHM (ANR-11-LABX-0010); the latter two are part of the French program
1287 "Investissements d'Avenir" operated by the French National Research Agency (ANR). Research on
1288 Fluvial Remote Sensing has been highly supported by river practitioners, such as the Agence de l'Eau
1289 Rhône-Méditerranée & Corse, the French Biodiversity Agency (AFB), some Regions (ARA, PACA,
1290 Occitanie, Grand Est...), the Compagnie Nationale du Rhône (CNR) and EDF (main electric French
1291 company). We also thank Stuart Lane, an associate editor and two external reviewers for their fruitful
1292 comments and suggestions.

1293

1294 **8. References**

1295

1296 Abad, J. D., & Garcia, M. H. (2006). RVR Meander: A toolbox for re-meandering of channelized
1297 streams. *Computers & Geosciences*, 32(1), 92–101.

1298 Abalharth, M., Hassan, M. A., Klinkenberg, B., Leung, V., & McCleary, R. (2015). Using LiDAR to
1299 characterize logjams in lowland rivers. *Geomorphology*, 246, 531-541.

1300 Adams J. 1979. Gravel size analysis from photographs. Journal of the Hydraulics Division of the
1301 American Society of Civil Engineers 105: 1247-1255 Aguiar, F. C., & Ferreira, M. T. (2005).
1302 Human-disturbed landscapes: effects on composition and integrity of riparian woody vegetation
1303 in the Tagus River basin, Portugal. *Environmental Conservation*, 32(1), 30-41.

1304 Alber, A., & Piégay, H. (2011). Spatial disaggregation and aggregation procedures for characterizing
1305 fluvial features at the network-scale: Application to the Rhône basin (France). *Geomorphology*,
1306 125(3), 343-360.

1307 Alber, A., & Piégay, H. (2017). Characterizing and modelling river channel migration rates at a
1308 regional scale: Case study of south-east France. *Journal of environmental management*, 202, 479-
1309 493.

1310 Allen, G. H., & Pavelsky, T. M. (2018). Global extent of rivers and streams. *Science*, 361(6402), 585-
1311 588. <https://doi.org/10.1126/science.aat0636>.

1312 Allred, T. M., & Schmidt, J. C. (1999). Channel narrowing by vertical accretion along the Green
1313 River near Green River, Utah. *Geological Society of America Bulletin*, 111(12), 1757-1772. DOI:
1314 10.1130/0016-7606(1999)111<1757.

1315 Amatulli, G., Domisch, S., Tuanmu, M. N., Parmentier, B., Ranipeta, A., Malczyk, J., & Jetz, W.
1316 (2018). A suite of global, cross-scale topographic variables for environmental and biodiversity
1317 modeling. *Scientific data*, 5, 180040. <http://www.earthenv.org/topography>.
1318 <https://doi.org/10.1038/sdata.2018.40>.

1319 Anderson, S. W. (2019). Uncertainty in quantitative analyses of topographic change: error
1320 propagation and the role of thresholding. *Earth Surface Processes and Landforms*, 44, 1015-1033.

1321 Antonarakis, A. S., Richards, K. S., Brasington, J., Bithell, M., & Muller, E. (2008). Retrieval of
1322 vegetative fluid resistance terms for rigid stems using airborne lidar. *Journal of Geophysical
1323 Research: Biogeosciences*, 113(G2).

1324 Antoniazza, G., Bakker, M., Lane, S. (2019). Revisiting the morphological method in two-dimensions
1325 to quantify bed-material transport in braided rivers. *Ear. Surf. Proc. Land*. Online Early View.

1326 Archer, L., Neal, J. C., Bates, P. D., & House, J. I. (2018). Comparing TanDEM-X Data With
1327 Frequently Used DEMs for Flood Inundation Modeling. *Water Resources Research*, 54(12), 10-
1328 205.

1329 Arnaud, F., Piégay, H., Schmitt, L., Rollet, A. J., Ferrier, V., & Béal, D. (2015). Historical
1330 geomorphic analysis (1932–2011) of a by-passed river reach in process-based restoration
1331 perspectives: The Old Rhine downstream of the Kembs diversion dam (France, Germany).
1332 *Geomorphology*, 236, 163-177.

1333 Atha, J. B. (2014). Identification of fluvial wood using Google Earth. *River research and
1334 applications*, 30(7), 857-864. <https://doi.org/10.1002/rra.2683>

1335 Atha, J. B., & Dietrich, J. T. (2016). Detecting fluvial wood in forested watersheds using LiDAR
1336 Data: a methodological assessment. *River Research and Applications*, 32(7), 1587-1596.
1337 doi:10.1002/rra.2989

- 1338 Ba, A., Laslier, M., Dufour, S., & Hubert-Moy, L. (2019). Riparian trees genuses identification based
 1339 on leaf-on/leaf-off airborne laser scanner data and machine learning classifiers in western France.
 1340 *International Journal of Remote Sensing*. <https://doi.org/10.1080/01431161.2019.1674457>
- 1341 Bailly J-S, Le Coarer Y, Languille P, Stigermark C-J, Allouis T. (2010). Geostatistical estimations of
 1342 bathymetric LiDAR errors on rivers. *Earth Surface Processes and Landforms*, **35**, 1199–1210.
- 1343 Bakker, M., & Lane, S. N. (2017). Archival photogrammetric analysis of river–floodplain systems
 1344 using Structure from Motion (SfM) methods. *Earth Surface Processes and Landforms*, **42**(8),
 1345 1274–1286. doi:10.1002/esp.4085
- 1346 Barker, D. M., Lawler, D. M., Knight, D. W., Morris, D. G., Davies, H. N., & Stewart, E. J. (2009).
 1347 Longitudinal distributions of river flood power: the combined automated flood, elevation and
 1348 stream power (CAFES) methodology. *Earth Surface Processes and Landforms*, **34**(2), 280–290.
- 1349 Bauer, M., Harzer, R., Strobl, K., & Kollmann, J. (2018). Resilience of riparian vegetation after
 1350 restoration measures on River Inn. *River research and applications*, **34**(5), 451–460.
- 1351 Bedell, E., Leslie, M., Fankhauser, K., Burnett, J., Wing, M. G., & Thomas, E. A. (2017). Unmanned
 1352 aerial vehicle-based structure from motion biomass inventory estimates. *Journal of Applied*
 1353 *Remote Sensing*, **11**(2), 026026.
- 1354 Belletti, B., Dufour, S., & Piégay, H. (2014). Regional assessment of the multi-decadal changes in
 1355 braided riverscapes following large floods (Example of 12 reaches in South East of France).
 1356 *Advances in Geosciences*, **37**, 57–71.
- 1357 Belletti, B., Dufour, S., & Piégay, H. (2015). What is the relative effect of space and time to explain
 1358 the braided river width and island patterns at a regional scale?. *River research and applications*,
 1359 **31**(1), 1–15.
- 1360 Belletti, B., Rinaldi, M., Bussettini, M., Comiti, F., Gurnell, A. M., Mao, L., ... & Vezza, P. (2017).
 1361 Characterising physical habitats and fluvial hydromorphology: A new system for the survey and
 1362 classification of river geomorphic units. *Geomorphology*, **283**, 143–157.
 1363 <https://doi.org/10.1016/j.geomorph.2017.01.032>
- 1364 Benacchio, V., Piégay, H., Buffin-Bélanger, T., & Vaudor, L. (2017). A new methodology for
 1365 monitoring wood fluxes in rivers using a ground camera: Potential and limits. *Geomorphology*,
 1366 **279**, 44–58. doi:10.1016/j.geomorph.2016.07.019
- 1367 Benjankar, R., Burke, M., Yager, E., Tonina, D., Egger, G., Rood, S. B., & Merz, N. (2014).
 1368 Development of a spatially-distributed hydroecological model to simulate cottonwood seedling
 1369 recruitment along rivers. *Journal of environmental management*, **145**, 277–288.
- 1370 Bertoldi, W., Gurnell, A. M., & Drake, N. A. (2011). The topographic signature of vegetation
 1371 development along a braided river: results of a combined analysis of airborne lidar, color air
 1372 photographs, and ground measurements. *Water Resources Research*,
 1373 **47**(6).<https://doi.org/10.1029/2010WR010319>.
- 1374 Bertoldi, W., Piégay, H., Buffin-Bélanger, T., Graham, D., Rice, S. (2012). Applications of Close-
 1375 range Imagery in River Research. In: Carbonneau, P.E., & Piégay, H. (Eds), *Fluvial Remote*
 1376 *Sensing for Science and Management*, Chichester, UK: John Wiley & Sons, Ltd,
- 1377 Bertoldi, W., Siviglia, A., Tettamanti, S., Toffolon, M., Vetsch, D., & Francalanci, S. (2014).
 1378 Modeling vegetation controls on fluvial morphological trajectories. *Geophysical Research Letters*,
 1379 **41**(20), 7167–7175.
- 1380 Bertrand, M., Piégay, H., Pont, D., Liébault, F., & Sauquet, E. (2013 a). Sensitivity analysis of
 1381 environmental changes associated with riverscape evolutions following sediment reintroduction:

- 1382 geomatic approach on the Drôme River network, France. *International journal of river basin*
 1383 *management*, 11(1), 19-32.
- 1384 Bertrand, M., Liébault, F., & Piégay, H. (2013 b). Debris-flow susceptibility of upland catchments.
 1385 *Natural Hazards*, 67(2), 497-511.
- 1386 Bertrand, M., Liébault, F., & Piégay, H. (2017). Regional Scale Mapping of Debris-Flow
 1387 Susceptibility in the Southern French Alps. *Journal of Alpine Research/ Revue de géographie*
 1388 *alpine*, (105-4).
- 1389 Bertrand, M., & Liébault, F. (2019). Active channel width as a proxy of sediment supply from mining
 1390 sites in New Caledonia. *Earth Surface Processes and Landforms*, 44(1), 67-76.
- 1391 Biedenharn, D. S., & Watson, C. C. (1997). Stage adjustment in the lower Mississippi River, USA.
 1392 *Regulated Rivers: Research & Management: An International Journal Devoted to River Research*
 1393 *and Management*, 13(6), 517-536.
- 1394 Bird, S., Hogan, D., & Schwab, J. (2010). Photogrammetric monitoring of small streams under a
 1395 riparian forest canopy. *Earth Surface Processes and Landforms*, 35(8), 952-970.
- 1396 Bizzi, S., & Lerner, D. N. (2015). The use of stream power as an indicator of channel sensitivity to
 1397 erosion and deposition processes. *River Research and Applications*, 31(1), 16-27. DOI:
 1398 10.1002/rra.2717
- 1399 Bizzi, S., L. Demarchi, R. C. Grabowski, C. J. Weissteiner, e W. Van de Bund. (2016). The Use of
 1400 Remote Sensing to Characterise Hydromorphological Properties of European Rivers. *Aquatic*
 1401 *Sciences* 78(1), 57–70. <https://doi.org/10.1007/s00027-015-0430-7>
- 1402 Bizzi, S., Piégay, H., Demarchi, L., Van de Bund, W., Weissteiner, C. J., & Gob, F. (2019). LiDAR-
 1403 based fluvial remote sensing to assess 50–100-year human-driven channel changes at a regional
 1404 level: The case of the Piedmont Region, Italy. *Earth Surface Processes and Landforms*, 44(2),
 1405 471-489.
- Blaschke, T. (2010). Object based image analysis for remote sensing. *ISPRS journal of*
photogrammetry and remote sensing, 65(1), 2-16. DOI: 10.1016/j.isprsjprs.2009.06.004
- 1406 Blaschke, T., Hay, G. J., Kelly, M., Lang, S., Hofmann, P., Addink, E., ... & Tiede, D. (2014).
 1407 Geographic object-based image analysis–towards a new paradigm. *ISPRS journal of*
 1408 *photogrammetry and remote sensing*, 87, 180-191. DOI: 10.1016/j.isprsjprs.2013.09.014
- 1409 Blench, T. (1969). *Mobile-bed fluviology: a regime theory treatment of rivers for engineers and*
 1410 *hydrologists*. University of Alberta Press: Edmonton.
- 1411 Boivin, M., Buffin-Bélangier, T., & Piégay, H. (2017). Estimation of large wood budgets in a
 1412 watershed and river corridor at interdecadal to interannual scales in a cold-temperate fluvial
 1413 system. *Earth Surface Processes and Landforms*, 42(13), 2199-2213.
- 1414 Bonin, L., Proulx, R., & Rheault, G. (2014). A digital photography protocol for the rapid assessment
 1415 of herbaceous communities in riparian buffers. *Riparian Ecology and Conservation*, 2(1), 35-44.
- 1416 Bracken, L. J., Turnbull, L., Wainwright, J., & Bogaart, P. (2015). Sediment connectivity: a
 1417 framework for understanding sediment transfer at multiple scales. *Earth Surface Processes and*
 1418 *Landforms*, 40(2), 177-188. DOI: 10.1002/esp.3635
- 1419 Brasington, J., Vericat, D., & Rychkov, I. (2012). Modeling river bed morphology, roughness, and
 1420 surface sedimentology using high resolution terrestrial laser scanning. *Water Resources Research*,
 1421 48(11).
- 1422 Brierley, G. J., & Fryirs, K. A. (2005). *Geomorphology and River Management: Applications of the*
 1423 *River Styles Framework*. Malden, MA: Blackwell Publishing.
 1424 <https://doi.org/10.1002/9780470751367>.

- 1425 Brierley, G.J., & Fryirs, K.A. (2008). *River futures: an integrative scientific approach to river repair*.
 1426 Island press
- 1427 Brierley, G., Fryirs, K., Cullum, C., Tadaki, M., Huang, H. Q., & Blue, B. (2013). Reading the
 1428 landscape: Integrating the theory and practice of geomorphology to develop place-based
 1429 understandings of river systems. *Progress in Physical Geography*, 37(5), 601-621. DOI:
 1430 10.1177/0309133313490007
- 1431 Brousse, G., Arnaud-Fassetta, G., Liébault, F., Bertrand, M., Melun, G., Loire, R., Malavoi, J.R.,
 1432 Fantino, G., Borgniet, L., *in review*. Monitoring of sediment replenishment in a large gravel-bed
 1433 river : the case of the Saint-Sauveur dam in the Buëch River (Southern Alps, France). *River*
 1434 *Research and Applications*.
- 1435 Brown, A. G., Tooth, S., Bullard, J. E., Thomas, D. S., Chiverrell, R. C., Plater, A. J., ... &
 1436 Wainwright, J. (2017). The geomorphology of the Anthropocene: emergence, status and
 1437 implications. *Earth Surface Processes and Landforms*, 42(1), 71-90.
- 1438 Brown, A. G., Lespez, L., Sear, D. A., Macaire, J. J., Houben, P., Klimek, K., ... & Pears, B. (2018).
 1439 Natural vs anthropogenic streams in Europe: history, ecology and implications for restoration,
 1440 river-rewilding and riverine ecosystem services. *Earth-science reviews*, 180, 185-205.
- 1441 Burtin A, Cattin R, Bollinger L, Vergne J, Steer P, Robert A, Findling N, Tiberi C. 2011. Towards
 1442 the hydrologic and bed load monitoring from high-frequency seismic noise in a braided river: The
 1443 "torrent de St Pierre", French Alps. *Journal of Hydrology* 408: 43-53
- 1444 Burtin, A., Hovius, N., & Turowski, J. M. (2016). Seismic monitoring of torrential and fluvial
 1445 processes. *Earth Surface Dynamics*, 4(2), 285-307. DOI: 10.5194/esurf-4-285-2016.
- 1446 Buscombe, D. (2008). Estimation of grain-size distributions and associated parameters from digital
 1447 images of sediment. *Sedimentary Geology*, 210(1-2), 1-10. DOI: 10.1016/j.sedgeo.2008.06.007
- 1448 Buscombe, D., & Masselink, G. (2009). Grain-size information from the statistical properties of
 1449 digital images of sediment. *Sedimentology*, 56(2), 421-438. DOI: 10.1111/j.1365-
 1450 3091.2008.00977.x
- 1451 Buscombe, D., Rubin, D. M., & Warrick, J. A. (2010). A universal approximation of grain size from
 1452 images of noncohesive sediment. *Journal of Geophysical Research: Earth Surface*, 115(F2). DOI:
 1453 10.1029/2009JF001477
- Buscombe, D., & Ritchie, A. (2018). Landscape classification with deep neural networks.
Geosciences, 8(7), 244. DOI: 10.3390/geosciences8070244
- 1454 Butler, J. B., Lane, S. N., & Chandler, J. H. (2001). Automated extraction of grain-size data from
 1455 gravel surfaces using digital image processing. *Journal of Hydraulic Research*, 39(5), 519-529.
- 1456 Bywater-Reyes, S., Wilcox, A. C., & Diehl, R. M. (2017). Multiscale influence of woody riparian
 1457 vegetation on fluvial topography quantified with ground-based and airborne LiDAR. *Journal of*
 1458 *Geophysical Research: Earth Surface*, 122(6), 1218-1235.
- 1459 Cadol, D., Rathburn, S. L., & Cooper, D. J. (2011). Aerial photographic analysis of channel narrowing
 1460 and vegetation expansion in Canyon de Chelly National Monument, Arizona, USA, 1935–2004.
 1461 *River Research and Applications*, 27(7), 841-856. <http://dx.doi.org/10.1002/rra.1399>
- 1462 Campana, D., Marchese, E., Theule, J. I., & Comiti, F. (2014). Channel degradation and restoration
 1463 of an Alpine river and related morphological changes. *Geomorphology*, 221, 230-241.
- 1464 Carbonneau, P. E., Lane, S. N., & Bergeron, N. E. (2004). Catchment-scale mapping of surface grain
 1465 size in gravel bed rivers using airborne digital imagery. *Water resources research*, 40(7).

- 1466 Carbonneau, P. E., Bergeron, N., & Lane, S. N. (2005). Automated grain size measurements from
 1467 airborne remote sensing for long profile measurements of fluvial grain sizes. *Water Resources*
 1468 *Research*, 41(11), W11426. DOI: 10.1029/2005WR003994
- 1469 Carbonneau PE, Lane SN, Bergeron N. (2006). Feature based image processing methods applied to
 1470 bathymetric measurements from airborne remote sensing in fluvial environments. *Earth Surface*
 1471 *Processes and Landforms*, 31, 1413–1423.
- 1472 Carbonneau, P., Fonstad, M. A., Marcus, W. A., & Dugdale, S. J. (2012). Making riverscapes real.
 1473 *Geomorphology*, 137(1), 74-86. DOI: 10.1016/j.geomorph.2010.09.030
- 1474 Carbonneau, P., & Piégay, H. (Eds.). (2012). *Fluvial remote sensing for science and management*,
 1475 Chichester, UK: John Wiley & Sons, Ltd,
- 1476 Carbonneau, P. E., & Dietrich, J. T. (2017). Cost-effective non-metric photogrammetry from
 1477 consumer-grade sUAS: implications for direct georeferencing of structure from motion
 1478 photogrammetry. *Earth Surface Processes and Landforms*, 42(3), 473-486. DOI:
 1479 10.1002/esp.4012
- 1480 Carbonneau, P. E., Bizzi, S., & Marchetti, G. (2018). Robotic photosieving from low-cost multirotor
 1481 sUAS: a proof-of-concept. *Earth Surface Processes and Landforms*, 43(5), 1160-1166. DOI:
 1482 10.1002/esp.4298
- 1483 Carbonneau, P.E., Dugdale, S.J., Breckon, T.P., Dietrich, J.D., Fonstad, M.A., Miyamoto, H., &
 1484 Woodget, A.S. (*in revision*). Generalised classification of fluvial scenes with deep learning
 1485 methods. In review, *Remote Sensing of Environment*.
- 1486 Carley, J. K., Pasternack, G. B., Wyrick, J. R., Barker, J. R., Bratovich, P. M., Massa, D. A., ... &
 1487 Johnson, T. R. (2012). Significant decadal channel change 58–67 years post-dam accounting for
 1488 uncertainty in topographic change detection between contour maps and point cloud models.
 1489 *Geomorphology*, 179, 71-88.
- 1490 Casado, M., Gonzalez, R., Kriechbaumer, T., & Veal, A. (2015). Automated identification of river
 1491 hydromorphological features using UAV high resolution aerial imagery. *Sensors*, 15(11), 27969-
 1492 27989. DOI: 10.3390/s151127969
- 1493 Cassel, M., Dépret, T., & Piégay, H. (2017). Assessment of a new solution for tracking pebbles in
 1494 rivers based on active RFID. *Earth Surface Processes and Landforms*, 42(13), 1938-1951. DOI:
 1495 10.1002/esp.4152.
- 1496 Cassel, M., Piégay, H., Lavé, J., Vaudor, L., Sri, D. H., Budi, S. W., & Lavigne, F. (2018). Evaluating
 1497 a 2D image-based computerized approach for measuring riverine pebble roundness.
 1498 *Geomorphology*, 311, 143-157. <https://doi.org/10.1016/j.geomorph.2018.03.020>.
- 1499 Cassel M, Guillaume F., Ludovic B., Kristell M., Perret F., Lejot J., Piégay H. (*accepted*).
 1500 Comparison of ground-based and UAV a-UHF artificial tracer mobility monitoring protocols on a
 1501 braided river. *Earth Surface Processes and Landforms*
- 1502 Chardon, V., Schmitt L, Piégay, H., Dimitri, L. (*in review*). Terrestrial photo-sieving and airborne
 1503 topographic LiDAR to assess bed grain size in large rivers: potentials and limits.
- 1504 Cavalli, M., Tarolli, P., Marchi, L., Dalla Fontana, G. (2008). The effectiveness of airborne LiDAR
 1505 data in the recognition of channel-bed morphology. *Catena*, 73(3), 249-260.
- 1506 Cavalli, M., Trevisani, S., Comiti, F., Marchi, L. (2013). Geomorphometric assessment of spatial
 1507 sediment connectivity in small Alpine catchments. *Geomorphology*, 188, 31–41.
- 1508 Charlton, M.E., Large, A.R., Fuller, I.C. (2003). Application of airborne LiDAR in river
 1509 environments: the River Coquet, Northumberland, UK. *Earth Surface Processes and*
 1510 *Landforms*, 28(3), 299-306.

- 1511 Chenorkian, R. (2012). A new tool to overall analyze the interactions between man and his
 1512 environment, along with their dynamics: the network of Human & Environmental Observatories.
 1513 Les Observatoires Hommes-Milieus: un nouveau dispositif pour une approche intégrante des
 1514 interactions environnements-sociétés et de leurs dynamiques. *Sud-Ouest européen. Revue*
 1515 *géographique des Pyrénées et du Sud-Ouest*, (33), 3-10.
- 1516 Cislighi, A., Rigon, E., Lenzi, M. A., & Bischetti, G. B. (2018). A probabilistic multidimensional
 1517 approach to quantify large wood recruitment from hillslopes in mountainous-forested catchments.
 1518 *Geomorphology*, 306, 108-127.
- 1519 Clerici, N., Paracchini, M. L., & Maes, J. (2014). Land-cover change dynamics and insights into
 1520 ecosystem services in European stream riparian zones. *Ecohydrology & Hydrobiology*, 14(2), 107-
 1521 120.
- 1522 Clubb, F. J., Mudd, S. M., Milodowski, D. T., Hurst, M. D., & Slater, L. J. (2014). Objective
 1523 extraction of channel heads from high-resolution topographic data. *Water Resources Research*,
 1524 50(5), 4283-4304.
- 1525 Clubb, F. J., Mudd, S. M., Milodowski, D. T., Valters, D. A., Slater, L. J., Hurst, M. D., & Limaye,
 1526 A. B. (2017). Geomorphometric delineation of floodplains and terraces from objectively defined
 1527 topographic thresholds. *Earth Surface Dynamics*, 5(3).
- 1528 Comiti, F., Da Canal, M., Surian, N., Mao, L., Picco, L., & Lenzi, M. A. (2011). Channel adjustments
 1529 and vegetation cover dynamics in a large gravel bed river over the last 200 years. *Geomorphology*,
 1530 125(1), 147-159.
- 1531 CEMS GloFAS (2019), River discharge and related historical data from the Global Flood Awareness
 1532 System, DOI: 10.24381/cds.a4fdd6b9
- 1533 Corenblit, D., Tabacchi, E., Steiger, J., Gurnell, A.M. (2007). Reciprocal interactions and adjustments
 1534 between fluvial landforms and vegetation dynamics in river corridors: A review of complementary
 1535 approaches. *Earth-Science Rev.* 84, 56–86. <https://doi.org/10.1016/j.earscirev.2007.05.004>
- 1536 Corenblit, D., Steiger, J., Gurnell, A.M., Tabacchi, E., Roques, L. (2009). Control of sediment
 1537 dynamics by vegetation as a key function driving biogeomorphic succession within fluvial
 1538 corridors. *Earth Surf. Process. Landforms* 34, 1790–1810.
 1539 <https://doi.org/10.1002/esp.1876>
- 1540 Crochemore, L., Isberg, K., Pimentel, R., Pineda, L., Hasan, A.,
 1541 & Arheimer, B. (2019). Lessons learnt from checking the quality of openly accessible river flow
 1542 data worldwide. *Hydrological Sciences Journal*, <https://doi.org/10.1080/02626667.2019.1659509>
- 1543 Crutzen, P.J. (2002). Geology of mankind. *Nature* 415, 23. DOI: [10.1038/415023a](https://doi.org/10.1038/415023a)
- 1544 Cunningham, S.C., Griffioen, P., White, M.D., & Nally, R.M. (2018). Assessment of ecosystems: A
 1545 system for rigorous and rapid mapping of floodplain forest condition for Australia's most
 1546 important river. *Land Degradation & Development* 29, 127–137.
- 1547 Czuba, J. A. (2018). A Lagrangian framework for exploring complexities of mixed-size sediment
 1548 transport in gravel-bedded river networks. *Geomorphology*, 321, 146-152. DOI:
 1549 10.1016/j.geomorph.2018.08.031
- 1550 Czuba, J. A., & Fofoula-Georgiou, E. (2014). A network-based framework for identifying potential
 1551 synchronizations and amplifications of sediment delivery in river basins. *Water Resources*
 1552 *Research*, 50(5), 3826-3851. DOI: 10.1002/2013WR014227
- 1553 Darby, S. E., Leyland, J., Kumm, M., Räsänen, T. A., & Lauri, H. (2013). Decoding the drivers of
 1554 bank erosion on the Mekong river: The roles of the Asian monsoon, tropical storms, and
 snowmelt. *Water Resources Research*, 49(4), 2146-2163.

- 1555 Demarchi, L., Bizzi, S., & Piégay, H. (2016). Hierarchical object-based mapping of riverscape units
1556 and in-stream mesohabitats using LiDAR and VHR imagery. *Remote Sensing*, 8(2), 97. DOI:
1557 10.3390/rs8020097
- 1558 Demarchi, L., Bizzi, S., & Piégay, H. (2017). Regional hydromorphological characterization with
1559 continuous and automated remote sensing analysis based on VHR imagery and low-resolution
1560 LiDAR data. *Earth Surface Processes and Landforms*, 42(3), 531-551. DOI: 10.1002/esp.4092
- 1561 Dépret, T., Riquier, J., & Piégay, H. (2017). Evolution of abandoned channels: Insights on controlling
1562 factors in a multi-pressure river system. *Geomorphology*, 294, 99-118.
- 1563 Detert, M., & Weitbrecht, V. (2012). Automatic object detection to analyze the geometry of gravel
1564 grains—a free stand-alone tool. In: River flow 2012: Proceedings of the international conference
1565 on fluvial hydraulics, San José, Costa Rica, 5-7. Taylor & Francis Group London, 595-600.
- 1566 Dewan, A., Corner, R., Saleem, A., Rahman, M.M., Haider, M.R., Rahman, M.M., Sarker, M.H.
1567 (2017). Assessing channel changes of the Ganges-Padma River system in Bangladesh using
1568 Landsat and hydrological data. *Geomorphology*, 276, 257–279.
- 1569 Dick, J., Orenstein, D. E., Holzer, J. M., Wohnner, C., Achard, A. L., Andrews, C., ... & Van
1570 Ryckegem, G. (2018). What is socio-ecological research delivering? A literature survey across 25
1571 international LTSER platforms. *Science of the Total Environment*, 622, 1225-1240.
- 1572 Diepenbroek, M, Bartholomä, A, Ibbeken, H. (1992). How round is round? A new approach to the
1573 topic ‘roundness’ by Fourier grain shape analysis. *Sedimentology* 39: 411–422. DOI:
1574 10.1111/j.1365-3091.1992.tb02125.x
- 1575 Dietrich, J.T. (2016). Riverscape mapping with helicopter-based Structure-from-Motion
1576 photogrammetry. *Geomorphology*, 252, 144-157.
- 1577 Dietrich, J. T. (2017). Bathymetric structure-from-motion: extracting shallow stream bathymetry
1578 from multi-view stereo photogrammetry. *Earth Surface Processes and Landforms*, 42(2), 355-364.
- 1579 Dietrich, W. E., Kirchner, J. W., Ikeda, H., & Iseya, F. (1989). Sediment supply and the development
1580 of the coarse surface layer in gravel-bedded rivers. *Nature*, 340(6230), 215-217.
- 1581 Do, H. X., Gudmundsson, L., Leonard, M., Westra, S., & Grabs, W. (2018). The Global Streamflow
1582 Indices and Metadata Archive (GSIM)-Part 1: The production of a daily streamflow archive and
1583 metadata. *Earth System Science Data*, 10(2).
- 1584 Domokos, G, Jerolmack, DJ, Sipos, AÁ, Török, Á. (2014). How river rocks round: Resolving the
1585 shape-size paradox. *PLoS ONE* 9: 1–7. DOI: 10.1371/journal.pone.0088657
- 1586 Donchyts, G, Baart, F., Winsemius, H., Gorelick, N., Kwadijk, J., Van De Giesen N. (2016). Earth’s
1587 surface water change over the past 30 years, 2016. *Nature Climate Change*, 6 (9), 810.
1588 <https://doi.org/10.1038/nclimate3111>
- 1589 Downs, P.W., Soar, P.J., Taylor, A. (2016). The anatomy of effective discharge: the dynamics of
1590 coarse sediment transport revealed using continuous bedload monitoring in a gravel-bed river
1591 during a very wet year. *Earth Surface Processes and Landforms*, 41(2), 147-161.
- 1592 Downs, P.W. & Piégay H. (2019). Catchment-scale cumulative impact of human activities on river
1593 channels in the late Anthropocene: implications, analytical limitations and prospect.
1594 *Geomorphology* 338, 88–104. <https://doi.org/10.1016/j.geomorph.2019.03.021>.
- 1595 Dufour, S., Barsoum, N., Muller, E., & Piégay, H. (2007). Effects of channel confinement on pioneer
1596 woody vegetation structure, composition and diversity along the River Drôme (SE France). *Earth
1597 Surface Processes and Landforms*, 32(8), 1244-1256.

- 1598 Dufour, S., & Piégay, H. (2009). From the myth of a lost paradise to targeted river restoration: forget
 1599 natural references and focus on human benefits. *River research and applications*, 25(5), 568-581.
 1600 DOI: 10.1002/rra.1239.
- 1601 Dufour, S., Muller, E., Straatsma, M., & Corgne, S. (2012). Image Utilisation for the Study and
 1602 Management of Riparian Vegetation: Overview and Applications. In: Carbonneau, P.E., & Piégay,
 1603 H. (Eds), *Fluvial Remote Sensing for Science and Management*, Chichester, UK: John Wiley &
 1604 Sons, Ltd, Chapter 10, 215–239.
- 1605 Dufour, S., Rinaldi, M., Piégay, H., & Michalon, A. (2015). How do river dynamics and human
 1606 influences affect the landscape pattern of fluvial corridors? Lessons from the Magra River,
 1607 Central–Northern Italy. *Landscape and Urban Planning*, 134, 107-118.
- 1608 Dunesme S., Melun G., Mustière S., Piégay H., 2018. Automatic vectorization of historical maps: a
 1609 way to characterize fluvial corridors evolution at a regional scale? Conference I.S.Rivers 2018,
 1610 Lyon, France, 3 p.
- 1611 Džubáková, K., Molnar, P., Schindler, K., & Trizna, M. (2015). Monitoring of riparian vegetation
 1612 response to flood disturbances using terrestrial photography. *Hydrology and Earth System
 1613 Sciences*, 19(1), 195-208. DOI: 10.5194/hess-19-195-2015.
- 1614 Entwistle, N. S., & Fuller, I. C. (2009). Terrestrial laser scanning to derive the surface grain size
 1615 facies character of gravel bars. *Laser Scanning for the Environmental Sciences*, 102-114.
- 1616 Entwistle, N., Heritage, G., & Milan, D. (2018). Recent remote sensing applications for hydro and
 1617 morphodynamic monitoring and modelling. *Earth Surface Processes and Landforms*, 43(10),
 1618 2283-2291. <https://doi.org/10.1002/esp.4378>
- 1619 Farid, A., Rautenkranz, D., Goodrich, D. C., Marsh, S. E., & Sorooshian, S. (2006). Riparian
 1620 vegetation classification from airborne laser scanning data with an emphasis on cottonwood trees.
 1621 *Canadian Journal of Remote Sensing*, 32(1), 15-18.
- 1622 Feurer D, Bailly J-S, Puech C, Le Coarer Y, Viau AA. (2008). Very-high-resolution mapping of river-
 1623 immersed topography by remote sensing. *Progress in Physical Geography*, 32, 403–419.
- 1624 Fonstad MA, Marcus WA. (2005). Remote sensing of stream depths with hydraulically assisted
 1625 bathymetry (HAB) models. *Geomorphology*, 72, 320–339.
- 1626 Fonstad, M. A., Dietrich, J. T., Courville, B. C., Jensen, J. L., & Carbonneau, P. E. (2013).
 1627 Topographic structure from motion: a new development in photogrammetric measurement. *Earth
 1628 Surface Processes and Landforms*, 38(4), 421-430.
- 1629 Fryirs, K. A., & Brierley, G. J. (2012). *Geomorphic analysis of river systems: an approach to reading
 1630 the landscape*. John Wiley & Sons.
- 1631 Fryirs, K. A., Brierley, G. J., & Erskine, W. D. (2012). Use of ergodic reasoning to reconstruct the
 1632 historical range of variability and evolutionary trajectory of rivers. *Earth Surface Processes and
 1633 Landforms*, 37(7), 763-773. DOI: 10.1002/esp.3210
- 1634 Fryirs, K. (2013). (Dis) Connectivity in catchment sediment cascades: a fresh look at the sediment
 1635 delivery problem. *Earth Surface Processes and Landforms*, 38(1), 30-46. DOI: 10.1002/esp.3242
- 1636 Fryirs, K. A. (2017). River sensitivity: a lost foundation concept in fluvial geomorphology. *Earth
 1637 Surface Processes and Landforms*, 42(1), 55-70. DOI: 10.1002/esp.3940
- 1638 Fryirs, K. A., Wheaton, J., Bizzi, S., Williams, R., & Brierley, G. J., (2019). To plug-in or not to plug-
 1639 in? Geomorphic analysis of rivers using the River Styles Framework in an era of big data
 1640 acquisition and automation, WiresWater, <https://doi.org/10.1002/wat2.1372> [on-line]
- 1641 Gasser, E, Schwarz, M, Simon, A, Perona, P, Phillips, C, Hübl, J, Dorren, L. (2019). A review of
 1642 modeling the effects of vegetation on large wood recruitment processes in mountain catchments.
 1643 *Earth-Science Reviews* DOI: 10.1016/j.earscirev.2019.04.013 [online]

- 1644 Geerling, G. W., Vreeken-Buijs, M. J., Jesse, P., Ragas, A. M. J., & Smits, A. J. M. (2009). Mapping
 1645 river floodplain ecotopes by segmentation of spectral (CASI) and structural (LiDAR) remote
 1646 sensing data. *River research and applications*, 25(7), 795-813.
- 1647 Gilbert, G. K. (1917). *Hydraulic-mining debris in the Sierra Nevada* (No. 105). US Government
 1648 Printing Office: Menlo Park, CA.
- 1649 Gilbert, J. T., Macfarlane, W. W., & Wheaton, J. M. (2016). The Valley Bottom Extraction Tool (V-
 1650 BET): A GIS tool for delineating valley bottoms across entire drainage networks. *Computers &
 1651 geosciences*, 97, 1-14. DOI: 10.1016/j.cageo.2016.07.014
- 1652 Gilvear, D., Winterbottom, S., & Sickingabula, H. (2000). Character of channel planform change and
 1653 meander development: Luangwa River, Zambia. *Earth Surface Processes and Landforms*, 25(4),
 1654 421-436.
- 1655 Gilvear, D., & Bryant, R. (2016). Analysis of remotely sensed data for fluvial geomorphology and
 1656 river science. In Kondolf, G.M. & Piégay, H. (eds.): *Tools in Fluvial Geomorphology, Second
 1657 Edition*. Chichester, UK: John Wiley & Sons, 103-132.
- 1658 Gilvear, D. J., Hunter, P., Stewardson, M., Greenwood, M. T., Thoms, M. C., & Wood, P. J. (2016).
 1659 Remote sensing: mapping natural and managed river corridors from the micro to the network scale.
 1660 In Gilvear, D. J., Greenwood, M. T., Thoms, M. C., & Wood, P. J. (eds): *River science: Research
 1661 and management for the 21st century*, 171-196.
- 1662 Giuliani, G, Chatenoux, B, De Bono, A, Rodila, D, Richard, J-P, Allenbach, K, Dao, H, Peduzzi, P.
 1663 (2017). Building an Earth Observations Data Cube: lessons learned from the Swiss Data Cube
 1664 (SDC) on generating Analysis Ready Data (ARD). *Big Earth Data* 1: 100–117. DOI:
 1665 10.1080/20964471.2017.1398903
- 1666 Gob, F., Bilodeau, C., Thommeret, N., Belliard, J., Albert, M. B., Tamisier, V., ... & Kreutzenberger,
 1667 K. (2014). Un outil de caractérisation hydromorphologique des cours d'eau pour l'application de
 1668 la DCE en France (CARHYCE). *Géomorphologie: relief, processus, environnement*, 20(1), 57-
 1669 72. DOI: 10.4000/geomorphologie.10497
- 1670 Goetz, S. J. (2006). Remote sensing of riparian buffers: Past progress and future prospects. *JAWRA
 1671 Journal of the American Water Resources Association*, 42(1), 133-143.
- 1672 Golly, A. and Turowski, J. M. (2017). Deriving principal channel metrics from bank and long-profile
 1673 geometry with the R package cmgo, *Earth Surf. Dynam.*, 5, 557-570,
 1674 <https://doi.org/10.5194/esurf-5-557-2017>.
- 1675 Grabowski, R.C., Surian, N., & Gurnell, A.M. (2014). Characterizing geomorphological change to
 1676 support sustainable river restoration and management. *WIREs Water* 2014, 1:483–512. doi:
 1677 10.1002/wat2.1037.
- 1678 Grabowski, R. C., & Gurnell, A. M. (2016). Using historical data in fluvial geomorphology. In:
 1679 Kondolf, G.M., & Piégay, H., (eds). *Tools in Fluvial Geomorphology*. Chichester, UK: John Wiley
 1680 & Sons, 56-76.
- 1681 Graham, D. J., Reid, I., & Rice, S. P. (2005 a). Automated sizing of coarse-grained sediments: image-
 1682 processing procedures. *Mathematical Geology*, 37(1), 1-28.
- 1683 Graham, D. J., Rice, S. P., & Reid, I. (2005 b). A transferable method for the automated grain sizing
 1684 of river gravels. *Water Resources Research*, 41(7).
- 1685 Green, R. H. (1979). *Sampling design and statistical methods for environmental biologists*. John
 1686 Wiley & Sons.

- 1687 Gregory, V. & Meleason, M. A. (2003). Modeling the Dynamics of Wood in Streams and Rivers
1688 History of Wood Models. In: Gregory, S. V, Boyer, K. L. & Gurnell, A. M. (Eds.). *The Ecology*
1689 *and Management of Wood in World Rivers*.
- 1690 Grigillo, D., Vrečko, A., Mikoš, M., Gvozdanović, T., Anžur, A., & Petrovič, D. (2015).
1691 Determination of large wood accumulation in a steep forested torrent using laser scanning. In
1692 *Engineering Geology for Society and Territory-Volume 3* (pp. 127-130). Springer, Cham.
- 1693 Grosso, C., & Azimi-Gaylon, S. (2018). Delta Environmental Data to Understand a California Estuary
1694 (DEDUCE): An Estuary-Wide Data Repository. In *I.S.Rivers International Conference 2018,*
1695 *Lyon, France*.
- 1696 Grill, G., B. Lehner, M. Thieme, B. Geenen, D. Tickner, F. Antonelli, S. Babu, P. Borrelli, L. Cheng,
1697 Crochetiere, H., ... & Zarfl, C. (2019). Mapping the world's free-flowing rivers. *Nature* 569, 7755:
1698 215.
- 1699 Guerit, L., Barrier, L., Narteau, C., Métivier, F., Liu, Y., Lajeunesse, E., ... & Ye, B. (2014). The
1700 Grain-size Patchiness of Braided Gravel-Bed Streams—example of the Urumqi River (northeast
1701 Tian Shan, China). *Advances in Geosciences*, 37, 27-39.
- 1702 Gurnell, A. M., Downward, S. R. Jones, R. (1994). Channel planform change on the river dee
1703 meanders, 1876–1992. *Regul. Rivers: Res. Mgmt.*, 9: 187-204.
- 1704 Gurnell, A.M., Bertoldi, W., Corenblit, D., (2012). Changing river channels: The roles of
1705 hydrological processes, plants and pioneer fluvial landforms in humid temperate, mixed load,
1706 gravel bed rivers. *Earth-Science Rev.* 111, 129–141.
1707 <https://doi.org/10.1016/j.earscirev.2011.11.005>
- 1708 Gurnell, A. M., Rinaldi, M., Belletti, B., Bizzi, S., Blamauer, B., Braca, G., ... & Demarchi, L. (2016).
1709 A multi-scale hierarchical framework for developing understanding of river behaviour to support
1710 river management. *Aquatic Sciences*, 78(1), 1-16. <https://doi.org/10.1007/s00027-015-0424-5>.
- 1711 Haase, P., Frenzel, M., Klotz, S., Musche, M., & Stoll, S. (2016). The long-term ecological research
1712 (LTER) network: Relevance, current status, future perspective and examples from marine,
1713 freshwater and terrestrial long-term observation. *Ecological Indicators*, (65), 1-3.
- 1714 Hammersmark, C. T., Dobrowski, S. Z., Rains, M. C., & Mount, J. F. (2010). Simulated effects of
1715 stream restoration on the distribution of wet-meadow vegetation. *Restoration Ecology*, 18(6), 882-
1716 893.
- 1717 Hayakawa, Y, Oguchi, T. (2005). Evaluation of gravel sphericity and roundness based on surface-
1718 area measurement with a laser scanner. *Computers and Geosciences* 31: 735–741. DOI:
1719 10.1016/j.cageo.2005.01.004
- 1720 Heckmann, T., & Schwanghart, W. (2013). Geomorphic coupling and sediment connectivity in an
1721 alpine catchment—Exploring sediment cascades using graph theory. *Geomorphology*, 182, 89-
1722 103. DOI: 10.1016/j.geomorph.2012.10.033.
- 1723 Heckmann, T., Schwanghart, W., & Phillips, J. D. (2015). Graph theory—Recent developments of
1724 its application in geomorphology. *Geomorphology*, 243, 130-146. DOI:
1725 10.1016/j.geomorph.2014.12.024.
- 1726 Heckmann, T., Haas, F., Abel, J., Rimböck, A., & Becht, M. (2017). Feeding the hungry river: Fluvial
1727 morphodynamics and the entrainment of artificially inserted sediment at the dammed river Isar,
1728 Eastern Alps, Germany. *Geomorphology*, 291, 128-142. DOI:
1729 <https://doi.org/10.1016/j.geomorph.2017.01.025>

- 1730 Heckmann, T., Cavalli, M., Cerdan, O., Foerster, S., Javaux, M., Lode, E., ... & Brardinoni, F. (2018).
 1731 Indices of sediment connectivity: opportunities, challenges and limitations. *Earth-science reviews*,
 1732 187, 77–108. DOI: 10.1016/j.earscirev.2018.08.004
- 1733 Henshaw, A. J., Gurnell, A. M., Bertoldi, W., & Drake, N. A. (2013). An assessment of the degree to
 1734 which Landsat TM data can support the assessment of fluvial dynamics, as revealed by changes in
 1735 vegetation extent and channel position, along a large river. *Geomorphology*, 202, 74-85.
- 1736 Hervouet, A., Dunford, R., Piégay, H., Belletti, B., & Trémélo, M. L. (2011). Analysis of post-flood
 1737 recruitment patterns in braided-channel rivers at multiple scales based on an image series collected
 1738 by unmanned aerial vehicles, ultra-light aerial vehicles, and satellites. *GIScience & Remote
 1739 Sensing*, 48(1), 50-73.
- 1740 Heritage, G. L., & Milan, D. J. (2009). Terrestrial laser scanning of grain roughness in a gravel-bed
 1741 river. *Geomorphology*, 113(1-2), 4-11.
- 1742 Hersbach, H., de Rosnay, P., Bell, B., Schepers, D., Simmons, A., Soci, C., Abdalla, S., Alonso-
 1743 Balmaseda, M., Balsamo, G., Bechtold, P., Berrisford, P., Bidlot, J.-R., de Boissésón, E., Bonavita,
 1744 M., Browne, P., Buizza, R., Dahlgren, P., Dee, D., Dragani, R., Diamantakis, M., Flemming, J.,
 1745 Forbes, R., Geer, A. J., Haiden, T., Hólm, E., Haimberger, L., Hogan, R., Horányi, A., Janiskova,
 1746 M., Laloyaux, P., Lopez, P., Muñoz-Sabater, J., Peubey, C., Radu, R., Richardson, D., Thépaut,
 1747 J.-N., Vitart, F., Yang, X., Zsótér, E., and Zuo, H.: (2018). Operational global reanalysis: progress,
 1748 future directions and synergies with NWP. European Centre for Medium Range Weather
 1749 Forecasts.
- 1750 Hicks, D. M., Shankar, U., Duncan, M. J., Rebuffé, M., & Aberle, J. (2009). Use of remote-sensing
 1751 with two-dimensional hydrodynamic models to assess impacts of hydro-operations on a large,
 1752 braided, gravel-bed river: Waitaki River, New Zealand. In: Sambrook Smith, G.H., Best, J.L.,
 1753 Bristow, C.S., Petts, G.E. & Jarvis, I. (eds) *Braided Rivers: Process, Deposits, Ecology and
 1754 Management*, John Wiley and Sons: Chichester, 311-326.
- 1755 Hirpa, F. A., Hopson, T. M., De Groeve, T., Brakenridge, G. R., Gebremichael, M., & Restrepo, P.
 1756 J. (2013). Upstream satellite remote sensing for river discharge forecasting: Application to major
 1757 rivers in South Asia. *Remote Sensing of Environment*, 131, 140-151.
- 1758 Hobbs, R. J., Arico, S., Aronson, J., Baron, J. S., Bridgewater, P., Cramer, V. A., ... & Norton, D.
 1759 (2006). Novel ecosystems: theoretical and management aspects of the new ecological world order.
 1760 *Global ecology and biogeography*, 15(1), 1-7.
- 1761 Hodge, R., Brasington, J., & Richards, K. (2009). In situ characterization of grain-scale fluvial
 1762 morphology using Terrestrial Laser Scanning. *Earth Surface Processes and Landforms*, 34(7),
 1763 954-968.
- 1764 Hooke, J. (2003). River meander behaviour and instability: a framework for analysis. *Transactions
 1765 of the Institute of British Geographers*, 28(2), 238-253.
- 1766 Horacio, J., Dunesme, S., Piégay, H. (on line) Comparison of historical topographic maps across four
 1767 countries to characterise river corridor evolution at a continental scale. River Research and
 1768 Applications
- 1769 Hortobágyi, B., Corenblit, D., Vautier, F., Steiger, J., Roussel, E., Burkart, A., & Peiry, J. L. (2017).
 1770 A multi-scale approach of fluvial biogeomorphic dynamics using photogrammetry. *Journal of
 1771 environmental management*, 202, 348-362.
- 1772 Huang, W. C., Young, C. C., & Liu, W. C. (2018). Application of an automated discharge imaging
 1773 system and LSPIV during typhoon events in Taiwan. *Water*, 10(3), 280.
 1774 <https://doi.org/10.3390/w10030280>.

- 1775 Husson, E., Ecke, F., & Reese, H. (2016). Comparison of manual mapping and automated object-
1776 based image analysis of non-submerged aquatic vegetation from very-high-resolution UAS
1777 images. *Remote Sensing*, 8(9), 724.
- 1778 Ibbeken, H., & Schleyer, R. (1986). Photo-sieving: A method for grain-size analysis of coarse-
1779 grained, unconsolidated bedding surfaces. *Earth Surface Processes and Landforms*, 11(1), 59-
1780 77. Isikdogan, F., Bovik, A., & Passalacqua, P. (2017). RivaMap: An automated river analysis and
1781 mapping engine. *Remote Sensing of Environment*, 202, 88-97.
1782 <https://doi.org/10.1016/j.rse.2017.03.044>.
- 1783 Jain, V., Preston, N., Fryirs, K., & Brierley, G. (2006). Comparative assessment of three approaches
1784 for deriving stream power plots along long profiles in the upper Hunter River catchment, New
1785 South Wales, Australia. *Geomorphology*, 74(1-4), 297-317.
- 1786 James, L. A. (1991). Incision and morphologic evolution of an alluvial channel recovering from
1787 hydraulic mining sediment. *Geological Society of America Bulletin*, 103(6), 723-736. DOI:
1788 10.1130/0016-7606(1991)103<0723.
- 1789 James, A. (1999). Time and the persistence of alluvium: River engineering, fluvial geomorphology,
1790 and mining sediment in California. *Geomorphology*, 31(1-4), 265-290. DOI: 10.1016/S0169-
1791 555X(99)00084-7.
- 1792 James, M. R., & Robson, S. (2012). Straightforward reconstruction of 3D surfaces and topography
1793 with a camera: Accuracy and geoscience application. *Journal of Geophysical Research: Earth
1794 Surface*, 117(F3).
- 1795 James LA, Hodgson ME, Ghoshal S, Latiolais MM. (2012). Geomorphic change detection using
1796 historic maps and DEM differencing: The temporal dimension of geospatial analysis.
1797 *Geomorphology*, 137, 181–198.
- 1798 James MR, Robson S. (2014). Mitigating systematic error in topographic models derived from UAV
1799 and ground-based image networks. *Earth Surface Processes and Landforms*, 39, 1413–1420.
- 1800 James, M. R., Robson, S., d'Oleire-Oltmanns, S., & Niethammer, U. (2017). Optimising UAV
1801 topographic surveys processed with structure-from-motion: Ground control quality, quantity and
1802 bundle adjustment. *Geomorphology*, 280, 51-66.
- 1803 Jodeau, M., Hauet, A., & Bercovitz, Y. (2017). Laboratory and field LSPIV measurements of flow
1804 velocities using Fudaa-LSPIV a free user-friendly software, In: HydroSenSoft, *Proc. 1st
1805 International Symposium and Exhibition on Hydro-Environment Sensors and Software*. 82-86.
- 1806 Johansen, K., Phinn, S., & Witte, C. (2010). Mapping of riparian zone attributes using discrete return
1807 LiDAR, QuickBird and SPOT-5 imagery: Assessing accuracy and costs. *Remote Sensing of
1808 Environment*, 114(11), 2679-2691.
- 1809 Johansen, K., Coops, N. C., Gergel, S. E., & Stange, Y. (2007). Application of high spatial resolution
1810 satellite imagery for riparian and forest ecosystem classification. *Remote sensing of Environment*,
1811 110(1), 29-44.
- 1812 Jugie, M., Gob, F., Virmoux, C., Brunstein, D., Tamisier, V., Le Coeur, C., & Grancher, D. (2018).
1813 Characterizing and quantifying the discontinuous bank erosion of a small low energy river using
1814 Structure-from-Motion Photogrammetry and erosion pins. *Journal of hydrology*, 563, 418-434.
- 1815 Kaneko, K., & Nohara, S. (2014). Review of effective vegetation mapping using the UAV
1816 (Unmanned Aerial Vehicle) method. *Journal of Geographic Information System*, 6(06), 733.
- 1817 Kasprak, A., Magilligan, F. J., Nislow, K. H., & Snyder, N. P. (2012). A LiDAR -derived evaluation
1818 of watershed-scale large woody debris sources and recruitment mechanisms: Coastal Maine, USA.
1819 *River Research and Applications*, 28(9), 1462-1476.

- 1820 Kondolf, G. M., Piégay, H., & Landon, N. (2007). Changes in the riparian zone of the lower Eygues
 1821 River, France, since 1830. *Landscape Ecology*, 22(3), 367-384.
- 1822 Kinzel PJ, Wright CW, Nelson JM, Burman AR. (2007). Evaluation of an experimental LiDAR for
 1823 surveying a shallow, braided, sand-bedded river. *Journal of Hydraulic Engineering*, **133**, 838–842.
- 1824 Kramer, N., & Wohl, E. (2014). Estimating fluvial wood discharge using time-lapse photography
 1825 with varying sampling intervals. *Earth Surface Processes and Landforms*, 39(6), 844-852.
 1826 <https://doi.org/10.1002/esp.3540>
- 1827 Kramer, N., Bangen, S. G., Wheaton, J. M., Bouwes, N., Wall, E., Saunders, C., ... & Fortney, S.
 1828 (2017). Geomorphic Unit Tool (GUT): Applications of Fluvial Mapping. In *AGU Fall Meeting*
 1829 *Abstracts*. EP11A-1546. AGU, New Orleans, LA, 11-15 Dec. DOI:
 1830 [10.13140/RG.2.2.30142.18241](https://doi.org/10.13140/RG.2.2.30142.18241)
- 1831 Kui, L., Stella, J. C., Shafroth, P. B., House, P. K., & Wilcox, A. C. (2017). The long-term legacy of
 1832 geomorphic and riparian vegetation feedbacks on the dammed Bill Williams River, Arizona, USA.
 1833 *Ecohydrology*, 10(4). <https://doi.org/10.1002/eco.1839>
- 1834 Lallias-Tacon, S., Liébault, F., & Piégay, H. (2014). Step by step error assessment in braided river
 1835 sediment budget using airborne LiDAR data. *Geomorphology*, 214, 307-323
- 1836 Lallias-Tacon, S., Liébault, F., & Piégay, H. (2017). Use of airborne LiDAR and historical aerial
 1837 photos for characterising the history of braided river floodplain morphology and vegetation
 1838 responses. *Catena*, 149, 742-759.
- 1839 Lane, S.N., Richards, K.S., & Chandler, J.H. (1994). Developments in monitoring and modelling
 1840 small-scale river bed topography. *Earth Surface Processes and Landforms*, **19**, 349–368.
- 1841 Lane, S.N., Richards, K.S., & Chandler, J.H. (1995). Morphological estimation of the time-integrated
 1842 bed load transport rate. *Water Resources Research*, **31**, 761–772.
- 1843 Lane, S. N. (2000). The measurement of river channel morphology using digital photogrammetry.
 1844 *The Photogrammetric Record*, 16(96), 937-961.
- 1845 Lane, S. N., Westaway, R. M., & Murray Hicks, D. (2003). Estimation of erosion and deposition
 1846 volumes in a large, gravel-bed, braided river using synoptic remote sensing. *Earth Surface*
 1847 *Processes and Landforms*, 28(3), 249-271.
- 1848 Lane SN, Widdison PE, Thomas RE, Ashworth PJ, Best JL, Lunt IA, Sambrook Smith GH, Simpson
 1849 CJ. (2010). Quantification of braided river channel change using archival digital image analysis.
 1850 *Earth Surface Processes and Landforms*, **35**, 971–985.
- 1851 Langhammer, J., & Vacková, T. (2018). Detection and mapping of the geomorphic effects of flooding
 1852 using UAV photogrammetry. *Pure and Applied Geophysics*, 175, 3223-3245.
 1853 doi:10.1007/s00024-018-1874-1
- 1854 Laslier, M., Hubert-Moy, L., & Dufour, S. (2019a). Mapping Riparian Vegetation Functions Using
 1855 3D Bispectral LiDAR Data. *Water*, 11(3), 483.
- 1856 Laslier, M., Corpetti, T., Hubert-Moy, L., & Dufour, S. (2019b). Monitoring the colonization of
 1857 alluvial deposits using multitemporal UAV RGB-imagery. *Applied Vegetation Science*, DOI:
 1858 [10.1111/avsc.12455](https://doi.org/10.1111/avsc.12455)
- 1859 Lassetre, N. S., Piégay, H., Dufour, S., & Rollet, A. J. (2008). Decadal changes in distribution and
 1860 frequency of wood in a free meandering river, the Ain River, France. *Earth Surface Processes and*
 1861 *Landforms*, 33(7), 1098-1112.
- 1862 Lauer, W. J. (2006). Planform Statistics, NCED Stream Restoration Toolbox. National Center for
 1863 Earth-Surface Dynamics, University of Minnesota, Minneapolis, MN, St. Anthony Falls Lab.

- 1864 Le Boursicaud, R., Pénard, L., Hauet, A., Thollet, F., & Le Coz, J. (2016). Gauging extreme floods
 1865 on YouTube: application of LSPIV to home movies for the post-event determination of stream
 1866 discharges. *Hydrological Processes*, *30*(1), 90-105. <https://doi.org/10.1002/hyp.10532>
- 1867 Le Coz, J., Hauet, A., Pierrefeu, G., Dramais, G., & Camenen, B. (2010). Performance of image-
 1868 based velocimetry (LSPIV) applied to flash-flood discharge measurements in Mediterranean
 1869 rivers. *Journal of hydrology*, *394*(1-2), 42-52. doi:10.1016/j.jhydrol.2010.05.049
- 1870 Le Coz, J., Patalano, A., Collins, D., Guillén, N. F., García, C. M., Smart, G. M., ... & Braud, I.
 1871 (2016). Crowdsourced data for flood hydrology: Feedback from recent citizen science projects in
 1872 Argentina, France and New Zealand. *Journal of Hydrology*, *541*, 766-777.
 1873 doi:10.1016/j.jhydrol.2016.07.036
- 1874 Lehmann, A, Giuliani, G, Ray, N, Rahman, K, Abbaspour, KC, Nativi, S, Craglia, M, Cripe, D,
 1875 Quevauviller, P, Beniston, M. (2014). Reviewing innovative Earth observation solutions for filling
 1876 science-policy gaps in hydrology. *Journal of DOI: 10.1016/j.jhydrol.2014.05.059*
- 1877 Lehmann, A, Chaplin-Kramer, R, Lacayo, M, Giuliani, G, Thau, D, Koy, K, Goldberg, G, Sharp, R.
 1878 (2017). Lifting the information barriers to address sustainability challenges with data from
 1879 physical geography and Earth observation. *Sustainability (Switzerland)* **9**: 1–15. DOI:
 1880 10.3390/su9050858
- 1881 Legleiter, C. J. (2012). Remote measurement of river morphology via fusion of LiDAR topography
 1882 and spectrally based bathymetry. *Earth Surface Processes and Landforms*, *37*(5), 499-518.
- 1883 Legleiter CJ, Overstreet BT, Glennie CL, Pan Z, Fernandez-Diaz JC, & Singhanian A. (2016).
 1884 Evaluating the capabilities of the CASI hyperspectral imaging system and Aquarius bathymetric
 1885 LiDAR for measuring channel morphology in two distinct river environments. *Earth Surface*
 1886 *Processes and Landforms*, **41**, 344–363.
- 1887 Lehner, B., Verdin, K., and Jarvis, A. 2008. New global hydrography derived from spaceborne
 1888 elevation data. *Eos, Trans. Am. Geophys. Union* *89*(10), 93–94.
- 1889 Lehner, B., Liermann, C. R., Revenga, C., Vörösmarty, C., Fekete, B., Crouzet, P., ... & Nilsson, C.
 1890 (2011). Global reservoir and dam (grand) database. *Technical Documentation, Version, 1*.
- 1891 Liébault, F., Piégay, H. (2002). Causes of 20th century channel narrowing in mountain and piedmont
 1892 rivers of Southeastern France. *Earth Surface Processes and Landforms*, **27**, 425-444
- 1893 Liébault, F., Clément, P., Piégay, H., Rogers, C. F., Kondolf, G. M., & Landon, N. (2002).
 1894 Contemporary channel changes in the Eygues basin, southern French Prealps: the relationship of
 1895 subbasin variability to watershed characteristics. *Geomorphology*, *45*(1-2), 53-66.
- 1896 Liébault, F., Bellot, H., Chapuis, M., Klotz, S., & Deschâtres, M. (2012). Bedload tracing in a high-
 1897 sediment-load mountain stream. *Earth Surface Processes and Landforms*, *37*(4), 385-399. DOI:
 1898 10.1002/esp.2245
- 1899 Liébault, F., Lallias-Tacon, S., Cassel, M., & Talaska, N. (2013). Long profile responses of alpine
 1900 braided rivers in SE France. *River Research and Applications*, *29*(10), 1253-1266.
- 1901 Lindsey, D.A., Langer, W.H., Van Gosen, B.S. (2007). Using pebble lithology and roundness to
 1902 interpret gravel provenance in piedmont fluvial systems of the Rocky Mountains, USA.
 1903 *Sedimentary Geology* **199**: 223–232. DOI: 10.1016/j.sedgeo.2007.02.006
- 1904 Litty, C, Schlunegger, F. (2016). Controls on Pebbles' Size and Shape in Streams of the Swiss Alps.
 1905 *The Journal of Geology* **125**: 101–112. DOI: 10.1086/689183
- 1906 Loicq, P., Moatar, F., Jullian, Y., Dugdale, S. J., & Hannah, D. M. (2018). Improving representation
 1907 of riparian vegetation shading in a regional stream temperature model using LiDAR data. *Science*
 1908 *of the Total Environment*, *624*, 480-490.

- 1909 Macfarlane, W. W., Gilbert, J. T., Jensen, M. L., Gilbert, J. D., Hough-Snee, N., McHugh, P. A., ...
1910 & Bennett, S. N. (2017). Riparian vegetation as an indicator of riparian condition: Detecting
1911 departures from historic condition across the North American West. *Journal of environmental*
1912 *management*, 202, 447-460. <https://doi.org/10.1016/j.jenvman.2016.10.054>
- 1913 MacVicar, B. J., Piégay, H., Henderson, A., Comiti, F., Oberlin, C., & Pecorari, E. (2009).
1914 Quantifying the temporal dynamics of wood in large rivers: field trials of wood surveying, dating,
1915 tracking, and monitoring techniques. *Earth Surface Processes and Landforms*, 34(15), 2031-2046.
- 1916 MacVicar, B.J., Hauet, A., Bergeron, N., Tougne, L., Ali, I. (2012). River Monitoring with Ground-
1917 based Videography. In: Carbonneau, P.E., & Piégay, H. (Eds), *Fluvial Remote Sensing for Science*
1918 *and Management*, Chichester, UK: John Wiley & Sons, Ltd
- 1919 MacVicar, B., & Piégay, H. (2012). Implementation and validation of video monitoring for wood
1920 budgeting in a wandering piedmont river, the Ain River (France). *Earth Surface Processes and*
1921 *Landforms*, 37(12), 1272-1289.
- 1922 Mandlbürger, G., Hauer, C., Wieser, M., & Pfeifer, N. (2015). Topo-bathymetric LiDAR for
1923 monitoring river morphodynamics and instream habitats—A case study at the Pielach River.
1924 *Remote Sensing*, 7(5), 6160-6195.
- 1925 Marchese, E., Scorpio, V., Fuller, I., McColl, S., & Comiti, F. (2017). Morphological changes in
1926 Alpine rivers following the end of the Little Ice Age. *Geomorphology*, 295, 811-826.
- 1927 Marcus WA. (2002). Mapping of stream microhabitats with high spatial resolution hyperspectral
1928 imagery. *Journal of geographical systems* 4, 113–126.
- 1929 Marcus, W. A., Marston, R. A., Colvard Jr, C. R., & Gray, R. D. (2002). Mapping the spatial and
1930 temporal distributions of woody debris in streams of the Greater Yellowstone Ecosystem, USA.
1931 *Geomorphology*, 44(3-4), 323-335.
- 1932 Marcus, W. A., Legleiter, C. J., Aspinall, R. J., Boardman, J. W., & Crabtree, R. L. (2003). High
1933 spatial resolution hyperspectral mapping of in-stream habitats, depths, and woody debris in
1934 mountain streams. *Geomorphology*, 55(1-4), 363-380.
- 1935 Marcus, W. A., & Fonstad, M. A. (2010). Remote sensing of rivers: the emergence of a subdiscipline
1936 in the river sciences. *Earth Surface Processes and Landforms*, 35(15), 1867-1872.
- 1937 Martínez--Fernández, V., González del Tánago, M., Maroto, J., & García de Jalón, D. (2017). Fluvial
1938 corridor changes over time in regulated and non-regulated rivers (Upper Esla River, NW Spain).
1939 *River research and applications*, 33(2), 214-223.
- 1940 Martinez, A.E., Adeyemo, A.E., & Walther, S.C. (2018). Riparian vegetation and digitized channel
1941 variable changes after stream impoundment: the Provo River and Jordanelle Dam, *Int. J. Appl.*
1942 *Geospatial Res.* 9, 19–35.
- 1943 Mazzorana, B., Zischg, A., Lurgiader, A., & Hübl, J. (2009). Hazard index maps for woody material
1944 recruitment and transport in alpine catchments. *Natural Hazards and Earth System Sciences*, 9(1),
1945 197-209.
- 1946 McKean, J., Nagel, D., Tonina, D., Bailey, P., Wright, C.W., Bohn, C., & Nayegandhi, A., 2009.
1947 Remote sensing of channels and riparian zones with a narrow-beam aquatic-terrestrial lidar.
1948 *Remote Sensing*, 1, 1065-1096. doi:10.3390/rs1041065.
- 1949 Meybeck, M., & Lestel, L. (2017). A Western European River in the Anthropocene: The Seine, 1870–
1950 2010. In: Kelly, J. et al. (eds), *Rivers of the Anthropocene*. California: University of California
1951 Press. DOI: <https://doi.org/10.1525/luminos.43.g>

- 1952 Michalková, M., Piégay, H., Kondolf, G. M., & Greco, S. E. (2011). Lateral erosion of the Sacramento
 1953 River, California (1942–1999), and responses of channel and floodplain lake to human influences.
 1954 *Earth Surface Processes and Landforms*, 36(2), 257-272.
- 1955 Michez, A., Piégay, H., Lisein, J., Claessens, H., & Lejeune, P. (2016). Classification of riparian
 1956 forest species and health condition using multi-temporal and hyperspatial imagery from unmanned
 1957 aerial system. *Environmental monitoring and assessment*, 188(3), 146.
- 1958 Michez, A., Piégay, H., Lejeune, P., & Claessens, H. (2017). Multi-temporal monitoring of a regional
 1959 riparian buffer network (> 12,000 km) with LiDAR and photogrammetric point clouds. *Journal of
 1960 environmental management*, 202, 424-436.
- 1961 Milan, D. J., Heritage, G. L., & Hetherington, D. (2007). Application of a 3D laser scanner in the
 1962 assessment of erosion and deposition volumes and channel change in a proglacial river. *Earth
 1963 Surface Processes and Landforms*, 32(11), 1657-1674.
- 1964 Milan, D. J., Heritage, G. L., Large, A. R. G., & Entwistle, N. S. (2010). Mapping hydraulic biotopes
 1965 using terrestrial laser scan data of water surface properties. *Earth Surface Processes and
 1966 Landforms*, 35(8), 918-931.
- 1967 Milan, D. J., Heritage, G. L., Large, A. R., & Fuller, I. C. (2011). Filtering spatial error from DEMs:
 1968 Implications for morphological change estimation. *Geomorphology*, 125(1), 160-171.
- 1969 Milan, D., Heritage, G., Tooth, S., Entwistle, N. (2018). Morphodynamics of bedrock-influenced
 1970 dryland rivers during extreme floods: Insights from the Kruger National Park, South Africa.
 1971 *GSA Bulletin*, 130(11-12), 1825-1841.
- 1972 Misset, C., Recking, A., Legout, C., Poirel, A., Cazihlac, M., Esteves, M., & Bertrand, M. (2019). An
 1973 attempt to Link suspended load hysteresis patterns and sediment sources configuration in alpine
 1974 catchments. *Journal of Hydrology*, <https://doi.org/10.1016/j.jhydrol.2019.06.039>.
 1975 (<http://www.sciencedirect.com/science/article/pii/S0022169419305864>)
- 1976 Moore, J. W. (2015). *Capitalism in the Web of Life: Ecology and the Accumulation of Capital*. Verso
 1977 Books. ISBN 9781781689035
- 1978 Mould, S., & Fryirs, K. (2018). Contextualising the trajectory of geomorphic river recovery with
 1979 environmental history to support river management. *Applied Geography*, 94, 130-146.
 1980 <https://doi.org/10.1016/j.apgeog.2018.03.008>
- 1981 Mudd, S. M., F. J. Clubb, B. Gailleton, M. D. Hurst, D. T. Milodowski, & Valters, D. A. (2018). "The
 1982 LSDTopo-Tools Chi Mapping Package (Version 1.11), Zenodo."
- 1983 Muste, M., Ho, H. C., & Kim, D. (2011). Considerations on direct stream flow measurements using
 1984 video imagery: Outlook and research needs. *Journal of Hydro-environment Research*, 5(4), 289-
 1985 300. doi:10.1016/j.jher.2010.11.002
- 1986 Norman, L., Villarreal, M., Pulliam, H. R., Minckley, R., Gass, L., Tolle, C., & Coe, M. (2014).
 1987 Remote sensing analysis of riparian vegetation response to desert marsh restoration in the Mexican
 1988 Highlands. *Ecological Engineering*, 70, 241-254.
- 1989 Notebaert, B., & Piégay, H. (2013). Multi-scale factors controlling the pattern of floodplain width at
 1990 a network scale: The case of the Rhône basin, France. *Geomorphology*, 200, 155-171.
- 1991 Nunes, S. S., Barlow, J., Gardner, T. A., Siqueira, J. V., Sales, M. R., & Souza, C. M. (2015). A 22
 1992 year assessment of deforestation and restoration in riparian forests in the eastern Brazilian
 1993 Amazon. *Environmental conservation*, 42(3), 193-203.
- 1994 Ollero, A. (2010). Channel changes and floodplain management in the meandering middle Ebro
 1995 River, Spain. *Geomorphology*, 117(3-4), 247-260.

- 1996 Ouellet Dallaire, C., Lehner, B., Sayre, R., & Thieme, M. (2019). A multidisciplinary framework to
 1997 derive global river reach classifications at high spatial resolution. *Environmental Research Letters*.
 1998 DOI: 10.1088/1748-9326/aad8e9
- 1999 Parker, C., Thorne, C. R., & Clifford, N. J. (2015). Development of ST: REAM: a reach-based stream
 2000 power balance approach for predicting alluvial river channel adjustment. *Earth Surface Processes
 2001 and Landforms*, 40(3), 403-413. DOI: 10.1002/esp.3641
- 2002 Passalacqua, P., Belmont, P., Staley, D. M., Simley, J. D., Arrowsmith, J. R., Bode, C. A., ... &
 2003 Wheaton, J. M. (2015). Analyzing high resolution topography for advancing the understanding of
 2004 mass and energy transfer through landscapes: A review. *Earth-Science Reviews*, 148, 174-193.
 2005 DOI: 10.1016/j.earscirev.2015.05.012
- 2006 Pearson, E., Smith, M.W., Klaar, M.J., & Brown, L.E. (2017). Can high resolution 3D topographic
 2007 surveys provide reliable grain size estimates in gravel bed rivers? *Geomorphology*, 293, 143–155.
- 2008 Peerbhay, K., Mutanga, O., Lottering, R., & Ismail, R. (2016). Unsupervised anomaly weed detection
 2009 in riparian forest areas using hyperspectral data and LiDAR, in: *Hyperspectral Image and Signal
 2010 Processing: Evolution in Remote Sensing (WHISPERS)*, 2016 8th Workshop On. IEEE, pp. 1–5.
- 2011 Pekel, J. F., Cottam, A., Gorelick, N., & Belward, A. S. (2016). High-resolution mapping of global
 2012 surface water and its long-term changes. *Nature*, 540(7633), 418-436.
 2013 <https://doi.org/10.1038/nature20584>.
- 2014 Perks, M. T., Russell, A. J., & Large, A. R. G. (2016). Technical Note: Advances in flash flood
 2015 monitoring using UAVs. *Hydrology and Earth System Sciences Discussions*. 1–18.
 2016 doi:10.5194/hess-2016-12
- 2017 Perucca, E., Camporeale, C., & Ridolfi, L. (2007). Significance of the riparian vegetation dynamics
 2018 on meandering river morphodynamics. *Water Resources Research*, 43(3), W03430.
- 2019 Petts, G.E., Moller, H., Roux, A.L. (1989). Historical change of large alluvial rivers: Western Europe.
 2020 *John Wiley & Sons, Chichester*, 355 p.
- 2021 Peucker-Ehrenbrink, B. (2009). Land2Sea database of river drainage basin sizes, annual water
 2022 discharges, and suspended sediment fluxes. *Geochemistry, Geophysics, Geosystems*, 10(6).
- 2023 Pickett, S.T.A. (1989). Space-for-Time Substitution as an Alternative to Long-Term Studies. In:
 2024 Likens G.E. (eds) *Long-Term Studies in Ecology*. Springer, New York, 110-135.
- 2025 Piégay, H., & Schumm, S. A. (2003). System approaches in fluvial geomorphology. In Kondolf,
 2026 G.M.& Piégay, H. (eds.): *Tools in Fluvial Geomorphology*. Chichester, UK: John Wiley & Sons,
 2027 103-134.
- 2028 Piégay, H., Grant, G., Nakamura, F., & Trustrum, N. (2006). Braided river management: from
 2029 assessment of river behaviour to improved sustainable development. *Braided rivers: process,
 2030 deposits, ecology and management*, 36, 257-275.
- 2031 Piégay, H., Kondolf, G. M., Minear, J. T., & Vaudor, L. (2015). Trends in publications in fluvial
 2032 geomorphology over two decades: A truly new era in the discipline owing to recent technological
 2033 revolution?. *Geomorphology*, 248, 489-500.
- 2034 Piégay, H., Ghaffarian, H., Lemaire, P., Zhang, Z., Boivin, M., Senter, A., ... & Michel, K. (2019).
 2035 Video-monitoring of wood flux: recent advances and next steps. In *4th international conference
 2036 in Wood in World Rivers Conference Proceedings*, Valdivia, Chile
- 2037 Pinter, N., & Heine, R. A. (2005). Hydrodynamic and morphodynamic response to river engineering
 2038 documented by fixed-discharge analysis, Lower Missouri River, USA. *Journal of Hydrology*,
 2039 302(1-4), 70-91. DOI:10.1016/j.jhydrol.2004.06.039.

- 2040 Pfeiffer, A. M., & Finnegan, N. J. (2018). Regional Variation in Gravel Riverbed Mobility, Controlled
 2041 by Hydrologic Regime and Sediment Supply. *Geophysical Research Letters*, 45(7), 3097-3106.
- 2042 Phillips, C. B., & Jerolmack, D. J. (2016). Self-organization of river channels as a critical filter on
 2043 climate signals. *Science*, 352(6286), 694-697.
- 2044 Purinton, B., & Bookhagen, B. (2019). Introducing
 2045 Pebble Counts: A grain-sizing tool for photo surveys of dynamic gravel-bed rivers. *Earth Surf.
 Dyn. Discuss.* 1–33. <https://doi.org/10.5194/esurf-2019-20>
- 2046 Räßle, B., Piégay, H., Stella, J. C., & Mercier, D. (2017). What drives riparian vegetation
 2047 encroachment in braided river channels at patch to reach scales? Insights from annual airborne
 2048 surveys (Drôme River, SE France, 2005–2011). *Ecohydrology*, 10(8), e1886.
- 2049 Ravazzolo, D., Mao, L., Mazzorana, B., & Ruiz-Villanueva, V. (2017). Brief communication: The
 2050 curious case of the large wood-laden flow event in the Pocuro stream (Chile). *Natural Hazards
 2051 and Earth System Sciences*, 17(11), 2053-2058. doi:10.5194/nhess-2017-154
- 2052 Ricaurte, L.F., Boesch, S., Jokela, J., Tockner, K. (2012). The distribution and environmental state of
 2053 vegetated islands within human-impacted European rivers. *Freshw. Biol.* 57, 2539–2549.
- 2054 Rice, S., & Church, M. (1998). Grain size along two gravel-bed rivers: statistical variation, spatial
 2055 pattern and sedimentary links. *Earth Surface Processes and Landforms*, 23(4), 345-363.
- 2056 Ridolfi, E., & Manciola, P. (2018). Water level measurements from drones: A pilot case study at a
 2057 dam site. *Water*, 10(3), 297. doi:10.3390/w10030297
- 2058 Riedler, B., Pernkopf, L., Strasser, T., Lang, S., & Smith, G. (2015). A composite indicator for
 2059 assessing habitat quality of riparian forests derived from Earth observation data. *International
 2060 Journal of Applied Earth Observation and Geoinformation*, 37, 114-123.
- 2061 Rodríguez-González, P. M., Albuquerque, A., Martínez-Almarza, M., & Díaz-Delgado, R. (2017).
 2062 Long-term monitoring for conservation management: Lessons from a case study integrating
 2063 remote sensing and field approaches in floodplain forests. *Journal of environmental management*,
 2064 202, 392-402.
- 2065 Rollet, A.J., Piégay, H., Bornette, G., Dufour, S., & Persat, H. (2013). Assessment of consequences
 2066 of sediment deficit on a gravel river-bed downstream of dams in restoration perspectives:
 2067 application of a multicriteria, hierarchical, and spatially explicit diagnosis. *River Research and
 2068 Applications*, 30(8), 939-953.
- 2069 Roussillon, T., Piégay, H., Sivignon, I., Tougne, L., & Lavigne, F. (2009). Automatic computation of
 2070 pebble roundness using digital imagery and discrete geometry. *Computers & Geosciences*, 35(10),
 2071 1992-2000.
- 2072 Roux, C., Alber, A., Bertrand, M., Vaudor, L., & Piégay, H. (2015). “Fluvial Corridor”: A new
 2073 ArcGIS toolbox package for multiscale riverscape exploration. *Geomorphology*, 242, 29-37. DOI:
 2074 10.1016/j.geomorph.2014.04.018
- 2075 Rubin, D. M. (2004). A simple autocorrelation algorithm for determining grain size from digital
 2076 images of sediment. *Journal of Sedimentary Research*, 74(1), 160-165. DOI:
 2077 10.1306/052203740160
- 2078 Ruiz-Villanueva, V., Díez-Herrero, A., Ballesteros, J. A., & Bodoque, J. M. (2014 a). Potential large
 2079 woody debris recruitment due to landslides, bank erosion and floods in mountain basins: a
 2080 quantitative estimation approach. *River Research and Applications*, 30(1), 81-97.
- 2081 Ruiz-Villanueva, V., Bladé, E., Sánchez-Juny, M., Martí-Cardona, B., Díez-Herrero, A., & Bodoque,
 2082 J. M. (2014 b). Two-dimensional numerical modeling of wood transport. *Journal of
 2083 Hydroinformatics*, 16(5), 1077-1096.

- 2084 Ruiz-Villanueva, V., Piégay, H., Gurnell, A. M., Marston, R. A., & Stoffel, M. (2016). Recent
 2085 advances quantifying the large wood dynamics in river basins: New methods and remaining
 2086 challenges. *Reviews of Geophysics*, 54(3), 611-652.
- 2087 Ruiz-Villanueva, V., Mazzorana, B., Bladé, E., Bürkli, L., Iribarren-Anacona, P., Mao, L., Nakamura,
 2088 F., Ravazzolo, D., Rickenmann, D., Sanz-Ramos, M., Stoffel, M., & Wohl, E. (2019).
 2089 Characterization of wood-laden flows in rivers. *Earth Surface Processes and Landforms*, 44,
 2090 1694–1709. <https://doi-org.acces.bibliotheque-diderot.fr/10.1002/esp.4603>
- 2091 Safran, S.M., Baumgarten, S.A., Beller, E.E., Crooks, J.A., Grossinger, R.M., Lorda, J., & Stein, E.D.
 2092 (2017). Tijuana River Valley Historical Ecology Investigation. Prepared for the State Coastal
 2093 Conservancy. A Report of SFEI-ASC’s Resilient Landscapes Program. SFEI Contribution No.
 2094 760. San Francisco Estuary Institute - Aquatic Science Center: Richmond, CA. p 230.
- 2095 Salo, J., Kalliola, R., Häkkinen, I., Mäkinen, Y., Niemelä, P., Puhakka, M., & Coley, P. D. (1986).
 2096 River dynamics and the diversity of Amazon lowland forest. *Nature*, 322(6076), 254-258.
- 2097 Sanhueza, D., Iroumé, A., Ulloa, H., Picco, L., & Ruiz-Villanueva, V. (2018). Measurement and
 2098 quantification of fluvial wood deposits using UAVs and structure from motion in the Blanco River
 2099 (Chile). 5th IAHR Europe Congress — New Challenges in Hydraulic Research and Engineering,
 2100 Proc. of the 5th IAHR Europe Congress. Editor(s) Armanini, A. & Nucci, E. , DOI:10.3850/978-
 2101 981-11-2731-1_216-cd.
- 2102 Santos, P.P., Tavares, A.O., & Andrade, A.I.A.S.S. (2011). Comparing historical-
 2103 hydrogeomorphological reconstitution and hydrological-hydraulic modelling in the estimation of
 2104 flood-prone areas-a case study in Central Portugal. *Natural Hazards and Earth System Sciences*,
 2105 11(6), 1669-1681.
- 2106 Schmitt, R.J., Bizzi, S., & Castelletti, A. (2014). Characterizing fluvial systems at basin scale by fuzzy
 2107 signatures of hydromorphological drivers in data scarce environments». *Geomorphology* 214
 2108 (2014), 69–83. <https://doi.org/10.1016/j.geomorph.2014.02.024>.
- 2109 Schmitt, R. J., Bizzi, S., & Castelletti, A. (2016). Tracking multiple sediment cascades at the river
 2110 network scale identifies controls and emerging patterns of sediment connectivity. *Water Resources*
 2111 *Research*, 52(5), 3941-3965. DOI: 10.1002/2015WR018097
- 2112 Schmitt, R. J., Bizzi, S., Castelletti, A., & Kondolf, G. M. (2018a). Improved trade-offs of
 2113 hydropower and sand connectivity by strategic dam planning in the Mekong. *Nature*
 2114 *Sustainability*, 1(2), 96. DOI: 10.1038/s41893-018-0022-3
- 2115 Schmitt, R. J., Bizzi, S., Castelletti, A. F., & Kondolf, G. M. (2018b). Stochastic modeling of sediment
 2116 connectivity for reconstructing sand fluxes and origins in the unmonitored Se Kong, Se San, and
 2117 Sre Pok tributaries of the Mekong River. *Journal of Geophysical Research: Earth Surface*, 123(1),
 2118 2-25. DOI: 10.1002/2016JF004105
- 2119 Schmitt, R. J. P., Bizzi, S., Castelletti, A., Opperman, J. J., Kondolf, G.M. (2019). Planning Dam
 2120 Portfolios for Low Sediment Trapping Shows Limits for Sustainable Hydropower in the Mekong.
 2121 *Science Advances*, 5(10), eaaw2175. <https://doi.org/10.1126/sciadv.aaw2175>
- 2122 Schumm, S. A. (1969). River metamorphosis. American Society of Civil Engineers, *Journal of the*
 2123 *Hydraulics division*, 95(1), 255-274.
- 2124 Schumm, S. A., Harvey, M. D., & Watson, C. C. (1984). *Incised channels: morphology, dynamics,*
 2125 *and control*. Water Resources Publications : Littleton, CO.
- 2126 Schwenk, J., Khandelwal, A., Fratkin, M., Kumar, V., & Fofoula-Georgiou, E. (2017). High
 2127 spatiotemporal resolution of river planform dynamics from Landsat: The RivMAP toolbox and
 2128 results from the Ucayali River. *Earth and Space Science*, 4(2), 46-75.

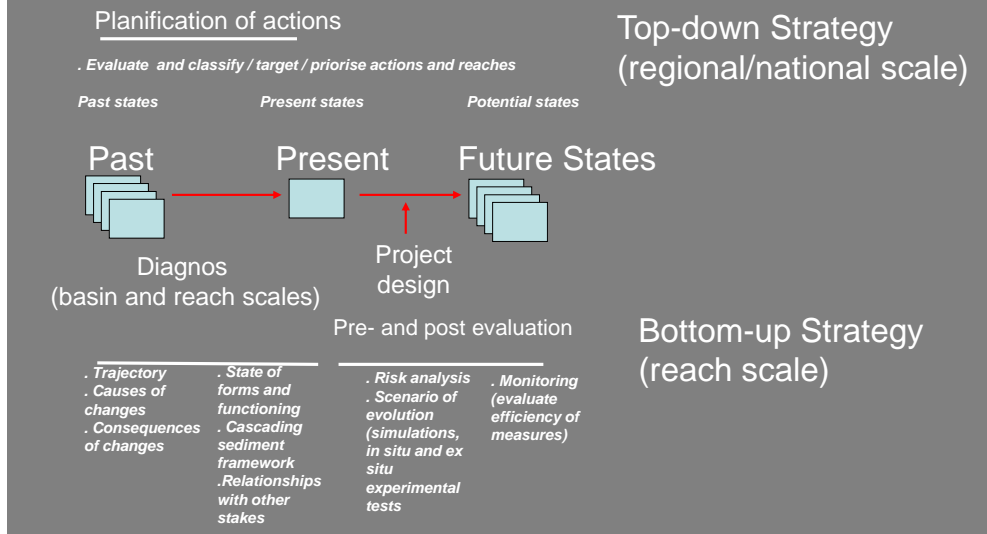
- 2129 Scorpio, V., Santangelo, N., & Santo, A. (2016). Multiscale map analysis in alluvial fan flood-prone
2130 areas. *Journal of Maps*, 12(2), 382-393.
- 2131 Scorpio, V., Surian, N., Cucato, M., Dai Prá, E., Zolezzi, G., & Comiti, F. (2018). Channel changes
2132 of the Adige River (Eastern Italian Alps) over the last 1000 years and identification of the historical
2133 fluvial corridor. *Journal of Maps*, 14(2), 680-691.
- 2134 Serlet, A. J., Gurnell, A. M., Zolezzi, G., Wharton, G., Belleudy, P., & Jourdain, C. (2018).
2135 Biomorphodynamics of alternate bars in a channelized, regulated river: An integrated historical
2136 and modelling analysis. *Earth Surface Processes and Landforms*, 43(9), 1739-1756.
- 2137 Simon, A., & Hupp, C. R. (1986). Channel Evolution in Modified Tennessee Channels. In
2138 *Proceedings of the 4th Federal Interagency Sedimentation Conference*, Las Vegas, Nevada. 5-71–
2139 5-82.
- 2140 Slater, L. J., & Singer, M. B. (2013). Imprint of climate and climate change in alluvial riverbeds:
2141 Continental United States, 1950-2011. *Geology*, 41(5), 595-598. DOI: 10.1130/G34070.1
- 2142 Slater L. J., Singer M. B., & Kirchner J. W. (2015). Hydrologic versus geomorphic drivers of trends
2143 in flood hazard. *Geophysical Research Letters* 42:1–7. DOI: 10.1002/2014GL062482
- 2144 Slater, L.J., Khouakhi, A., Wilby R.L. (2019a). River channel conveyance capacity adjusts to modes
2145 of climate variability. *Scientific Reports*, 9:12619, DOI: 10.1038/s41598-019-48782-1
- 2146 Slater, L.J., Thirel, G., Harrigan, S., Delaigue, O., Hurley, A., Khouakhi, A., Prosdocimi, I., Vitolo,
2147 C., & Smith, K. (2019b). Using R in hydrology: a review of recent developments and future
2148 directions. *Hydrology and Earth System Sciences*, 23, 2939-2963. DOI: 10.5194/hess-23-2939-
2149 2019
- 2150 Solins, J. P., Thorne, J. H., & Cadenasso, M. L. (2018). Riparian canopy expansion in an urban
2151 landscape: Multiple drivers of vegetation change along headwater streams near Sacramento,
2152 California. *Landscape and Urban Planning*, 172, 37-46.
- 2153 Spada, D., Molinari, P., Bertoldi, W., Vitti, A., & Zolezzi, G. (2018). Multi-Temporal Image Analysis
2154 for Fluvial Morphological Characterization with Application to Albanian Rivers. *ISPRS*
2155 *International Journal of Geo-Information*, 7(8), 314, DOI:10.3390/ijgi7080314.
- 2156 Spiekermann, R., Betts, H., Dymond, J., & Basher, L. (2017). Volumetric measurement of river bank
2157 erosion from sequential historical aerial photography. *Geomorphology*, 296, 193-208.
- 2158 Stähly, S., Friedrich, H., & Detert, M. (2017). Size ratio of fluvial grains' intermediate axes assessed
2159 by image processing and square-hole sieving. *J. Hydraul. Eng.* 143, 06017005.
2160 [https://doi.org/10.1061/\(asce\)hy.1943-7900.0001286](https://doi.org/10.1061/(asce)hy.1943-7900.0001286)
- 2161 Steeb, N., Rickenmann, D., Badoux, A., Rickli, C., & Waldner, P. (2017). Large wood recruitment
2162 processes and transported volumes in Swiss mountain streams during the extreme flood of August
2163 2005. *Geomorphology*, 279, 112-127.
- 2164 Steffen, W., Crutzen, P.J., & McNeill, J.R.. (2007). The Anthropocene: are humans now
2165 overwhelming the great forces of nature? *AMBIO: A Journal of the Human Environment* 16(8),
2166 614-621.
- 2167 Stover, S. C., & Montgomery, D. R. (2001). Channel change and flooding, Skokomish River,
2168 Washington. *Journal of Hydrology*, 243(3-4), 272-286. DOI: 10.1016/S0022-1694(00)00421-2
- 2169 Straatsma, M. W., & Baptist, M. J. (2008). Floodplain roughness parameterization using airborne
2170 laser scanning and spectral remote sensing. *Remote Sensing of Environment*, 112(3), 1062-1080.
- 2171 Surian, N., & Rinaldi, M. (2003). Morphological response to river engineering and management in
2172 alluvial channels in Italy. *Geomorphology*, 50(4), 307-326.

- 2173 Surian, N., Ziliani, L., Comiti, F., Lenzi, M. A., & Mao, L. (2009). Channel adjustments and alteration
 2174 of sediment fluxes in gravel-bed rivers of North-Eastern Italy: potentials and limitations for
 2175 channel recovery. *River Research and Applications*, 25, 551-567.
- 2176 Surian, N., Barban, M., Ziliani, L., Monegato, G., Bertoldi, W., & Comiti, F. (2015). Vegetation
 2177 turnover in a braided river: frequency and effectiveness of floods of different magnitude. *Earth
 2178 Surface Processes and Landforms*, 40(4), 542-558.
- 2179 Tamminga, A. D., Eaton, B. C., & Hugenholtz, C. H. (2015). UAS-based remote sensing of fluvial
 2180 change following an extreme flood event. *Earth Surface Processes and Landforms*, 40(11), 1464-
 2181 1476. <https://doi.org/10.1002/esp.3728>
- 2182 Tangi, M., Schmitt, R., Bizzi, S., & Castelletti, A. (2019). The CASCADE toolbox for analyzing river
 2183 sediment connectivity and management. *Environmental Modelling and Software*, 119, 400-406,
 2184 <https://doi.org/10.1016/j.envsoft.2019.07.008>
- 2185 Tauro, F., Olivieri, G., Petroselli, A., Porfiri, M., & Grimaldi, S. (2016). Flow monitoring with a
 2186 camera: A case study on a flood event in the Tiber River. *Environmental monitoring and
 2187 assessment*, 188(2), 118. doi:10.1007/s10661-015-5082-5
- 2188 Tauro, F., Selker, J., Van De Giesen, N., Abrate, T., Uijlenhoet, R., Porfiri, M., ... & Ciruolo, G.
 2189 (2018). Measurements and observations in the XXI century (MOXXI): Innovation and multi-
 2190 disciplinarity to sense the hydrological cycle. *Hydrological sciences journal*, 63(2), 169-196.
 2191 doi:10.1080/02626667.2017.1420191
- 2192 Tauro, F., Piscopia, R., & Grimaldi, S. (2019). PTV-Stream: A simplified particle tracking
 2193 velocimetry framework for stream surface flow monitoring. *Catena*, 172, 378-386.
 2194 doi:10.1016/j.catena.2018.09.009
- 2195 Tena, A., Piégay, H., Seignemartin, G., Barra, A., Berger, J.F., Mourier, B., & Winiarski, T. (*in
 2196 review*). Cumulative effects of channel engineering and bypassing on floodplain terrestrialisation
 2197 patterns and connectivity.
- 2198 Thoma, D. P., Gupta, S. C., Bauer, M. E., & Kirchoff, C. E. (2005). Airborne laser scanning for
 2199 riverbank erosion assessment. *Remote sensing of Environment*, 95(4), 493-501.
- 2200 Thorel, M., Piégay, H., Barthelemy, C., Räßple, B., Gruel, C. R., Marmonier, P., ... & Stella, J. C.
 2201 (2018). Socio-environmental implications of process-based restoration strategies in large rivers:
 2202 should we remove novel ecosystems along the Rhône (France)?. *Regional environmental change*,
 2203 18(7), 2019-2031. <https://doi.org/10.1007/s10113-018-1325-7>.
- 2204 Tomsett, C., & Leyland, J., (2019). Remote sensing of river corridors: A review of current trends and
 2205 future directions. *River Research and Applications*. DOI: 10.1002/rra.3479
- 2206 Tonon, A., Picco, L., Ravazzolo, D., & Lenzi, M. (2014). Using a terrestrial laser scanner to detect
 2207 wood characteristics in gravel-bed rivers. *Journal of Agricultural Engineering*, 45(4), 161-167.
 2208 <https://doi.org/10.4081/jae.2014.431>
- 2209 Toone, J., Rice, S. P., & Piégay, H. (2014). Spatial discontinuity and temporal evolution of channel
 2210 morphology along a mixed bedrock-alluvial river, upper Drôme River, southeast France:
 2211 Contingent responses to external and internal controls. *Geomorphology*, 205, 5-16.
- 2212 Tormos, T., Kosuth, P., Durrieu, S., Dupuy, S., Villeneuve, B., & Wasson, J. G. (2012). Object-based
 2213 image analysis for operational fine-scale regional mapping of land cover within river corridors
 2214 from multispectral imagery and thematic data. *International journal of remote sensing*, 33(14),
 2215 4603-4633.

- 2216 Truksa, T. (2017). Can drones measure LWD?: high resolution aerial imagery and structure from
2217 motion as a method for quantifying instream wood. Geological Society of America *Abstracts with*
2218 *Programs*. Vol. 49, No. 6, Paper No. 354-12. doi: 10.1130/abs/2017AM-308662
- 2219 Ulloa, H., Iroumé, A., Mao, L., Andreoli, A., Diez, S., & Lara, L. E. (2015). Use of remote imagery
2220 to analyse changes in morphology and longitudinal large wood distribution in the Blanco River
2221 after the 2008 Chaitén volcanic eruption, southern Chile. *Geografiska Annaler: Series A, Physical*
2222 *Geography*, 97(3), 523-541.
- 2223 Van Der Knijff, J. M., Younis, J., & De Roo, A. P. J. (2010). LISFLOOD: a GIS-based distributed
2224 model for river basin scale water balance and flood simulation. *International Journal of*
2225 *Geographical Information Science*, 24(2), 189-212. DOI: 10.1080/13658810802549154
- 2226 Vauclin, S., Mourier, B., Seignemartin, G., Tena, A., Develle, A.L., Piégay, H., Berger, J.F.,
2227 Winiarski, T. (*in review*). Characterizing the infrastructure-induced legacy sediments by a
2228 combined geophysical and coring approach.
- 2229 Vázquez-Tarrío, D., Borgniet, L., Liébault, F., & Recking, A. (2017). Using UAS optical imagery
2230 and SfM photogrammetry to characterize the surface grain size of gravel bars in a braided river
2231 (Vénéon River, French Alps). *Geomorphology*, 285, 94-105. DOI:
2232 <https://doi.org/10.1016/j.geomorph.2017.01.039>
- 2233 Vericat, D., Brasington, J., Wheaton, J., & Cowie, M. (2009). Accuracy assessment of aerial
2234 photographs acquired using lighter-than-air blimps: low-cost tools for mapping river corridors.
2235 *River Research and Applications*, 25(8), 985-1000.
- 2236 Vericat, D., Wheaton, J. M., & Brasington, J. (2017). Revisiting the morphological approach:
2237 opportunities and challenges with repeat high-resolution topography. In: Tsutsumi D, Laronne JB
2238 (eds) *Gravel-Bed Rivers Processes and Disasters*. John Wiley and Sons: Chichester; 121-158.
- 2239 Wackrow R, Chandler JH. (2008). A convergent image configuration for DEM extraction that
2240 minimises the systematic effects caused by an inaccurate lens model. *The Photogrammetric*
2241 *Record* 23, 6–18.
- 2242 Wackrow R, Chandler JH. (2011). Minimising systematic error surfaces in digital elevation models
2243 using oblique convergent imagery. *The Photogrammetric Record* 26, 16–31.
- 2244 Wadell, H., (1932). Volume, shape, and roundness of rock particles. *Journal of Geology*, 40:443-51.
- 2245 Wawrzyniak, V., Räßple, B., Piégay, H., Michel, K., Parmentier, H., & Couturier, A. (2014). Analyse
2246 multi-temporelle des marges fluviales fréquemment inondées à partir d'images satellites Pléiades.
2247 *Revue Française de Photogrammétrie et de Télédétection*.
- 2248 Wawrzyniak, V., Piégay, H., Allemand, P., Vaudor, L., Goma, R., & Grandjean, P. (2016). Effects
2249 of geomorphology and groundwater level on the spatio-temporal variability of riverine cold water
2250 patches assessed using thermal infrared (TIR) remote sensing. *Remote Sensing of Environment*,
2251 175, 337-348. <https://doi.org/10.1016/j.rse.2015.12.050>
- 2252 Westaway RM, Lane SN, Hicks DM. (2003). Remote survey of large-scale braided, gravel-bed rivers
2253 using digital photogrammetry and image analysis. *International Journal of Remote Sensing* 24,
2254 795–815.
- 2255 Wheaton, J.M., Brasington, J., Darby, S.E., Sear, D.A. (2010). Accounting for Uncertainty in DEMs
2256 from Repeat Topographic Surveys: Improved Sediment Budgets. *Earth Surface Processes and*
2257 *Landforms*, 35(2), 136-156.
- 2258 Wheaton, J.M., Fryirs, K.A., Brierley, G., Bangen, S.G., Bouwes, N., O'Brien, G., (2015).
2259 Geomorphic mapping and taxonomy of fluvial landforms. *Geomorphology* 248, 273–295.
2260 <https://doi.org/10.1016/j.geomorph.2015.07.010>

- 2261 Williams, R. D., Brasington, J. , Vericat, D. and Hicks, D. M. (2014), Hyperscale terrain modelling
2262 of braided rivers: fusing mobile terrestrial laser scanning and optical bathymetric mapping. *Earth*
2263 *Surface Processes and Landforms*, 39: 167-183. doi:[10.1002/esp.3437](https://doi.org/10.1002/esp.3437)
- 2264 Winterbottom SJ, Gilvear DJ. (1997). Quantification of channel bed morphology in gravel-bed rivers
2265 using airborne multispectral imagery and aerial photography. *Regulated Rivers: Research &*
2266 *Management: An International Journal Devoted to River Research and Management* **13**, 489–499.
- 2267 Woodget AS, Carbonneau PE, Visser F, Maddock IP. (2015). Quantifying submerged fluvial
2268 topography using hyperspatial resolution UAS imagery and structure from motion
2269 photogrammetry. *Earth Surface Processes and Landforms* **40**, 47–64.
- 2270 Woodget, A.S., Austrums, R., (2017). Subaerial gravel size measurement using topographic data
2271 derived from a UAV-SfM approach. *Earth Surf. Process. Landforms* 42, 1434–1443.
2272 <https://doi.org/10.1002/esp.4139>
- 2273 Woodget, A.S., Fyffe, C., Carbonneau, P.E., (2018). From manned to unmanned aircraft: Adapting
2274 airborne particle size mapping methodologies to the characteristics of sUAS and SfM. *Earth*
2275 *Surface Processes and Landforms* 43, 857–870. <https://doi.org/10.1002/esp.4285>
2276

improving river management, restoration or conservation
 => wider scope in term of spatial and temporal scales

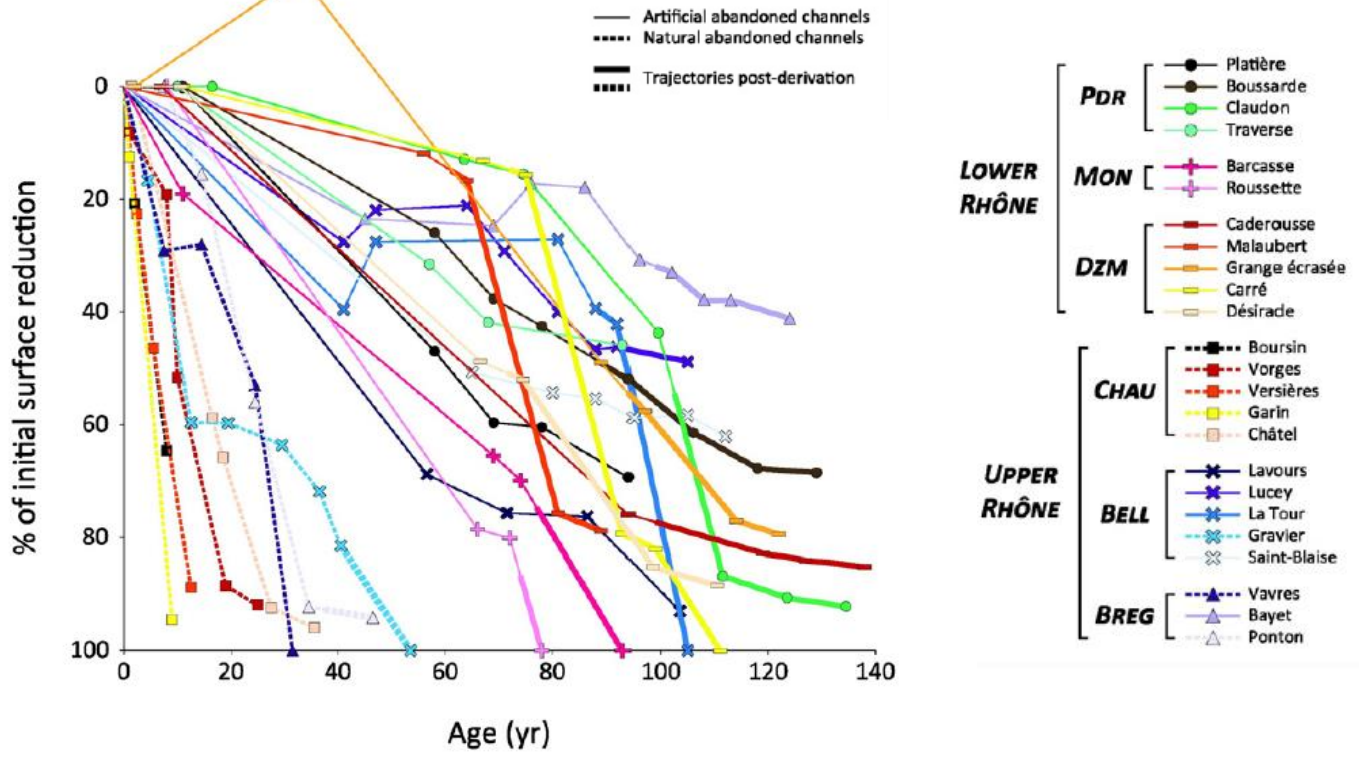


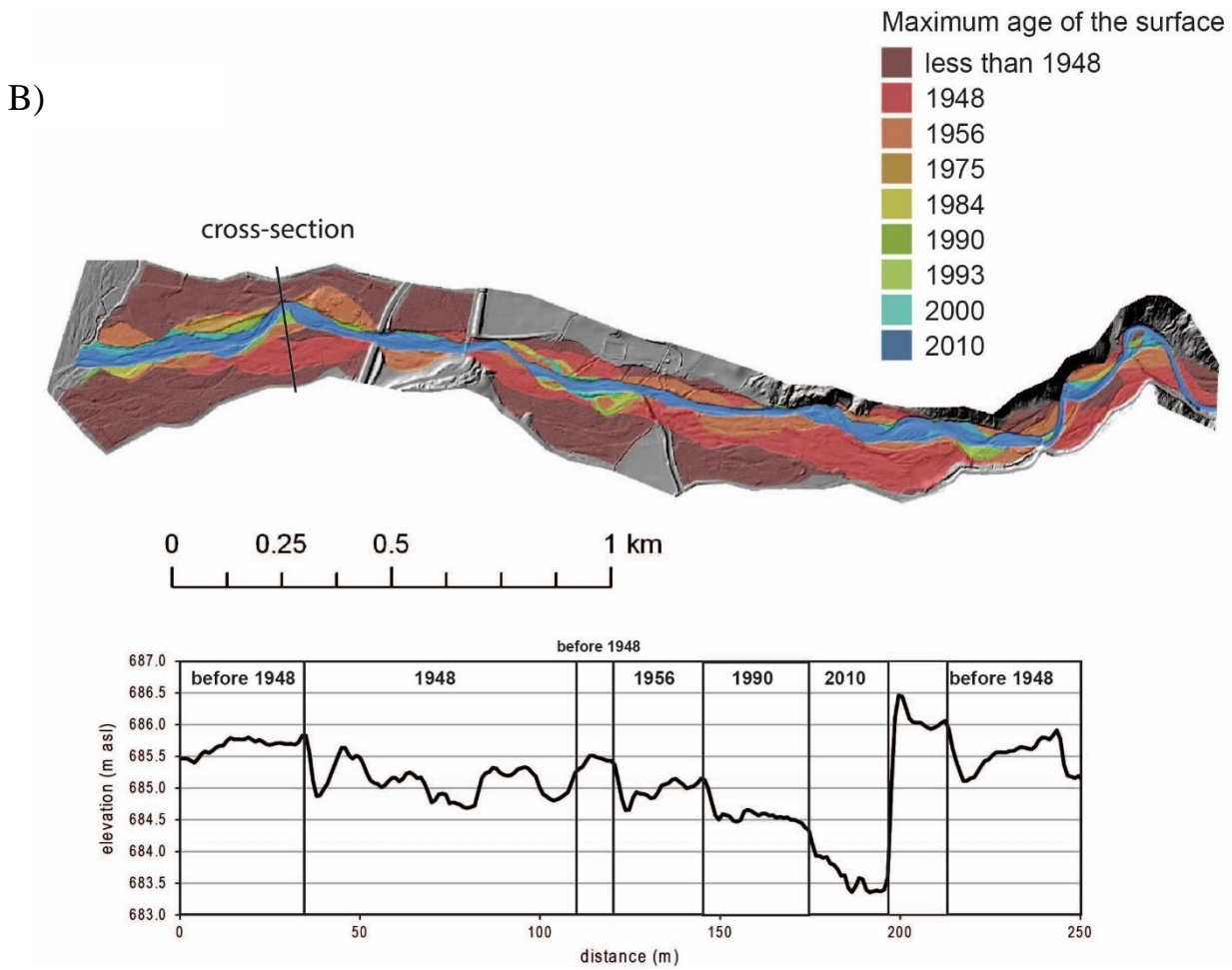
2277

2278 *Figure 1. General framework of geomorphic studies: diagnosis and project appraisal, top-down*
 2279 *and bottom-up strategies (source: Piégay et al. 2016, chapter 22)*

2280
 2281
 2282
 2283
 2284
 2285
 2286
 2287
 2288
 2289
 2290
 2291
 2292
 2293

A)

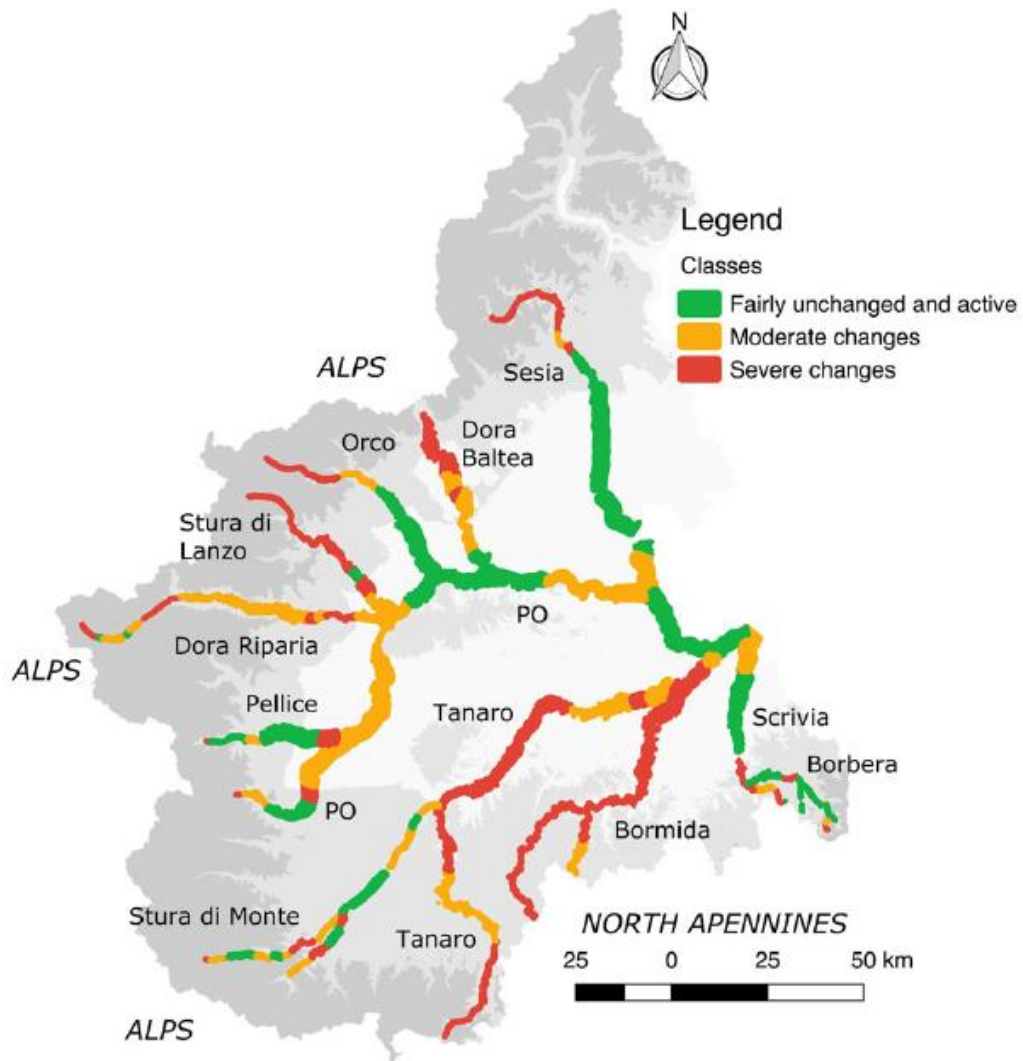




2295
2296

2297 *Figure 2. Temporal evolution of surface areas through time based on a series of aerial photographs:*
 2298 *(A) example of the terrestrialisation of the natural (dashed line) and artificial (thick line) abandoned*
 2299 *channels of the Rhône River – Grange Ecrasée is the only one of expansion right after cut-off*
 2300 *and then shrinking (Source: Figure 1, Dépret et al. 2017, Geomorphology) (B) reconstruction of bed-*
 2301 *level evolution of a small alpine gravel-bed stream from the combination of historical aerial*
 2302 *photographs (from 1948 to 2010) and a recent airborne LiDAR survey (2010) (modified after Lallias-*
 2303 *Tacon et al., 2017); historical aerial photographs have been used to date recent terraces, and*
 2304 *airborne LiDAR data to extract elevation differences between dated terraces to reconstruct the*
 2305 *floodplain formation history*

2306
2307

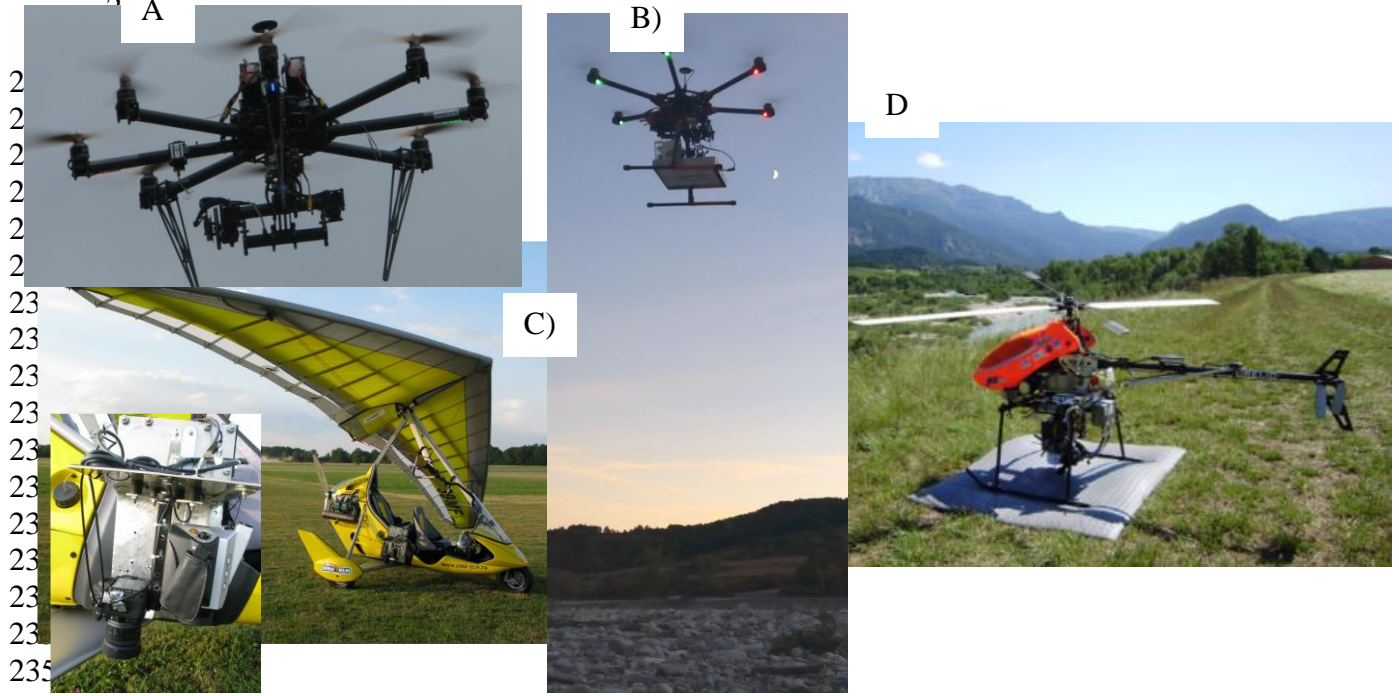


2308
 2309
 2310
 2311
 2312
 2313
 2314
 2315
 2316
 2317
 2318
 2319
 2320
 2321
 2322
 2323
 2324
 2325
 2326
 2327
 2328
 2329
 2330

Figure 3. Classes of channel changes combining incision and narrowing based on regional LiDAR, aerial photos and field/archived data to established reference: severe changes indicate significant narrowing (>50-100% of their current width) and riverbed incision (2-5 m) over the last century, moderate changes indicate mostly river reaches that show substantial narrowing and moderate channel incision (source: Figure 12, Bizzi et al., 2018 in ESPL)

2331
 2332
 2333
 2334
 2335
 2336
 2337
 2338
 2339

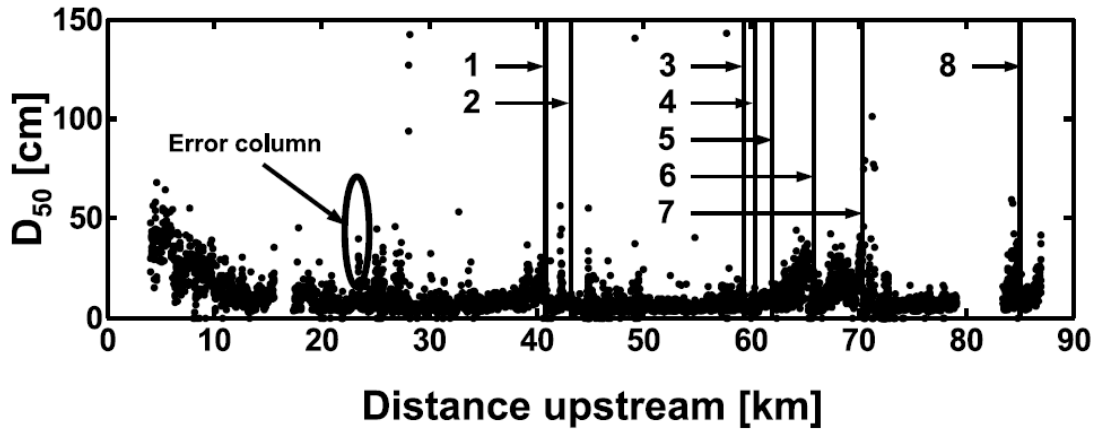
2340



2
 2
 2
 2
 2
 2
 23
 23
 23
 23
 23
 23
 23
 23
 23
 23
 235

2360
 2361
 2362
 2363
 2364
 2365
 2366

Figure 4. Example of platforms used by scientific teams to acquire hyperspatial imagery : A) Octocopter ; B) Hexacopter equipped with an active RFID antenna; C) Ultralight trike equipped with RGB and thermal cameras; D) Unmanned Control Helicopter (Sources : A) Franck Perret ; B) Mathieu Cassel; C) Baptiste Marteau and D) Kristell Michel)



2368

2369

2370

2371

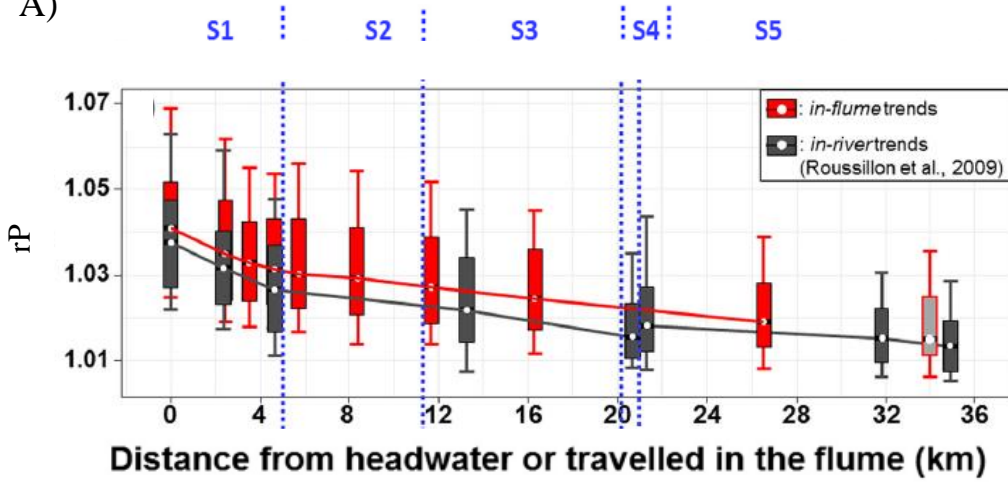
2372

2373

Figure 5. Long profile of median grain size over 80 km of the Sainte Marguerite River, Québec from image processing and showing link cutoff points (vertical lines), numbered 1–8 as determined by Davey and Lapointe (unpublished report, 2004) and an example of an “error column” structure caused by glare at the water surface (Source : Figure 5. Carbonneau et al., 2005).

2374
 2375
 2376
 2377
 2378

A)



2379

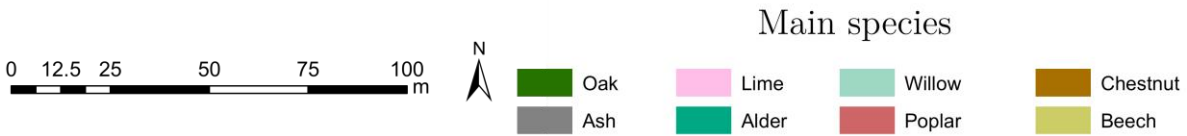
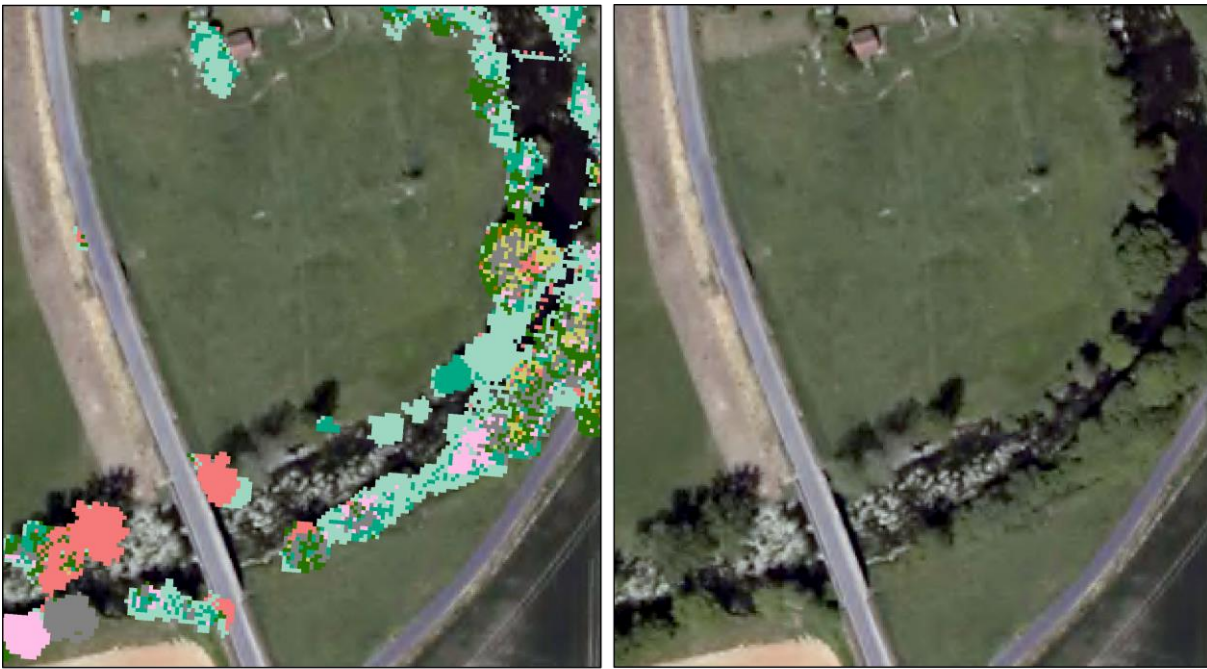
2380
 2381

B)



2382
 2383
 2384
 2385
 2386
 2387
 2388
 2389
 2390
 2391
 2392
 2393
 2394
 2395
 2396
 2397

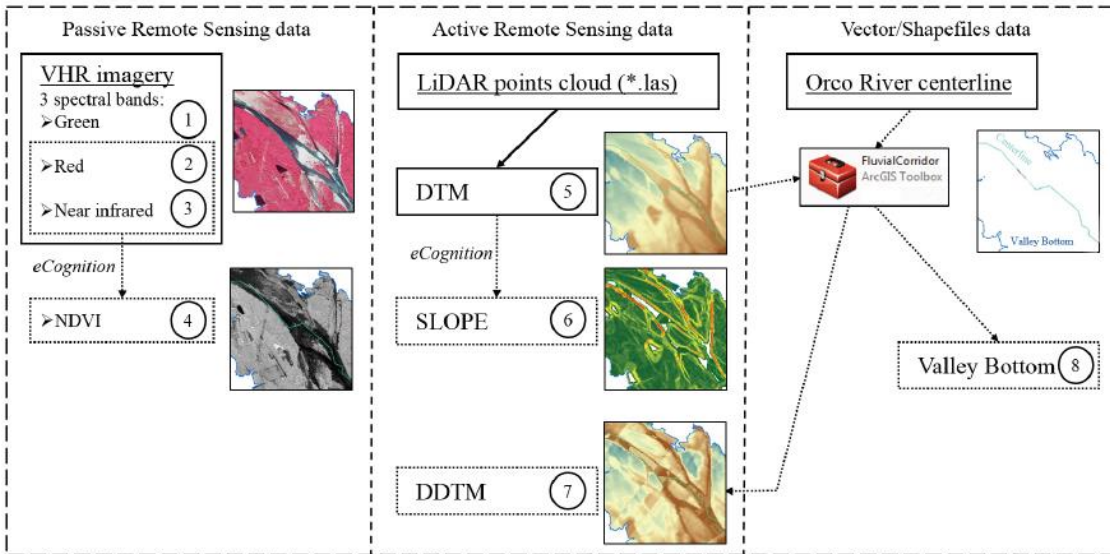
Figure 6. (A) Evolutions of the ratios of perimeters rP according to the distance travelled through 36 km from the headwater of Progo river (Indonesia) (dark grey) or in an annular flume (red). $rP = P_g/P_e$ with P_g the pebble perimeter and P_e the ellipse perimeter, both having the same surface area. The single clear grey boxplot with red borders represents values distributions of rounded pebbles which were collected 30 km downstream the Progo spring. Boxplots represent distributions of shape parameter values at a given distance and provide 10th, 25th, 50th, 75th and 90th percentiles values. White circles represent median values. (B) Example of picture of angular pebbles taken for roundness analysis. (Source: Cassel et al., 2018, Figure 11 and Figure 3).



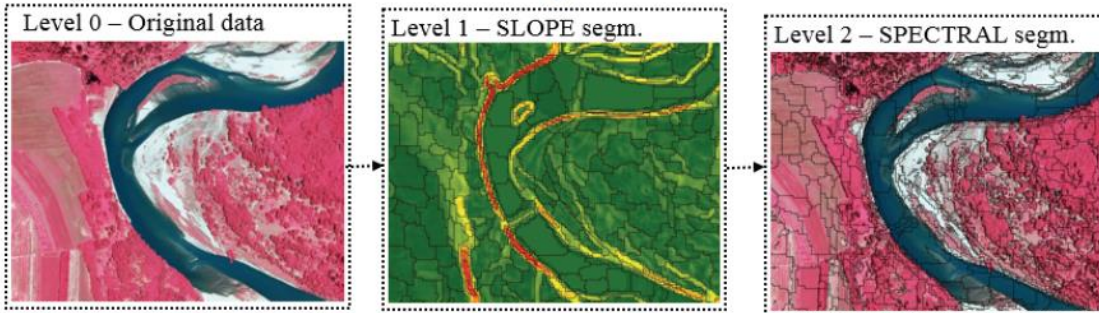
2398
 2399
 2400
 2401
 2402
 2403
 2404
 2405
 2406
 2407
 2408
 2409
 2410
 2411

Figure 7. Riparian genres map obtained from LiDAR data and tree morphological patterns (Sélune River, western France). Tree crown morphology and internal structure indicators were computed from the 3D points clouds of two surveys (summer and winter; $n = 144$ indicators) and the most discriminant indicators were selected using a stepwise Quadratic Discriminant Analysis allowing the number of indicators to be reduced to less than 10 relevant indicators. The selected indicators were used as variables for classification using Support Vector Machine. Overall accuracy ranges from 80% for 3 genres to 50% for 8 genres. With 8 genres, the identification remains a challenge as for one tree crown predicted pixels can be mixed (Source: Ba et al., 2019)

Data and pre-processing



Segmentation

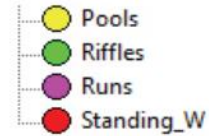


Classification

Riverscape units

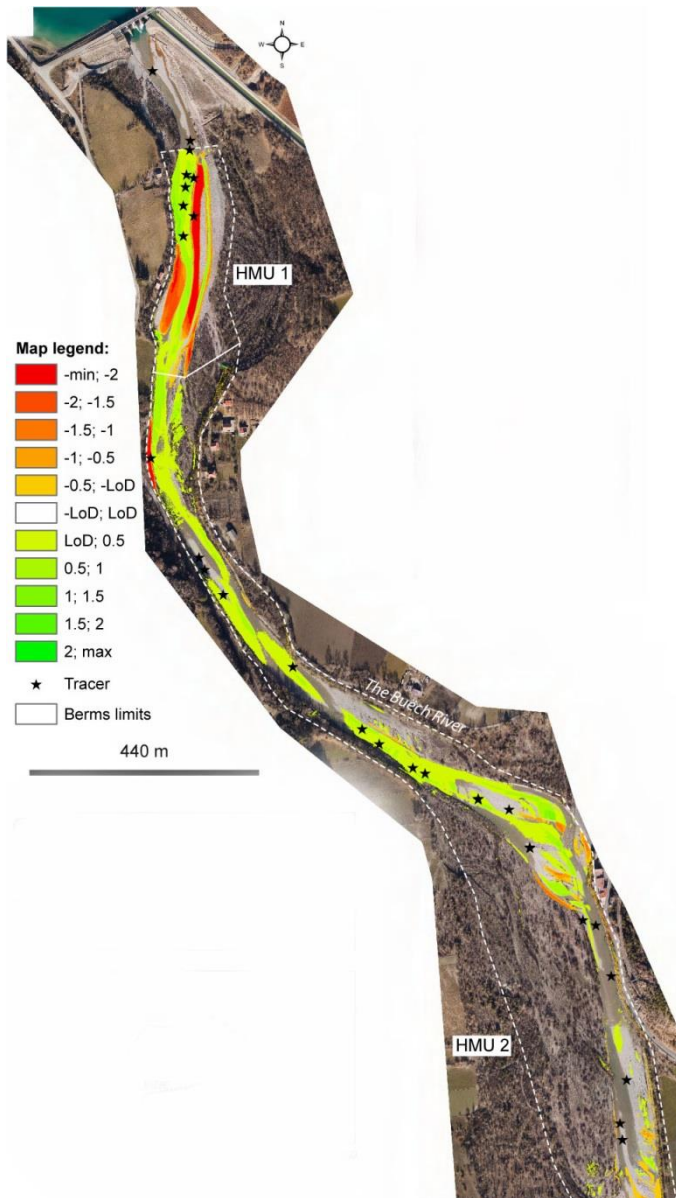


Mesohabitats



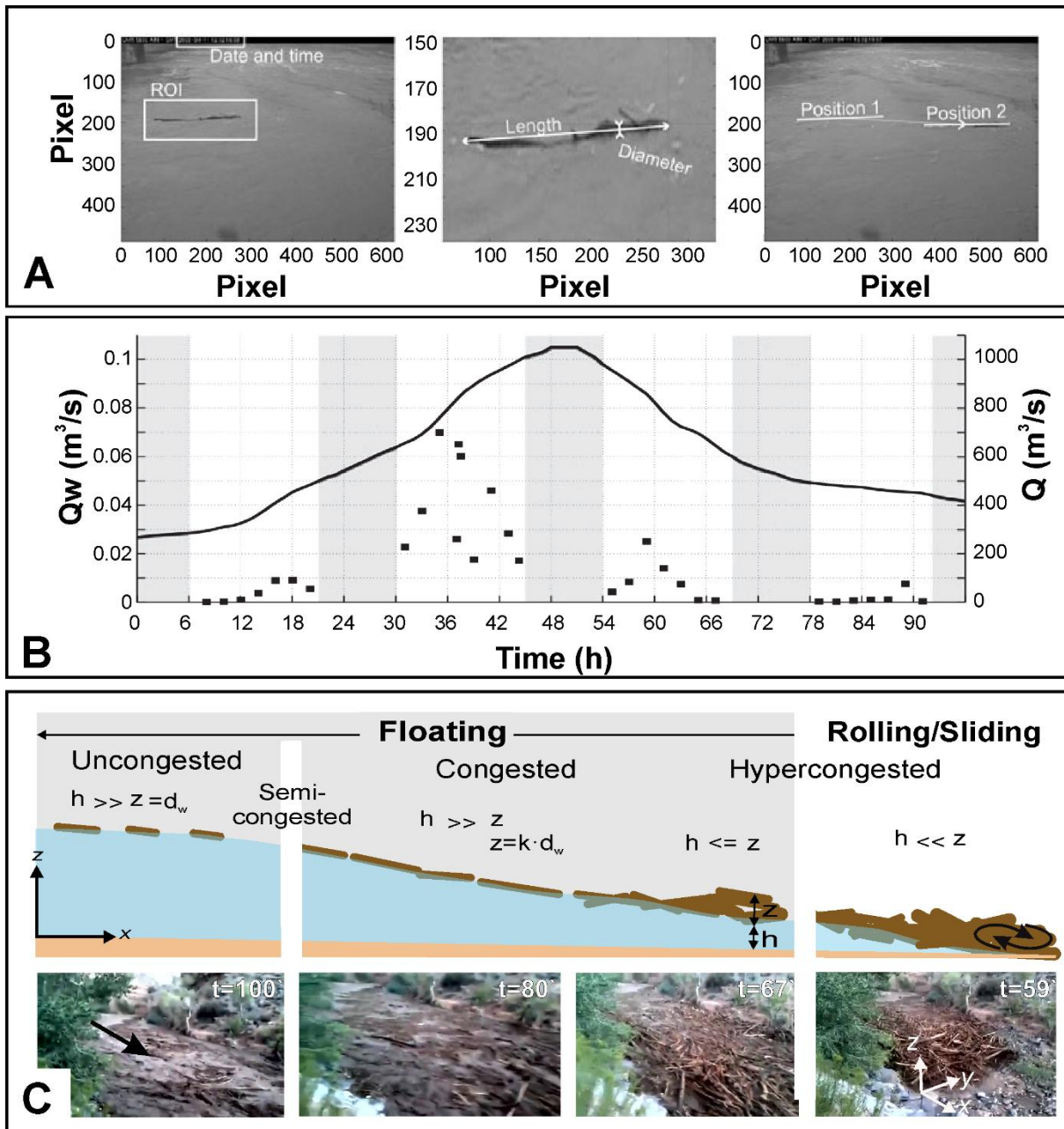
2412
2413
2414
2415
2416
2417
2418
2419

Figure 8. Workflow of the multilevel, object-based methodology developed for the classification of riverscape units and in-stream mesohabitats. Top row shows data type used (multispectral and Lidar derived DTM); central row describes the OBIA steps to derive topographically and spectrally homogenous units; the bottom row displays classification results for riverscape units (on the left) and mesohabitats (on the right). (Source: Demarchi et al. 2016 Figure 5)



2420
 2421
 2422
 2423
 2424
 2425
 2426
 2427
 2428

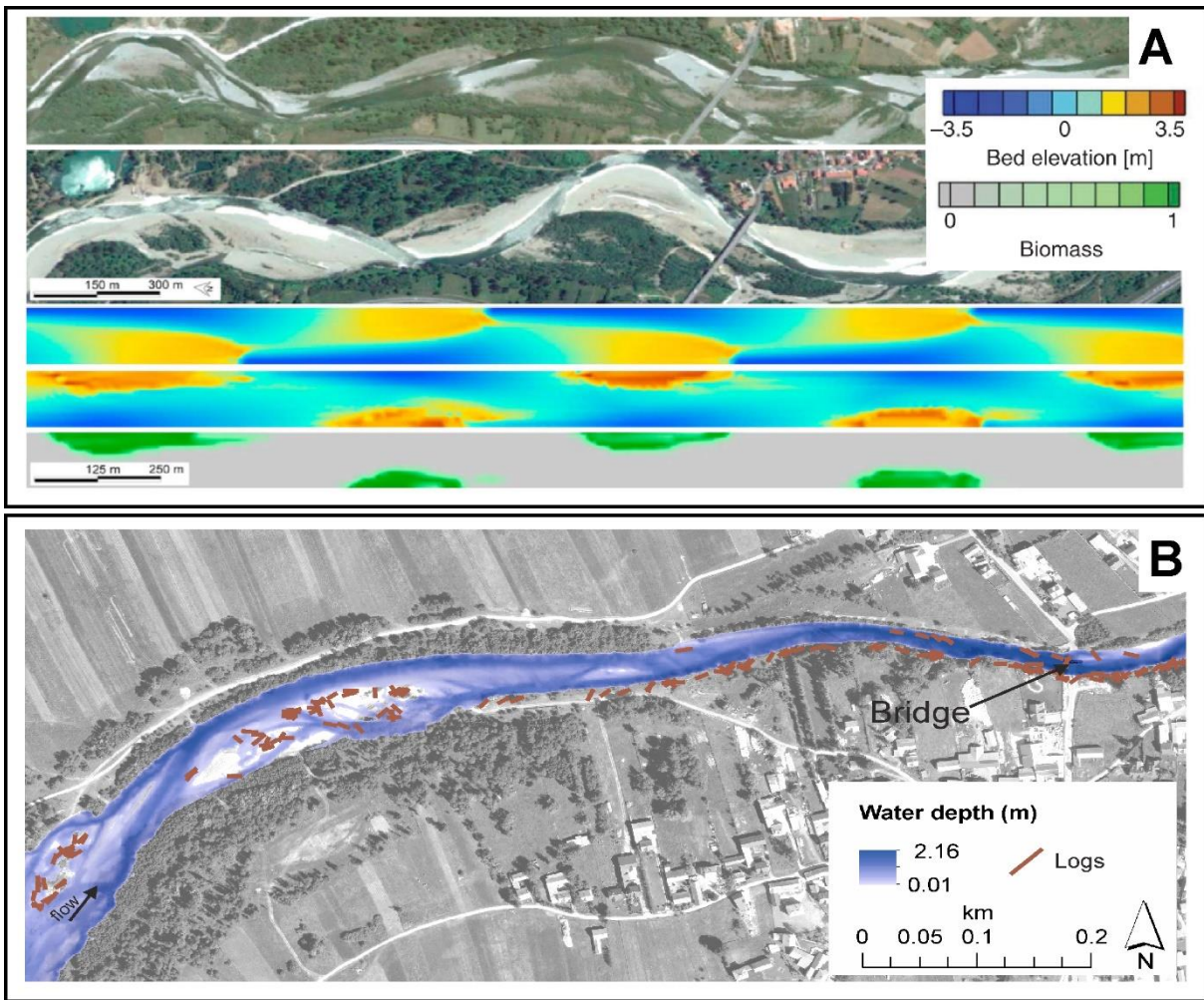
Figure 9. Monitoring of sediment wave propagation following a gravel replenishment operation downstream of a dam in the Buëch River (Southern French Prealps), using repetitive airborne LiDAR surveys and UHF active RFID tags (source: Brousse et al, online); the combination of HR topographic differencing before and after a 5-yr flood and bedload tracing successfully allow to detect the propagation of the artificially-induced sediment wave, with a front located at 2.5 km from the dam



2430

2431 *Figure 10: (A) Wood detection procedure using a video camera in the Ain River, France. Images*
 2432 *show the region of interest (ROI) based on a visual detection of wood including measurement of date*
 2433 *and time from time stamp, the precise location of end and side points to define the piece length,*
 2434 *diameter, and first position, and the definition of second position after advancing a user-determined*
 2435 *number of frames to allow calculation of velocity and angular velocity;* (B) *Flood hydrograph and*
 2436 *wood flux estimated based on video records during the event on April 10–13, 2008 (Modified from*
 2437 *MacVicar and Piégay, 2012); (C) Wood transport regimes characterized using home movies; the*
 2438 *small images show the same river section (North Creek, US) at different times (t), h: water depth*
 2439 *and z: wood flow depth; d_w: wood piece diameter; k: coefficient >1 (Modified from Ruiz-Villanueva*
 2440 *et al., 2019).*

2441



2442

2443 *Figure 11: (A) Aerial images of the Magra River near Aulla (Italy) in 2007 (up) and in 2011 (down)*
 2444 *and bed topography before a simulated flood sequence, after four floods and simulated biomass*
 2445 *distribution (From Bertoldi et al., 2014).(B) Simulated water depth and logs deposited along the*
 2446 *Czarny Dunajec River reach at a discharge of 28m³/s. From Ruiz-Villanueva et al., 2017.*

2447

2448

2449
 2450
 2451
 2452
 2453
 2454
 2455
 2456
 2457
 2458
 2459
 2460
 2461
 2462
 2463
 2464
 2465
 2466
 2467
 2468
 2469
 2470
 2471
 2472
 2473
 2474
 2475
 2476
 2477
 2478
 2479
 2480
 2481
 2482
 2483
 2484
 2485
 2486
 2487
 2488
 2489
 2490
 2491
 2492
 2493

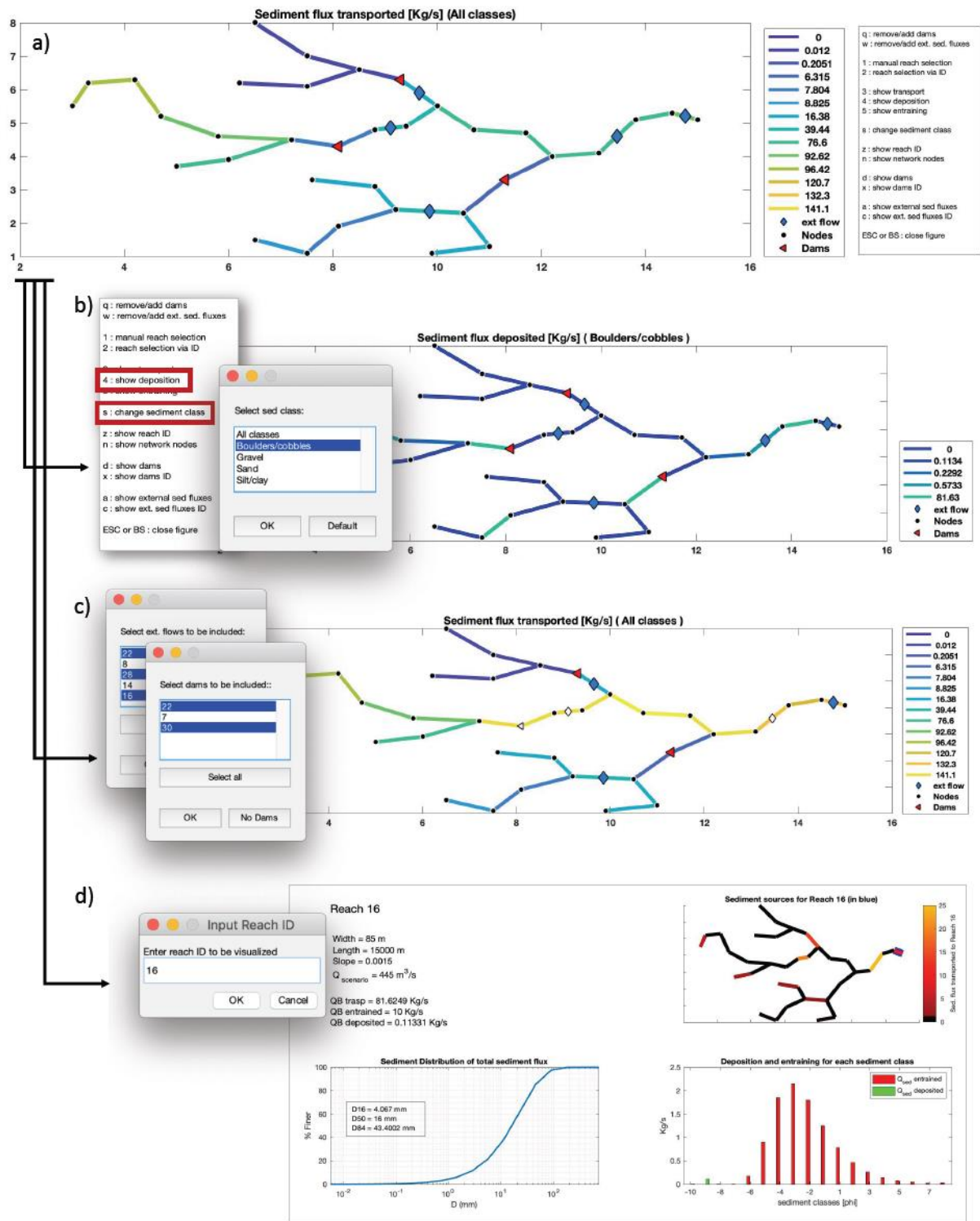


Figure 12. Examples of plots obtained from CASCADE toolbox (source: Tangi et al, 2019). The tool allows analysing various properties of sediment connectivity in an interactive manner. Panel a shows the total sediment transported in Kg/s in the network. b visualizes patterns of deposition for a single sediment class out of the 18 considered in the model (in this case boulders/cobbles). c shows the changes in total sediment transport caused by the removal of one dam and two external sediment flows. d shows an analysis of grain size distribution, sediment sources and deposition and entrainment in a specific reach. Each step can be interactively controlled by the user using a graphical interface.

2494
 2495
 2496
 2497
 2498
 2499
 2500
 2501
 2502
 2503
 2504
 2505
 2506
 2507
 2508
 2509
 2510
 2511
 2512
 2513
 2514
 2515
 2516
 2517
 2518
 2519
 2520

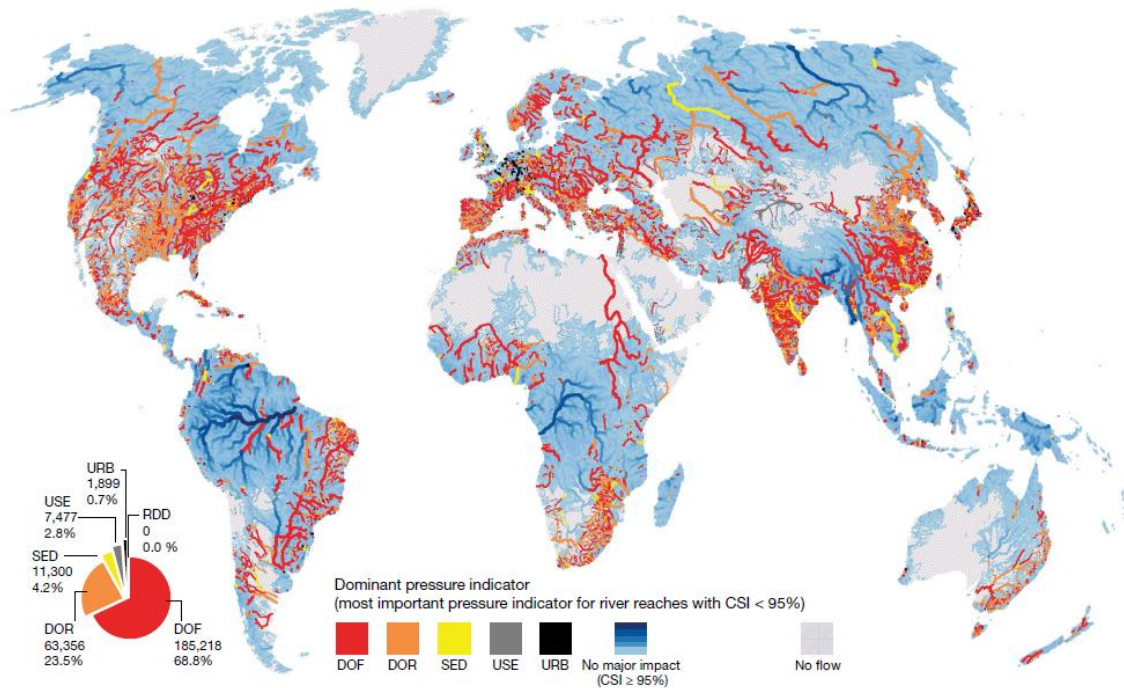
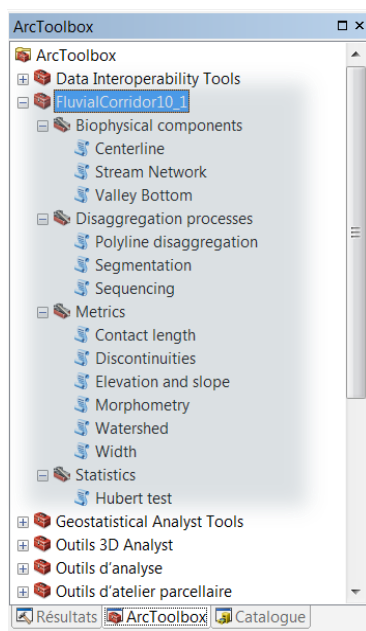


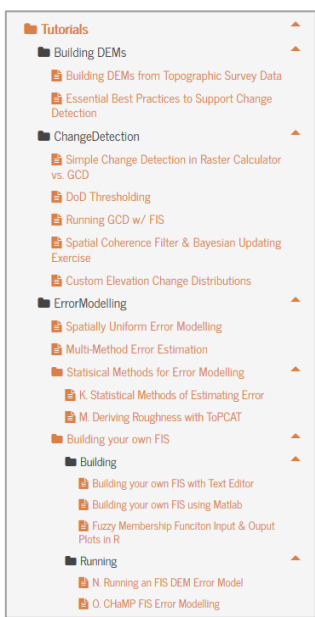
Figure 13. Dominant pressure indicator for global river reaches below a given Connectivity Status Index (CSI) threshold (95%). Pressure indicators include the DOF (degree of fragmentation), DOR (degree of regulation), SED (sediment trapping), USE (consumptive water use) and URB (urban areas). The inset shows the number and proportion of river reaches per dominant pressure indicator at the global scale. (Source: Grill et al., 2019; Figure 2)

2521
2522
2523
2524
2525
2526
2527
2528
2529
2530
2531
2532
2533
2534
2535
2536
2537
2538
2539
2540
2541
2542
2543
2544
2545
2546
2547
2548
2549
2550
2551
2552
2553
2554
2555
2556
2557
2558
2559
2560
2561
2562
2563
2564
2565
2566
2567
2568
2569
2570

A)



B)



C)

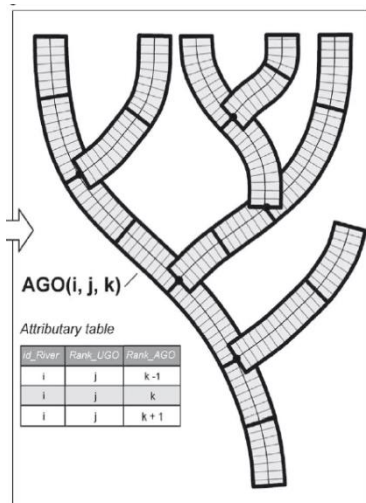
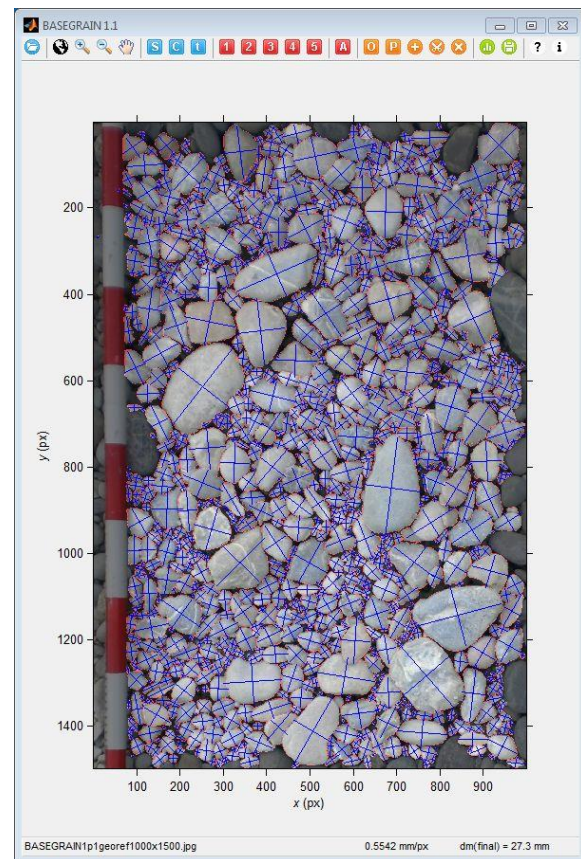


Figure 14. Example of tools/interfaces available online to measure characters of fluvial corridors : A) The Fluvial Corridor Toolbox – FCT - within the ArcGIS Arc Toolbox (Roux et al. 2015) and view of generic spatial units for characterizing aggregated geographical objects at the network-scale (<https://github.com/EVS-GIS/Fluvial-Corridor-Toolbox-ArcGIS>); B) website views (tutorial and dataset example) of the Geomorphic Change Detection software (<http://gcd.riverscapes.xyz/>) (Wheaton et al., 2010a); and C) Example of image output showing grain detection using BaseGrain software (<https://www.ethz.ch/content/specialinterest/baug/laboratory-vaw/basement/en/download/tools/basegrain.html>) (Detert et Weitbrecht, 2012)